

博 士 論 文

関節不安定性の制動が関節軟骨変性に与える影響

埼玉県立大学大学院

保健医療福祉研究科

博士論文

2018年3月

村 田 健 児



博士論文

関節不安定性の制動が関節軟骨変性に与える影響  
(Controlling joint instability delays the degeneration of articular cartilage)

埼玉県立大学大学院

保健医療福祉研究科

博士論文

村田健児



目次	
図表一覧.....	3
要旨.....	4
Graphical Abstract.....	9
1. 略語一覧.....	10
2. 研究の背景と目的.....	11
-1 本邦における変形性膝関節症の位置づけ.....	11
-2 関節軟骨の構成組織.....	11
-3 関節軟骨変性メカニズムと現在の治療法.....	12
-4 膝関節における関節不安定性と変形性膝関節症の関連.....	14
-5 本研究の目的.....	15
3. 関節不安定性が軟骨変性の進行に及ぼす影響.....	17
-1 目的.....	17
-2 実験方法.....	17
1) 倫理的配慮.....	17
2) 研究デザイン.....	17
3) ACL-T モデル、CAJM モデルの手術方法.....	17
4) 軟 X 線による脛骨の前方関節不安定性の計測.....	18
5) 膝関節軟骨、滑膜、骨棘の組織学的評価および分析.....	19
6) 関節軟骨と滑膜の免疫組織化学分析.....	20
7) リアルタイム PCR 法を用いた関節軟骨における mRNA 発現.....	21
8) 統計解析.....	22
4. 研究結果.....	30
-1 CAJM モデルは前方への関節不安定性を制動する.....	30

-2 異常関節運動の制動は軟骨変性を遅延させる .....	30
-3 異常関節運動の制動は関節軟骨(軟骨厚・乱れ・染色性)を維持する .....	31
-4 異常関節運動の制動が関節軟骨の炎症メディエータを抑制する .....	32
-5 異常関節運動の制動は関節軟骨の炎症メディエータ mRNA を抑制する .....	32
-6 異常関節運動の制動は滑膜の炎症所見を低減する .....	33
-7 異常関節運動の制動が滑膜組織の炎症メディエータを抑制する .....	33
-8 異常関節運動の制動は骨棘を抑制する .....	33
5. 考察 .....	43
6. 研究の限界と今後の展望 .....	48
7. 結語 .....	50
8. 謝辞 .....	51
9. 引用文献 .....	52

## 図表一覧

Fig.1. The pathogenesis of osteoarthritis .....	17
Fig.2. Experimental protocol .....	25
Fig.3. Surgery of CAJM model.....	26
Fig.4. Osteoarthritis Research Society International score .....	27
Fig.5. Histological analysis point and method of surface roughness.....	28
Fig.6. Influence of controlling joint instability by CAJM surgery .....	36
Fig.7. Cartilage histological findings and OARSI degeneration score comparison .....	37
Fig.8. Influence of controlling joint instability for cartilage.....	38
Fig.9. Controlling joint instability inhibits inflammatory factors observed using immune-histochemical analysis in cartilage .....	39
Fig.10. Synovial membrane histological findings and synovial membrane inflammation score.....	40
Fig.11. Controlling abnormal joint movement inhibits inflammatory factors in synovial membrane .....	41
Fig.12. Histological osteophyte formation scoring system (HOFSS) .....	42
Table 1. Histological osteophyte formation scoring system .....	29
Table 2. Synovial membrane inflammation score.....	30
Table 3. Controlling joint instability inhibits mRNA expression of inflammatory factors as a proportion of the normal tissue samples .....	43

## 要旨

超高齢社会を迎えた日本において、運動器疾患の予防は喫緊の課題であるといえる。なかでも変形性膝関節症（Osteoarthritis: OA）は、日常生活の様々な場面において膝関節痛に伴う活動障害を引き起こす運動器疾患であり、その罹患者数も多いことから病態解明と予防ならびに治療法の開発が国内外で期待されている。しかしながら、OA に対する主たる治療法は対症療法が主であり、根治を目指した治療法は現在までに十分なエビデンスは得られていない。この理由として、OA 発症要因の本質が機械的ストレスであり、具体的な進行メカニズムについて十分に解明されていないことが一要因である。

関節軟骨は、主にゲル状に保持された水とプロテオグリカンで構成され、低摩擦潤滑機能という重要な機能を有している。この機能は、荷重や関節運動に伴う応力負荷を分散することで関節への機械的ストレスを巧妙に軽減している。しかしながら、関節軟骨が耐え得る生理的な限界を超過した機械的ストレスが加えられた際に生じる摩耗や変性、関節辺縁部での骨棘は OA の特徴といえる。現在までに明らかにされている関節軟骨の進行要因や病態については、損傷した軟骨の治癒能力の限界、軟骨細胞自身の貧食作用によるアポトーシス、損傷に伴う滑膜や滑液などの膝関節内炎症による関節軟骨組織の分解促進、軟骨下骨における軟骨内骨化、骨棘の形成とその微細骨折に伴う貧食作用と様々であるが、少なくともその根本には機械的ストレスの関与が存在するといえる。しかし、機械的ストレスが示す具体的な損傷メカニズムについて検証した報告はなく、関節軟骨の機能維持に関する過去の報告では、適度な運動が推奨されるに留まっている。

脛骨と大腿骨から構成される膝関節は、骨形状のみでは不安定であるため、その安定性を靭帯や半月板などに依存している。特に、膝前十字靭帯は

脛骨の前方引出しを制動することで、膝関節の機能的安定性維持し、正常な関節運動学を保つ上で重要な軟部組織である。しかし、前十字靭帯の損傷に伴う脛骨の前方不安定性は、正常から逸脱した関節運動を惹起し、関節機能の低下や関節自体への力学的ストレスを増加させる。膝関節の機能的安定性によって維持される関節運動学は、関節軟骨の変性が進行する過程において、機械的ストレスとの関連性を明らかにする上で重要な視点である。本研究は、前十字靭帯断裂後の関節不安定性に伴う異常な関節運動学という機械的ストレスが OA 進行に関与する具体的な機械的ストレスであると仮説を立て、OA に対する異常な関節運動の関与とその制動する効果について検証することを目的とした。

この目的を達成するために、OA の病態解明において従来から利用されている前十字靭帯断裂によって異常関節運動が惹起された前十字靭帯損傷モデル (Anterior cruciate ligament transection model; ACL-T) と靭帯損傷させることで惹起された異常な関節運動を正常な状態へ制動する新たな異常関節運動制動モデル (Controlling abnormal joint movement model; CAJM) を用いた。まず、異常関節運動における制動効果の検証について、定性ばねを用いた前方引出しテストでは、制動した CAJM モデルと比較して、制動していない ACL-T モデルの大腿骨に対する脛骨の前方引出し量が有意に増大し、前方への関節不安定性が顕著であった。さらに、膝関節の最大伸展位ならびに最大屈曲位においても、ACL-T モデルで顕著に前方引出しを確認した。また、CAJM モデルでは最大伸展位ならびに最大屈曲位は正常膝関節と顕著な差はなく、ギプス固定やワイヤー固定の関節固定術とは異なり、関節可動域制限が生じていないことが確認された。これらの結果は、ACL-T モデルにおいて矢状面上で異常関節運動が生じ、CAJM モデルはその制動効

果を有していることから異なる関節不安定性の再現が可能であった。

これらのモデルを用いて、関節軟骨の変性について検証するため、組織学的な観察を行った。4 週目時点では ACL-T モデルで表層のフィブリル化ならびに軟骨構成組織であるグルコサミノグリカンを染色するサフラニン O の染色性が表層部で低下した。一方、CAJM モデルにおいても表層のフィブリル化やサフラニン O 染色性の低下が確認されたが、ACL-T モデルに比較して顕著ではなかった。12 週時点では、ACL-T モデルの関節軟骨厚の減少、表層のフィブリル化、グルコサミノグリカンの染色性が著しく低下し、関節軟骨の変性が顕著であった。大腿骨においても、関節軟骨表層のフィブリル化、グルコサミノグリカンの染色性の低下を認め、CAJM モデルよりも関節軟骨の変性が重症化していた。

軟骨の組織学的変性を半定量化する国際基準である OARSI スコアにおいて評価した結果、12 週時点で CAJM モデルに比較して ACL-T モデルで有意にスコアが高く、軟骨の変性が顕著であった。また、脛骨の軟骨厚、表層のフィブリル化を示す Roughness、そしてグルコサミノグリカンの染色性について、組織学的分析を行った。結果、軟骨厚については、12 週目時点で ACL-T モデルで有意に減少し、CAJM モデルで軟骨厚が維持された。また、Roughness についても、12 週目時点において顕著に ACL-T モデルで増大し、フィブリル化が顕著であった。また、軟骨の構成成分であるグルコサミノグリカンの染色性について、4 週目時点では CAJM モデルと ACL-T モデルの双方で正常軟骨に比較して有意に低下したが、12 週目時点では、ACL-T モデルが CAJM モデルよりも顕著に低下していた。このことから、異常関節運動の制動が関節軟骨の変性を遅延できることを組織学的分析によって示した。

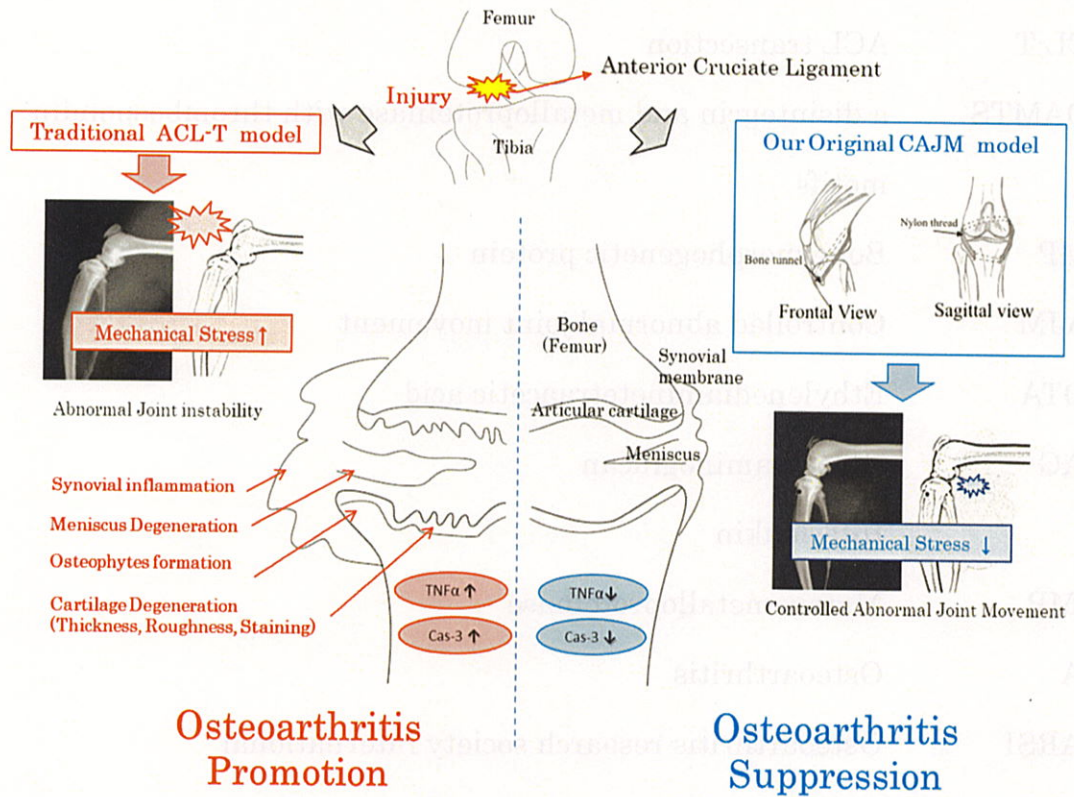
関節軟骨の変性過程において発現する炎症メディエータの腫瘍壊死因子- $\alpha$  (Tumor necrosis factor- $\alpha$ ; TNF- $\alpha$ )、インターロイキン- $\beta$  (Interleukin- $\beta$ ; IL- $\beta$ )、そして軟骨細胞のアポトーシス誘導因子である Caspase-3 の活性化を免疫組織化学染色法で評価した。結果、TNF- $\alpha$  は 4 週時点において CAJM モデルと比較して ACL-T モデルで有意な発現を認めた。また、Caspase-3 は、4 週時点ならびに 12 週時点において CAJM モデルと比較して ACL-T モデルにおいて顕著な発現を認めた。脛骨の軟骨から採取した mRNA 発現量についても CAJM モデルと比較して ACL-T モデルでは、TNF- $\alpha$  と Caspase-3 の有意な発現を認めており、異常な関節運動の制動が、軟骨炎症メディエータである TNF- $\alpha$  や軟骨細胞のアポトーシスに関連する Caspase-3 の抑制に機能したといえる。

滑膜の炎症が関節軟骨の変性に影響を及ぼすことから、異常関節運動の制動が滑膜に与える影響について、半定量解析である Synovial membrane inflammation スコアを用いて組織学的に評価した。結果、12 週時点の滑膜において、線維芽細胞の増殖が前方滑膜に観察され、滑膜の肥厚は後方に顕著に確認された。Synovial membrane inflammation スコアは、前方滑膜には、ACL-T モデルと CAJM モデルで有意な差を認めなかったが、後方滑膜組織について ACL-T モデルは CAJM モデルに比較してスコアが有意に大きかった。炎症メディエータである TNF- $\alpha$  と IL- $\beta$  についても免疫組織学的染色にて、ACL-T モデルで濃染を認めたことから、継続した滑膜炎が CAJM モデルに比較して ACL-T モデルで引き起こされていた可能性を示唆した。

最後に、変形性膝関節症の診断として用いられる骨棘について、骨棘の大きさならびに成熟度について **Histological osteophyte formation scoring system** を用いて評価した。結果、骨棘の大きさについて、ACL-T モデルは CAJM モデルに比較して骨棘の大きさについて高いスコアを示した。骨棘の成熟度についても同様に、ACL-T モデルは CAJM モデル比較して成熟度スコアが有意に大きかった。このことは、異常な機械的ストレスが検知され、骨形成が促進された可能性を示し、先の滑膜増殖の結果を合わせて異常関節運動の制動が後方部における骨棘形成を抑制することを示唆している。

以上の結果から、異常関節運動は関節軟骨の変性を遅延させ、OA の発症と進行に重要な役割を果たすと考えられる。

## Graphical Abstract



In recent years, joint instability has been recognized as a significant cause of cartilage degeneration. This study is unique in that it is approached from the novel perspective that controlling joint instability can inhibit cartilage degeneration. We analyzed the effect of joint instability on articular cartilage. We found that joint instability promotes the progression of osteoarthritis and controlling joint instability inhibits cartilage degeneration.

## 1. 略語一覧

ACL	Anterior cruciate ligament
ACL-T	ACL transection
ADAMTS	a disintegrin and metalloproteinase with thrombospondin motifs
BMP	Bone morphogenetic protein
CAJM	Controlled abnormal joint movement
EDTA	Ethylenediaminetetraacetic acid
GAG	Glycosaminoglycan
IL	Interleukin
MMP	Matrix metalloproteinase
OA	Osteoarthritis
OARSI	Osteoarthritis research society international
PBS	Phosphate buffered saline
PCR	polymerase chain reaction
PFA	Paraformaldehyde
RANKL	Receptor activator of nuclear factor kappa- $\beta$ ligand
TGF	Transforming growth factor
TNF	Tumor necrosis factor
VEGF	Vascular endothelial growth factor

## 2. 研究の背景と目的

### -1 本邦における変形性膝関節症の位置づけ

超高齢社会を迎えた本邦において、骨・関節機能の低下を予防することは重要な課題となっている。なかでも、変形性膝関節症（Osteoarthritis; OA）は、関節軟骨の変性を主病変とし、膝関節痛や歩行障害、延いては日常生活障害を引き起こす運動器疾患であり、その罹患者数は700万人を超える<sup>1)</sup>。疼痛や機能障害は自覚しなくとも、X線撮影上で変性を認めた潜在的なOAを含めると国内の罹患者数は2,800万人を超えると推測され、OAの予防的戦略は我が国の重要な位置づけにある。しかしながら、その病態解明と予防法ならびに治療法の開発が国内外で期待されていながら、根本的な解決には至っていない<sup>2)</sup>。

### -2 関節軟骨の構成組織

関節軟骨は、血管、神経、そしてリンパ管が存在していない硝子軟骨であり、荷重緩衝作用という優れた機能を有している<sup>3)</sup>。主な構成組織は、約80%が水分、残る20%は軟骨細胞や細胞外マトリックス（プロテオグリカンやII型コラーゲン）によって構成される。主成分であるプロテオグリカンは、コンドロイチン硫酸、ヘパラン硫酸、ケラタン硫酸、デルマタン硫酸、そしてヒアルロン酸といった高分子糖タンパク質で構成され、硫酸基やヒドロキシル基を有する構造上の特徴から水分をゲル状に保持し、荷重や関節運動に伴う局所的な応力負荷を分散することで、関節軟骨へ加わる機械的ストレスを巧妙に軽減している<sup>4)</sup>。しかしながら、プロテオグリカンの減少やII型コラーゲンの分解によって、関節軟骨に加わる機械的ストレスが生理的な限界を超越した場合、関節軟骨の摩耗や変性を特徴としたOAが発症する。

### -3 関節軟骨変性メカニズムと現在の治療法

前述のごとく、関節軟骨は高分子タンパク質であるプロテオグリカンやヒアルロン酸、そしてⅡ型コラーゲンを主とした細胞外マトリックスで構成される。しかしながら、血管やリンパ管が欠如する関節軟骨は損傷後の修復能力が著しく低いことから、軟骨を“損傷させない・変性させない”ことが OA の予防として重要な視点であるといえる。関節軟骨変性に関連するカスケードは複数存在し、すべてが解明されていないものの、機械的ストレスが OA 発症メカニズムに寄与する重要なターゲットであることは一定の見解を得ている<sup>5),6)</sup>。

強い機械的ストレスが関節軟骨に生じた場合、損傷した軟骨組織の貧食作用に伴う分解能と軟骨組織を修復させるための合成能との間で、分解能が相対的に増加することにより関節軟骨の恒常性が維持できなくなる。すなわち、血管やリンパ管が存在していない関節軟骨は、もとより損傷時の治癒能力が劣ることから、関節軟骨の分解能が相対的に増大し、この合成能と分解能の不均衡が関節軟骨の変性を進行させる要因の一つとされている<sup>7)</sup>。同時に、損傷した軟骨組織で炎症性サイトカインであるインターロイキン (Interleukin; IL) や腫瘍壊死因子 (Tumor necrosis factor; TNF) の分泌が増大し、なかでも軟骨変性メディエータである IL-1<sup>8),9)</sup>や TNF- $\alpha$ <sup>10),11)</sup>は、プロテオグリカンの分解作用を有するマトリックスメタロプロテアーゼ (Matrix metalloproteinase; MMP) やアグリカナーゼ (a disintegrin and metalloproteinase with thrombospondin motifs; ADAMTS) を誘導し、関節軟骨の変性を一層促進する<sup>12),13),14),15),16)</sup>。

一方、関節軟骨を損傷するほどの強い機械的ストレスに至らなくとも、軟骨に加わる継続的な機械的ストレスによって、徐々に変性が進行するケース

が一般的であるといえる<sup>17)</sup>。半月板損傷や膝関節靭帯（前十字靭帯、後十字靭帯、内側側副靭帯や外側側副靭帯）を損傷した場合、将来的な OA 発症のリスクが高まると報告されており<sup>18)</sup>、半月板や靭帯損傷後に生じる機械的ストレスの変化が長期的に軟骨変性に関連している可能性も報告されている<sup>19)</sup>。近年は「滑膜性 OA」や「脂肪性 OA」というように半月板や靭帯損傷後に生じる滑膜や膝蓋下脂肪体組織の炎症が軟骨変性に寄与するという報告も散見される<sup>20),21)</sup>。特に、滑膜は滑液を生成する重要な役割を持ち、滑膜や滑液から分泌される軟骨変性メディエータやタンパク質分解酵素は関節軟骨の分解作用を促進すると報告されている<sup>22),23),24),25),26),27)</sup>。また、滑膜は OA 進行の目安とされる骨棘の形成過程にも深く関連し、関節軟骨辺縁部において滑膜から血液供給を受けることで異常な関節力学に起因する骨の成長の結果として形成される<sup>28)</sup>。過度な機械的ストレスによって軟骨細胞が異常分化および肥大化し、コラーゲンタイプ X 型の発現が活性化され、軟骨基質の石灰化が進行していく内軟骨骨化過程を辿る。この過程における滑膜や軟骨下骨からの血管新生刺激因子ある血管内皮細胞増殖因子 (vascular endothelial growth factor; VEGF)<sup>29),30),31)</sup>や骨棘誘導因子である骨形成タンパク質(Bone Morphogenetic Protein ; BMP)<sup>32)</sup>、トランスフォーミング増殖因子(Transforming growth factor beta ; TGF- $\beta$ )<sup>33),34)</sup>の発現は、骨棘形成過程に必要不可欠であることが明らかとなっている<sup>35)</sup>。骨棘は、関節軟骨の潤滑性を低下させるのみならず、可動域の制限や骨棘の骨折に伴う貧食作用によって、IL-1 $\beta$  や TNF- $\alpha$  などの炎症性サイトカインを誘導し、MMP や ADAMTS といった基質分解酵素の発現を刺激することで関節軟骨の変性を促進する<sup>36)</sup>。また、関節軟骨の深層に位置する軟骨下骨では、過度な機械的ストレスによって内軟骨骨化シグナルが活性化される<sup>37),38)</sup>。低活性状態で維持されている正常な軟骨細胞が生理的な限界を超過した機械的ストレスによ

って、異常分化が進行することで内軟骨骨化が進行する<sup>39)</sup>。

このように正常を逸脱する機械的ストレスによって軟骨変性は進行し、最大の特徴である荷重緩衝作用を失うと、膝関節痛や歩行障害、延いては日常生活障害を引き起こす。その治療法は、筋力強化運動や関節可動域運動などの運動療法、低周波や超音波といった物理療法、ヒアルロン酸やステロイドの関節内注射、消炎鎮痛効果を有する内服、人工関節置換術や骨切り術といった手術療法が選択される<sup>40)</sup>。近年では、根本的な治療を目的とした滑膜由来の間葉系幹細胞を用いた軟骨再生療法の研究も行われており、治療の発展性が期待されている<sup>41)</sup>。しかしながら、対症療法が主となり根本的治療が確立されていないのは、変形性膝関節症の発症要因の本質が機械的ストレスであり、具体的な機械的ストレスと進行メカニズムが十分解明されていないことが原因として考えられる。

#### -4 膝関節における関節不安定性と変形性膝関節症の関連

OAの要因は多因子に渡り、加齢<sup>42),43),44)</sup>、性別<sup>45),46)</sup>、遺伝的要因<sup>47)</sup>、肥満に伴う体重増加<sup>48),49)</sup>といった全身的な要因、筋力低下<sup>50),51)</sup>、半月板・靭帯損傷<sup>52),53)</sup>などの膝関節周囲の機能的要因がOAの発症と進行に深く関連することが明らかとなっている。

一方、近年、関節の弛緩性といった膝関節自体の不安定性が機械的ストレスとして軟骨変性を進行させる一因であることが報告されている<sup>54)</sup>。前十字靭帯、内側側副靭帯、内側半月板の損傷や大腿四頭筋萎縮に伴う二次的な関節不安定性によって、OAの代表的な病態的特徴の関節軟骨の変性、滑膜組織や滑液中の炎症性サイトカインの増加、そして骨棘の形成が報告されている<sup>55),56),57),58)</sup>。また、OA患者は関節不安定性に伴う内転モーメントの増加<sup>59),60),61)</sup>や自覚的な関節不安定性を訴えることから<sup>62),63),64),65)</sup>、関節不安定性

と OA の関連は容易に想定でき、これらの現象を臨床現場では経験的に理解している。従来から OA の進行機序の解明に用いられている膝前十字靭帯断裂モデルは、脛骨の過度な前方引き出しが生じることから、関節不安定性が惹起されている代表的なモデルである。しかしながら、膝前十字靭帯断裂は、一度関節内に剪刀を挿入し靭帯を切断することから、純粋な脛骨の前方不安定性という異常関節運動が OA 進行に関与していることを完全に示すことはできていない。それらの解決のためには、関節内侵襲によって惹起された脛骨の異常な前方不安定性を制動する新たなモデルが必要であり、一度不安定性が生じた膝関節を外科的に制動する新たなモデルラットを開発することで、その機序を解明できると考えている。近年、Kokubun らは前十字靭帯損傷後に生じた前方引出しを関節包外で制動する異常関節運動を制動する新たなモデルを提唱した<sup>66)</sup>。このモデルを用いることによって、OA の進行や発症に関与する具体的な機械的ストレスについて、明確にする一つの解決策となり得ると考えられる。

#### -5 本研究の目的

本研究では、関節不安定性に伴う脛骨の異常な関節運動が関節軟骨に対する機械的ストレスとなり、関節軟骨変性の進行や骨棘形成に関連していると仮説を立て、その制動によって関節軟骨の変性が抑制できるかを検証することで、変形性膝関節症の発症進行における機械的ストレスの関与について明らかにすることを目的とした。

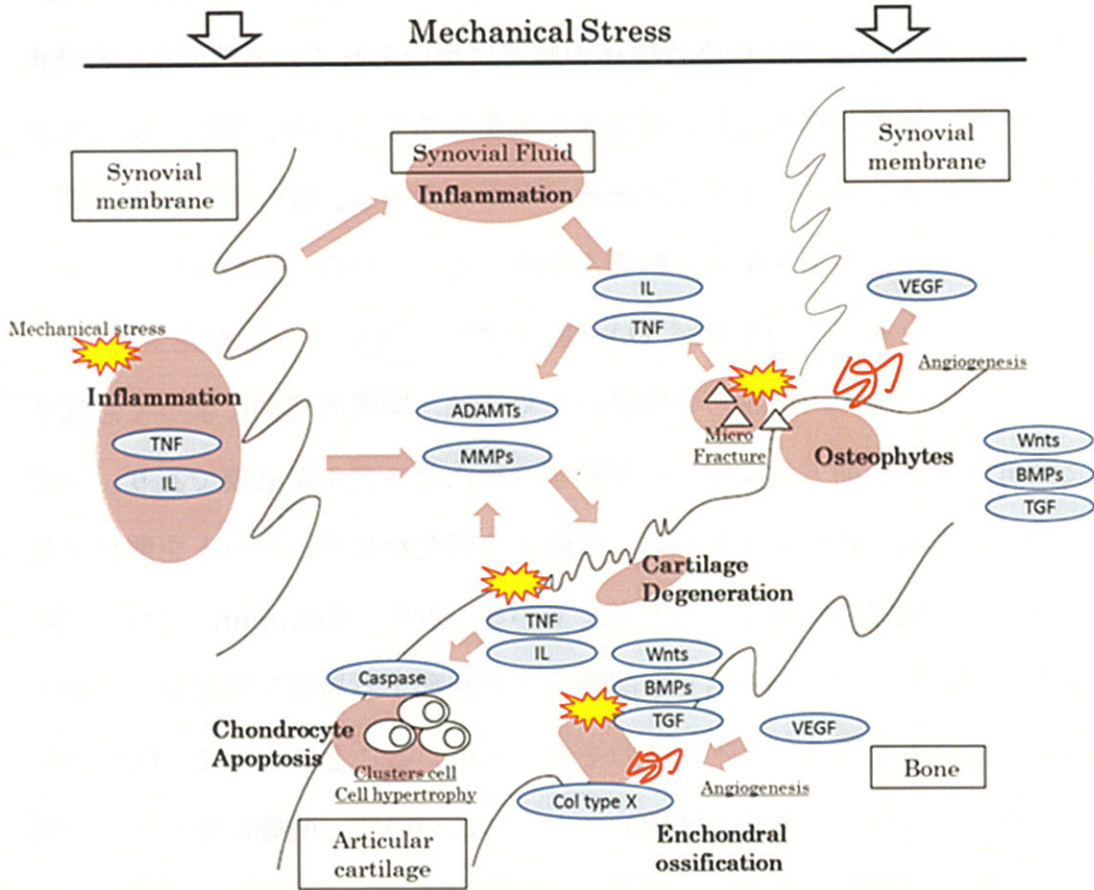


Fig.1. In recent years, joint instability has been recognized as a significant cause of cartilage degeneration. This study is unique in that it is approached from the novel perspective that controlling joint instability can inhibit cartilage degeneration. In this study, we analyzed the effect of joint instability on articular cartilage. We found that joint instability promotes the progression of osteoarthritis and controlling joint instability inhibits cartilage degeneration.

### 3. 関節不安定性が軟骨変性の進行に及ぼす影響

#### -1 目的

関節不安定性の制動が関節軟骨に及ぼす影響について、組織学的、免疫組織学的、生化学的手法を用いて検証することを目的とした。

#### -2 実験方法

##### 1) 倫理的配慮

本学研究推進委員会の承認を得た後、動物実験基本計画書ならびに動物実験実施計画書に従い、研究を推進した（承認番号 26-9）。また、本研究は *Animal Research: Reporting of In Vivo Experiments* ガイドラインに従い<sup>67)</sup>、実施した。

##### 2) 研究デザイン

6ヶ月齢 Wistar 系雄性ラット 65 匹 (Sankyo Labo Service Corporation, INC, JPN) を用いた。対象は、外科的な手術を行わない INTACT 群、膝関節の前十字靭帯 (Anterior cruciate ligament; ACL) を外科的に断裂させることで脛骨の前方関節不安定性を惹起した群 (ACL-T 群)、ACL 断裂後に脛骨の前方関節不安定性を制動した関節制動群 (Controlled abnormal joint movement; CAJM 群) の 3 群に分類した (Fig. 2)。

##### 3) ACL-T モデル、CAJM モデルの手術方法

ジエチルエーテル (Wako Pure Chemical Industries, Ltd., JPN) で吸入麻酔後、ソムノペンチル (Kyoritsu Seiyaku Corporation, JPN) 0.8ml/kg を腹腔内に投与、抗精神薬レペタン (Otsuka Pharmaceutical Co., Ltd. JPN) 0.8ml/kg を背部皮下に投与し、深麻酔ならびに苦痛緩和処置を行った。膝

関節内側をメスで縦切開し(Fig. 3a)、膝蓋腱を露出した後、膝蓋腱内側の関節包から関節内へ侵入した剪刀を用いて、ACLを完全断裂させることで脛骨の前方関節不安定性が惹起されたことを確認した(Fig. 3b)。ACL-T群は、関節包と皮膚を縫合糸(Johnson & Johnson K.K., JPN)を用いて閉創した。CAJM群は、歯科用ドリルNSKアルチメイトXL(Nakanishi Co., Ltd. JPN)を用いて脛骨内側から脛骨外側に向けて開孔した(Fig. 3c)。骨孔に4-0 ナイロン糸(Akiyama seisakusyo Co., Ltd. JPN)を脛骨内側から脛骨外側に貫通させ(Fig. 3d)、ループ状に大腿骨後顆の外側から内側にかけて緊縛し、前方への関節不安定性を制限した後、閉創した(Fig. 3e-g)。術後の飼育条件は、温度23℃、湿度55%に設定されたポリカーボネイト製ケージ内(2匹/ケージ)で、運動を制限することなく飼育した。照明は昼夜12時間サイクルで明暗を管理し、固形飼料と給水は自由摂取可能とした。

#### 4) 軟X線による脛骨の前方関節不安定性の計測

関節不安定性の評価として、術後直ぐに各群5匹ずつ15匹を分析に供した。股関節を含むラット右後肢を採取し、大腿骨近位1/2の大腿四頭筋を剪定した後、自作した前方引出し装置に大腿骨近位1/2をクランプで固定した。撮影肢位は、膝関節最大伸展位、最大屈曲位、90度屈曲位とし、定性ばね(Sanko spring Co., Ltd. JPN)を用いて脛骨を前方へ0.2kgfの力で牽引しながら、軟X線装置M-60(Softex Co., Ltd. JPN)で撮像した。撮影条件は、管電圧28kV、電流1mA、露光時間1秒と設定し、画像はデジタル画像センサーNAOMI(RF Co., Ltd. JPN)によって、デジタル化した。90度屈曲位の脛骨前方移動量は、画像処理ソフトウェアImage Jを用いて定量化した。

## 5) 膝関節軟骨、滑膜、骨棘の組織学的評価および分析

術後 4 週、12 週時点で、右後肢膝関節を採取した (n = 5/群, 30 肢)。採  
した膝関節は生理食塩水で洗浄後、直ちに 4%PFA/リン酸緩衝液 (Wako  
Pure Chemical Industries, Ltd., JPN) で浸漬固定した (48 時間, 4°C)。固  
定後、PBS で洗浄し、10%エチレンジアミン四酢酸 (Sigma-Aldrich Co.  
LLC, JPN) 溶液で脱灰した (60 日間, 4°C)。脱灰終了後、スクロース置換処  
理として 10%スクロース溶液 (4 時間)、15%スクロース溶液 (4 時間)、20%  
スクロース溶液 (12 時間)の順で浸潤し、OCT compound (Sakura Finetek  
Japan Co., Ltd. JPN) で包埋した。クライオスタット CM3050S (Leica  
Microsystems GmbH, GER) を用いて、矢状面 14 $\mu$ m で薄切し、凍結切片  
を作成し、サフラニン O・ファストグリーン染色を実施した。半定量的解  
析として、関節軟骨の変性について、Osteoarthritis Research Society  
International (OARSI) スコアを用いた<sup>68),69),70)</sup>。OARSI スコアは、グレー  
ド(0-6)とステージ(0-4)の積算、合計 24 点で構成され、点数が高いほ  
ど関節軟骨の変性が著しいことを示す軟骨の組織学的解析手法である (Fig.  
4)。2 名の独立した評価者が、一肢に対して 3 スライドの評価を行い、その  
平均点を OARSI スコアとした。解析部位は、1 スライドの内は内側と外側  
それぞれ、前方部、中央部、後方部の 6 カ所でスコアリングし、平均化し  
た。骨棘スコアは、Kaneko らの手法 (Histological osteophyte formation  
scoring system, HOFSS) を用いて評価した<sup>71)</sup>。HOFSS スコアは、骨棘の  
大きさ (0-3) と骨棘の成熟度 (0-3) の加算、合計 6 点で構成され、点数  
が高いほど組織学的に骨棘が形成されていることを示すスコアである  
(Table.1)。解析部位は、内側の脛骨後方部において、一肢に対して 3 スラ  
イドの評価を行い、平均化した。滑膜は、Synovial membrane  
inflammation スコア<sup>69)</sup>を用いた。Synovial membrane inflammation スコ

アは、滑膜組織の層構造と線維芽細胞の増殖に着目し、合計 4 点で構成される (Table.2)。解析部位は、前方および後方の滑膜において、一肢に対して 3 スライドの評価を行い、平均化した。

軟骨厚の評価は、50 倍で撮像された関節軟骨を 1 スライドにつきランダムに選択された 6 か所の軟骨厚を測定し、その平均値を軟骨厚とした。軟骨表層 Roughness は、400 倍で撮像された関節軟骨表層について直線近似と仮定し (Approximation of the straight length)、実際の軟骨表層の長さを計測し (True length)、True length/ Approximation of the straight length で割合を算出した<sup>72)</sup> (Fig. 5)。1 スライドにつきランダムに選択された 2 か所の軟骨表層 Roughness を算出し、平均化した。グリコサミノグリカンを示すサフラニン O の染色性は、切片をグレースケール化した後、256 階調で 10,000  $\mu\text{m}^2$  の範囲を 1 肢につき 9 か所 (1 切片につき 3 か所を 3 切片) 測定した。INTACT 群を 100% となるように正規化し、その割合を算出した。

## 6) 関節軟骨と滑膜の免疫組織化学分析

アビジン・ビオチン複合体法を用いて免疫組織化学染色を実施した。凍結した組織切片を 30 分間室温で風乾させた後、リン酸緩衝液で 5 分間 3 回洗浄した。内因性ペルオキシダーゼ活性の抑制のため、エタノール(Wako Pure Chemical Industries, Ltd., JPN) で希釈した 3%過酸化水素溶液 (Wako Pure Chemical Industries, Ltd., JPN) で 30 分間反応させた。リン酸緩衝液で 5 分間 3 回の洗浄後、ヤギ血清アルブミン(Vector Laboratories, USA) を用いて組織切片をブロッキングし、室温で 30 分間反応させた。一次抗体として、抗ウサギ TNF- $\alpha$  (Bioss, USA) ポリクローナル抗体、抗ウサギ IL-1 $\beta$  (Bioss, USA) ポリクローナル抗体、抗ウサギ Caspase-3 (Bioss,

USA) ポリクローナル抗体を Antibody Diluent (DAKO Agilent Pathology Solutions, USA) を用いて、すべての抗体は濃度 1:250 で希釈し、一晚反応させた(4°C)。ポジティブコントロールとして、抗ウサギ Collagen-type II (Abcam, USA) ポリクローナル抗体を用いて、濃度 1:400 で希釈し、同様に一晚反応させた。二次抗体として、ビオチン標識抗ウサギ IgG ヤギポリクローナル抗体 (Vector Laboratories, USA)を用いて、室温で1時間反応させた後、3,3'-ジアミノベンジジン (DAKO Agilent Pathology Solutions, USA) で発色した。関節軟骨における解析は、20 倍で撮像された関節軟骨の面積における陽性細胞が占める密度を算出した。滑膜の解析は、染色性を5つのカテゴリー (negative (0), weakly positive (1), positive (2); strongly positive (3), high staining intensity (4)) に分類した。

#### 7) リアルタイム PCR 法を用いた関節軟骨における mRNA 発現

術後 2 週、4 週で CAJM 群と ACL-T 群の右後肢脛骨から関節軟骨を採取、さらに ACL-T 群の左後肢脛骨から基準肢として関節軟骨を採取した (n = 5/群, 20 匹 30 肢)。採取した関節軟骨は、RNA later Stabilization Solution (Thermo Fisher Scientific K.K., JPN) で RNA を安定化させ、全てのサンプルを採取後、RNeasy Lipid Tissue Mini Kit (QIAGEN, GER) のプロトコールに従い、フェノールクロロホルム抽出法によって Total RNA を抽出した。具体的には、2ml サンプルチューブに Kit 内付属の TRIzol reagent 1ml と軟骨組織を混合し、Tissue Lyser LT (QIAGEN, GER) を用いて、50Hz で 3 分間ホモジナイズした。その後、クロロホルム (Wako Pure Chemical Industries, Ltd., JPN) 200 $\mu$ l を添加し、15 秒間激しく攪拌させた。実験台上で 5 分間静置し、15 分間遠心した後 (12, 000g, 4°C)、約 600 $\mu$ l の上清を新しい 2ml サンプルチューブに移し、QIAQUBE

(QIAGEN, GER)を用いて、Total RNA 抽出した。抽出された Total RNA は、NanoDrop Lite (Thermo Fisher Scientific K.K., JPN) によって、RNA 濃度を測定した。cDNA の合成は、High Capacity cDNA Reverse Transcription kit (Thermo Fisher Scientific K.K., JPN) に従い、サーマルクライマーPalm-Cycler (Cprbett Research, AUS)を用いた。逆転写反応時間は、25°C10分、37°C120分、85°C5分の反応後、4°Cまで冷却した。リアルタイム PCR は、Taqman プローブ法を用いた。利用機器は Step one Puls (Applied Biosystems, USA) を使用し、Fast Advanced Master Mix (Thermo Fisher Scientific K.K., JPN) のプロトコールに従った。PCR 条件は 95°C20 秒の熱変性後、アニーリング時間 20 秒 60°Cのサイクルを 40 回行った。ターゲット遺伝子は、*TNF- $\alpha$*  (Rn01753871\_m1)、*IL-1 $\beta$*  (Rn00580432\_m1)、そして *Caspase-3* (Rn00563902\_m1)とし、内因性標準遺伝子として glyceraldehyde-3-phosphate dehydrogenase (GAPDH: Rn0177563\_g1) を利用した。得られた Ct 値は、比較 Ct 法によって基準肢を 1 として CAJM 群と ACL-T 群の相対値を算出した。

## 8) 統計解析

統計解析は、SPSS 21.0J for Windows (SPSS Japan Inc, JPN) を用いた。組織学的スコアのデータは、Shapiro-Wilk の検定による正規性の検証を行い、一元配置分散分析法または Kruskal-Wallis 法で群間比較を実施した。後検定は、Tukey 法または Mann-Whitney 検定 (Bonferroni 法による補正) を採用した。データは、平均値 (95%信頼区間) または中央値 (25% タイル値, 75%タイル値) で示した。リアルタイム PCR 法は比較 Ct 法を用いた CTR を 1 とする相対値で表記し、統計解析は ACL-T 群と CAJM 群との間で Mann-Whitney 検定を用いた。全ての有意水準は  $p < 0.05$  と

した。

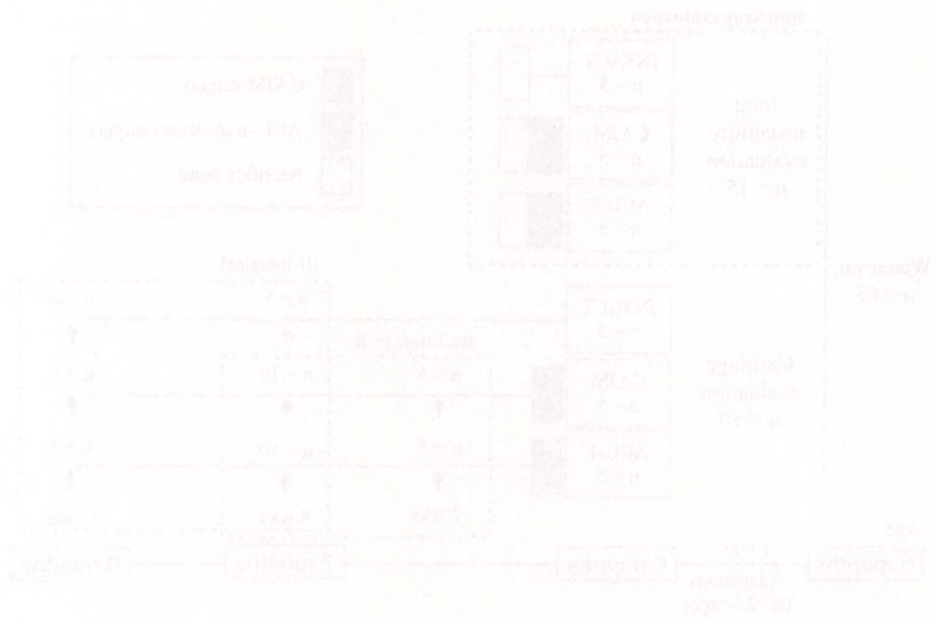


Fig. 2. Experimental protocol. A total of 66 Wistar rats were divided into three experimental groups: an intact group (INT, n=18), a controlled abnormal joint movement group (CAJM, n=22), and an abnormal joint movement group (AJM, n=26).

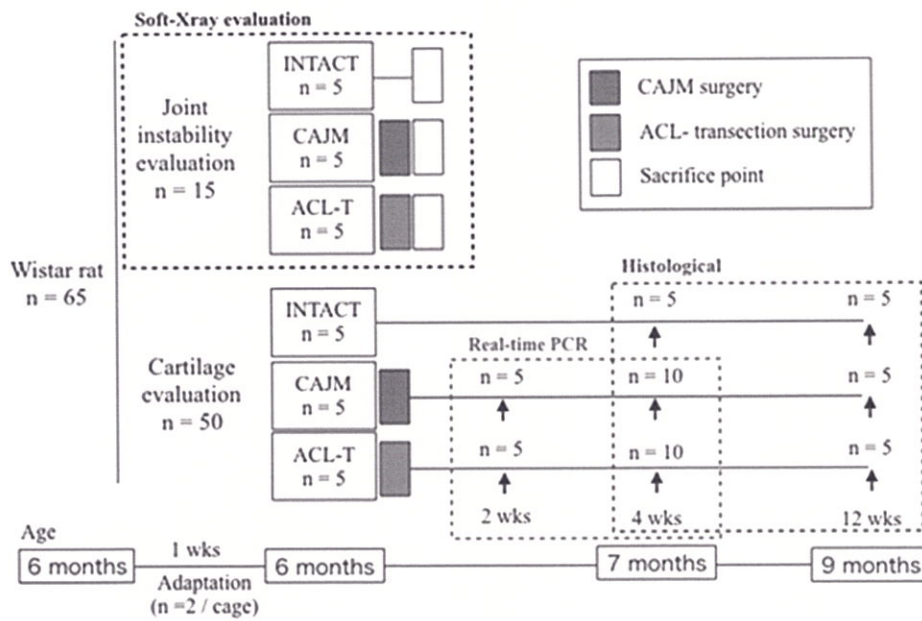


Fig.2. Experimental protocol. A total of 65 Wistar rats were divided into three experimental groups: an intact group (INTACT, n=15), a controlled abnormal joint movement group (CAJM, n=25), and an ACL transection group (ACL-T, n=25).

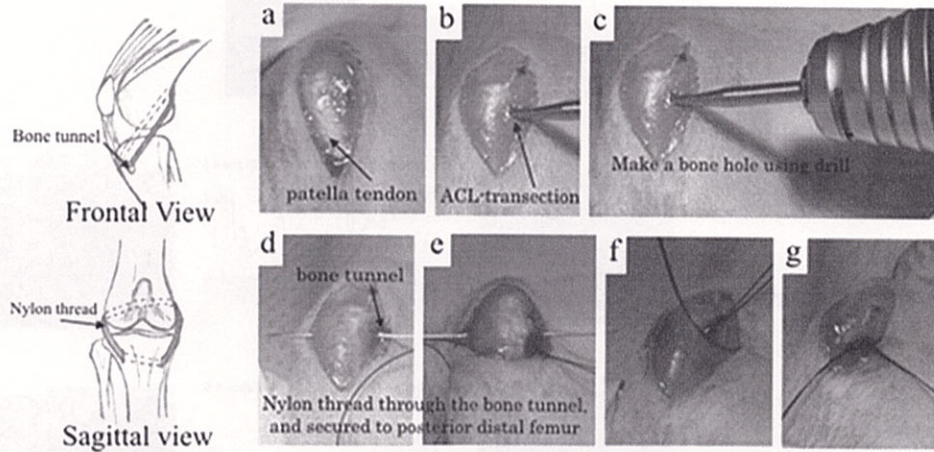


Fig.3. Surgery of CAJM model. Schematic frontal and sagittal views of a controlled abnormal joint movement (CAJM) model showing tibia achieved by creating bone tunnel using rotary drill and nylon thread passed beside the femur condyle. The medial capsule of the right knee joint was exposed without disrupting the patellar tendon (a), and the ACL was completely transected (b). To achieve a damping force in the knee joint after the ACL transection, a bone tunnel to the anterior proximal tibia was created, and a nylon thread was passed through the tunnel (c). The thread was tied and secured to the posterior distal femur (d), thereby damping the anterior drawing force of the femur on the tibia (e). A schematic representation of the surgical procedure is provided in the bottom panel (f-g)

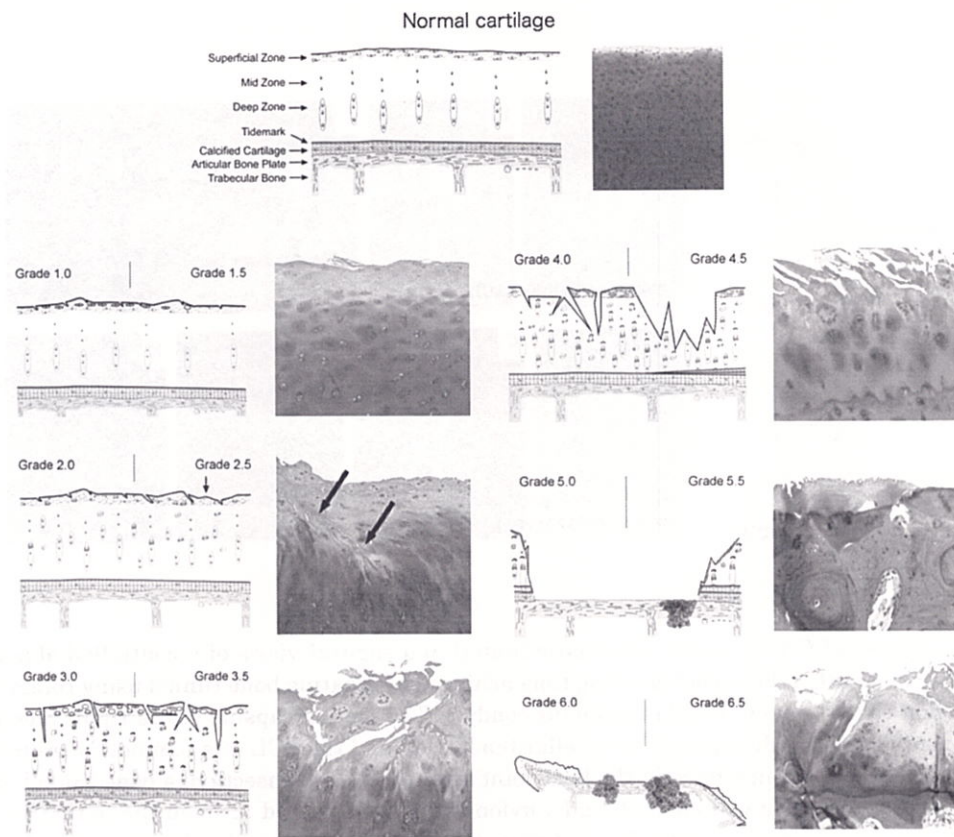
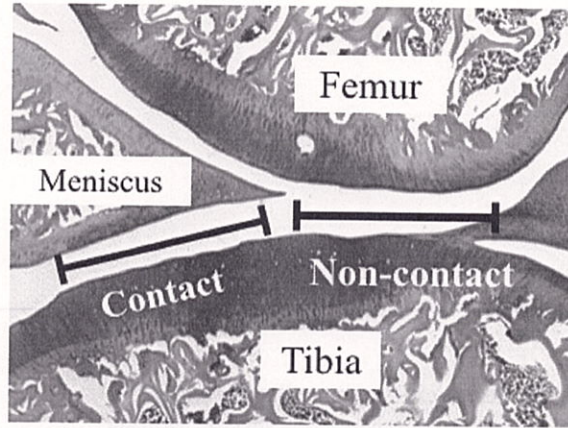
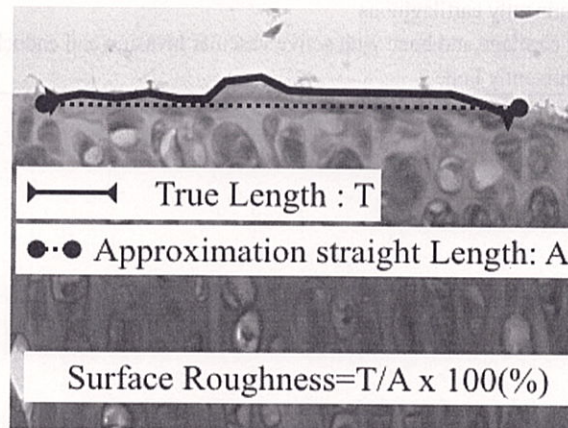


Fig.4. Osteoarthritis Research Society International (OARSI) Score <sup>70)</sup>



*Evaluation of Cartilage thickness*



*Methods for evaluation of surface roughness*

Fig.5. Histological analysis point and method of surface

Table.1. Histological osteophyte formation scoring system <sup>71)</sup>

---

<b>Osteophyte size</b>	
0	none
1	small ~ the same thickness as the adjacent cartilage
2	medium ~ 1-3 × the thickness as the adjacent cartilage
3	large >3 × the thickness as the adjacent cartilage

---

<b>Osteophyte maturity</b>	
0	none
1	predominantly cartilaginous
2	mixed cartilage and bone with active vascular invasion and endochondral ossification
3	predominantly bone

---

Table.2. Synovial membrane inflammation score<sup>69)</sup>

0	No changes (1–2 layers of synovial lining cells)
1	Increased number of lining cell layers ( $\geq 3$ –4 layers) or slight proliferation of subsynovial tissue.
2	Increased number of lining cell layers ( $\geq 3$ –4 layers) and/or proliferation of subsynovial tissue.
3	Increased number of lining cell layers ( $> 4$ layers) and/or proliferation of subsynovial tissue and infiltration of few inflammatory cells
4	Increased number of lining cell layers ( $> 4$ layers) and/or proliferation of subsynovial tissue, infiltration of large number of inflammatory cells.

## 4. 研究結果

### -1 CAJM モデルは前方への関節不安定性を制動する

自作した前方引出し装置と軟 X 線装置を Fig.6A に示した。手術による関節可動域運動への影響について、膝関節最大屈曲ならびに最大伸展の可動域に顕著な差は認めなかった (Fig.6B)。膝関節最大屈曲位、最大伸展位、屈曲 90°での脛骨の前方引出しは、すべての角度で ACL-T 群において顕著に前方引出しが確認され、続いて CAJM 群、INTACT 群の順に前方引き出し量の増加確認された (Fig.6C)。膝関節屈曲 90°での脛骨の前方引出し距離を算出したところ、ACL-T 群、CAJM 群、INTACT 群の順で不安定性が増大し、3 群すべてにおいて有意差を認めた (INTACT, 0.23 [0.16-0.30] mm; CAJM, 1.26 [1.00-1.52] mm; ACL-T, 2.43 [2.32-2.54] mm) (Fig.6D)。

### -2 異常関節運動の制動は軟骨変性を遅延させる

12 週時点では、ACLT 群の関節軟骨厚の減少、表層のフィブリル化、グリコサミノグリカンの染色性が低下し、関節軟骨の変性が著しく重症化した。大腿骨においても、関節軟骨表層のフィブリル化、グリコサミノグリカンの染色性の低下を認め、INTACT 群ならびに CAJM 群よりも変性が重症化していた (Fig.7A, B)。これらの組織学的変性における OARSI スコアは (Fig.7C)、4 週目時点で INTACT 群と比較して、ACL-T 群が有意に変性していた ( $p = 0.013$  with post-hoc Mann-Whitney U 検定 with Bonferroni 補正) (INTACT, 2 [1-2]; CAJM, 2 [2-3]; ACLT, 5 [4-6])。12 週目時点においても、INTACT 群と比較して、ACL-T 群が有意に変性していた ( $p = 0.001$ , with post-hoc Mann-Whitney U 検定 with Bonferroni 補正) (INTACT, 2 [1-4]; CAJM, 3 [1-4]; ACLT, 8 [6-12])。また、12 週目時点では CAJM 群と比

較して、ACL-T 群が有意に変性していた ( $p = 0.021$ , both with post-hoc Mann-Whitney U 検定 with Bonferroni 補正)。

### -3 異常関節運動の制動は関節軟骨(軟骨厚・乱れ・染色性)を維持する

関節軟骨厚は、4 週目時点で有意差は認められなかったが ( $p = 0.363$  with ANOVA)、12 週時点で ACL-T 群は INTACT 群ならびに CAJM 群と比較して、有意に減少していた ([INTACT vs ACL-T]  $p = 0.040$ , [CAJM vs ACL-T]  $p = 0.042$  with post-hoc Tukey test) (INTACT, 125.6 [114.8-136.4]  $\mu\text{m}$ ; CAJM, 126.5 [115.1-137.1]  $\mu\text{m}$ ; ACL-T, 106.6 [91.8-121.3]  $\mu\text{m}$ ) (Fig. 8)。表層ラフネスは、4 週目時点で有意差は認められなかったが ( $p = 0.237$  with ANOVA)、12 週目時点では INTACT 群ならびに CAJM 群と比較して、有意に高値を示した ([INTACT vs ACL-T]  $p = 0.007$ , [CAJM vs ACL-T]  $p = 0.025$  with post-hoc Tukey test) (INTACT, 105.4 [103.4-107.4] %; CAJM, 110.5 [103.6-117.5] %; ACL-T, 136.7 [111.8-161.5] %) (Fig. 8)。染色性について、4 週目時点で既に、CAJM 群および ACL-T 群は INTACT 群と比較して、有意に減少していたが ([INTACT vs ACL-T]  $p < 0.001$ , [CAJM vs ACL-T]  $p < 0.001$  with post-hoc Tukey test) (INTACT, 100.0 [97.6-102.4] %; CAJM, 88.5 [85.1-92.0] %; ACL-T, 85.5 [81.7-89.3] %)、CAJM 群と ACL-T 群に有意者認めなかった ( $p = 0.513$  with post-hoc Tukey methods)。一方、12 週時点では、ACL-T 群にのみ著明な染色性の低下を確認した ([INTACT vs ACL-T]  $p < 0.001$ , [CAJM vs ACL-T]  $p = 0.006$  with post-hoc Tukey test) ( $p < 0.001$ ; INTACT, 100.0 [102.4-97.6] %; CAJM, 94.9 [91.1-98.6] %; ACL-T 83.1 [78.4-87.8] %) (Fig. 8)。

#### -4 異常関節運動の制動が関節軟骨の炎症メディエータを抑制する

TNF- $\alpha$  は、4 週目時点で ACL-T 群、CAJM 群、INTACT 群の順で高い発現を示した ([INTACT vs ACL-T]  $p < 0.001$ , [INTACT vs CAJM]  $p = 0.004$ , [CAJM vs ACL-T]  $p = 0.012$  with post-hoc Tukey test) (INTACT, 4.09 [2.69-5.48] %; CAJM, 9.40 [7.39-11.40] %; ACL-T, 14.83 [11.55-18.11] %)。しかし、12 週時点では、3 群間で差を認めなかった ( $p = 0.267$  with ANOVA) (Fig. 9)。Caspase-3 は、4 週目時点で ACL-T 群、CAJM 群、INTACT 群の順で高い発現を示した ([INTACT vs ACL-T]  $p < 0.001$ , [INTACT vs CAJM]  $p = 0.011$ , [CAJM vs ACL-T]  $p < 0.001$  with post-hoc Tukey test) (INTACT, 6.30 [5.17-7.43] %; CAJM, 9.24 [8.40-10.09] %; ACL-T, 14.39 [12.61-16.17] %)。また、12 週目時点でも ACL-T 群、CAJM 群、INTACT 群の順で高い発現を示した ([INTACT vs ACL-T]  $p < 0.001$ , [INTACT vs CAJM]  $p = 0.027$ , [CAJM vs ACL-T]  $p = 0.036$  with post-hoc Tukey test) (INTACT, 4.81 [3.70-5.91] %; CAJM, 7.89 [6.49-9.28] %; ACL-T, 10.71 [9.25-12.17] %)。

一方、IL-1 $\beta$  は 4 週目 ( $p = 0.123$  with ANOVA) ならびに 12 週目時点 ( $p = 0.078$  with ANOVA) で有意差は確認できなかった。

#### -5 異常関節運動の制動は関節軟骨の炎症メディエータ mRNA を抑制する

関節軟骨における mRNA 発現量 (Table. 3) は、2 週目時点の CAJM 群と ACL-T 群との間では、すべての因子において有意な差を認めなかった (IL-1 $\beta$ :  $p = 0.685$ , TNF- $\alpha$ :  $p = 0.741$ , Caspase-3:  $p = 0.201$ , Mann-Whitney U 検定)。一方、2 週目時点では、TNF- $\alpha$  において CAJM 群と比較して、ACL-T 群で有意に発現量が増加していた (TNF- $\alpha$ :  $p = 0.007$ , Mann-Whitney U 検定)。

#### -6 異常関節運動の制動は滑膜の炎症所見を低減する

12 週時点の滑膜の細胞増殖ならびに肥厚について組織学的に評価した (Fig. 10)。INTACT 群は脂肪層ならび滑膜層が確認できるが、ACL-T 群ならびに CAJM 群では滑膜層の肥厚が確認できた。前方滑膜組織について、ACL-T 群は INTACT 群に比較してスコアが有意に大きかったが、ACL-T 群と CAJM 群では有意な差は認めなかった ([INTACT vs ACL-T]  $p = 0.018$ , with post-hoc Mann-Whitney U 検定 with Bonferroni 補正) (INTACT, 1 [0-1]; CAJM, 1 [1-3]; ACL-T, 2[1-3])。後方滑膜組織について、ACL-T 群は CAJM 群と INTACT 群に比較してスコアが有意に大きかった ([INTACT vs ACL-T]  $p = 0.018$ , [CAJM vs ACL-T]  $p = 0.017$ , with post-hoc Mann-Whitney U 検定 with Bonferroni 補正) (INTACT, 1 [1-1]; CAJM, 2 [2-3]; ACL-T, 4[4-4])。

#### -7 異常関節運動の制動が滑膜組織の炎症メディエータを抑制する

滑膜の組織学的所見を Fig.10、TNF- $\alpha$  ならびに IL-1 $\beta$  の免疫組織学的所見を Fig. 11 に示した。TNF- $\alpha$  の CAJM 群と ACL-T 群は、滑膜辺縁部で濃染を認めたが、ACL-T 群でより顕著だった (Anterior: INTACT, 1[1-2]; CAJM, 1[1-2]; ACL-T, 3[1-3]) (Posterior: INTACT, 1[1-1]; CAJM, 1 [1-1]; ACL-T, 2[1-3])。IL-1 $\beta$  でも同様の傾向を認め、前方ならびに後方滑膜において ACL-T 群で濃染を認めた (Anterior: INTACT, 1[0-2]; CAJM, 2[1-2]; ACL-T, 2[1-3]) (Posterior: INTACT, 1[1-1]; CAJM, 1 [1-2]; ACL-T, 2[2-3])。

#### -8 異常関節運動の制動は骨棘を抑制する

12 週時点の骨棘の大きさならびに成熟度を評価した (Fig. 12)。骨棘の大きさについて、ACL-T 群は CAJM 群と INTACT 群に比較して骨棘が有意に大きかった ([INTACT vs ACL-T]  $p < 0.001$ , [CAJM vs ACL-T]  $p = 0.025$ , with post-

hoc Mann-Whitney U 検定 with Bonferroni 補正) (INTACT, 0[0-0]; CAJM, 1 [0-2]; ACL-T, 3[2-3])。骨棘の成熟度についても、ACL-T 群は CAJM 群と INTACT に比較して成熟度スコアが有意に大きかった

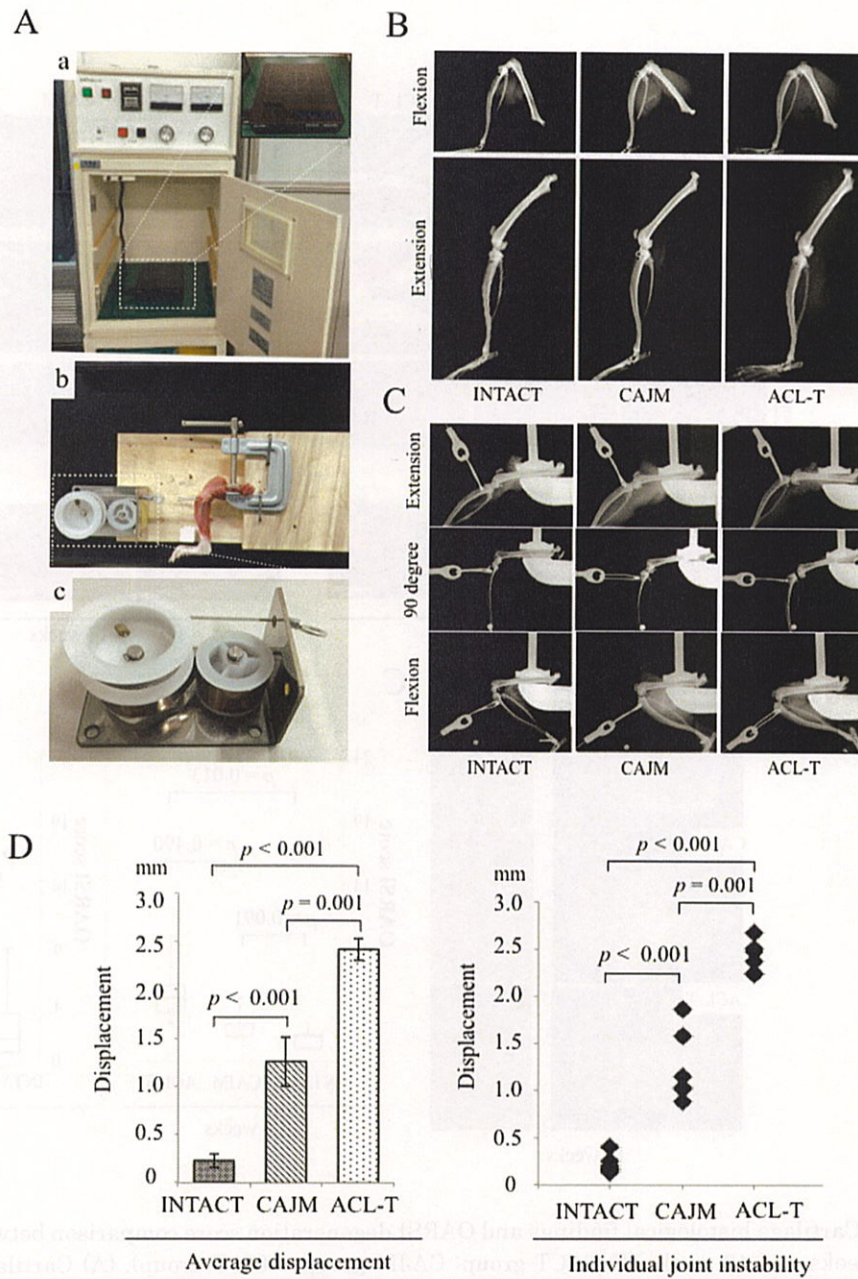


Fig.6. Influence of controlling joint instability by controlled abnormal joint movement (CAJM) surgery. (A) System for examination of joint instability. The femur was set into the examination system, and knee instability was maintained by anterior traction using a 0.2 kgf constant force spring. Soft x-ray radiographs were taken using a soft radiogram M-60. (B) Soft x-ray radiography was performed at 28 kV and 1 mA for 1.5 s. Difference of range of motion among three groups. Flexion and extension range was not limited. However, ACLT group was confirmed little excessive extension angle. The excessive range seems to be the influence of joint instability with ACL injury. (C) Examination systems of joint instability evaluation at flexion and extension angle. CAJM model was braced anterior instability compared to ACL-T group at both angles (flexion and extension angle). (D) Differences in joint instability were compared across the INTACT, CAJM, and anterior cruciate ligament transection (ACL-T) groups. The ACL-T model is shown with the tibia positioned such that the resulting abnormality can be observed. The CAJM model is shown with external bracing of the anterior motion of the tibia, as provided by the nylon thread.

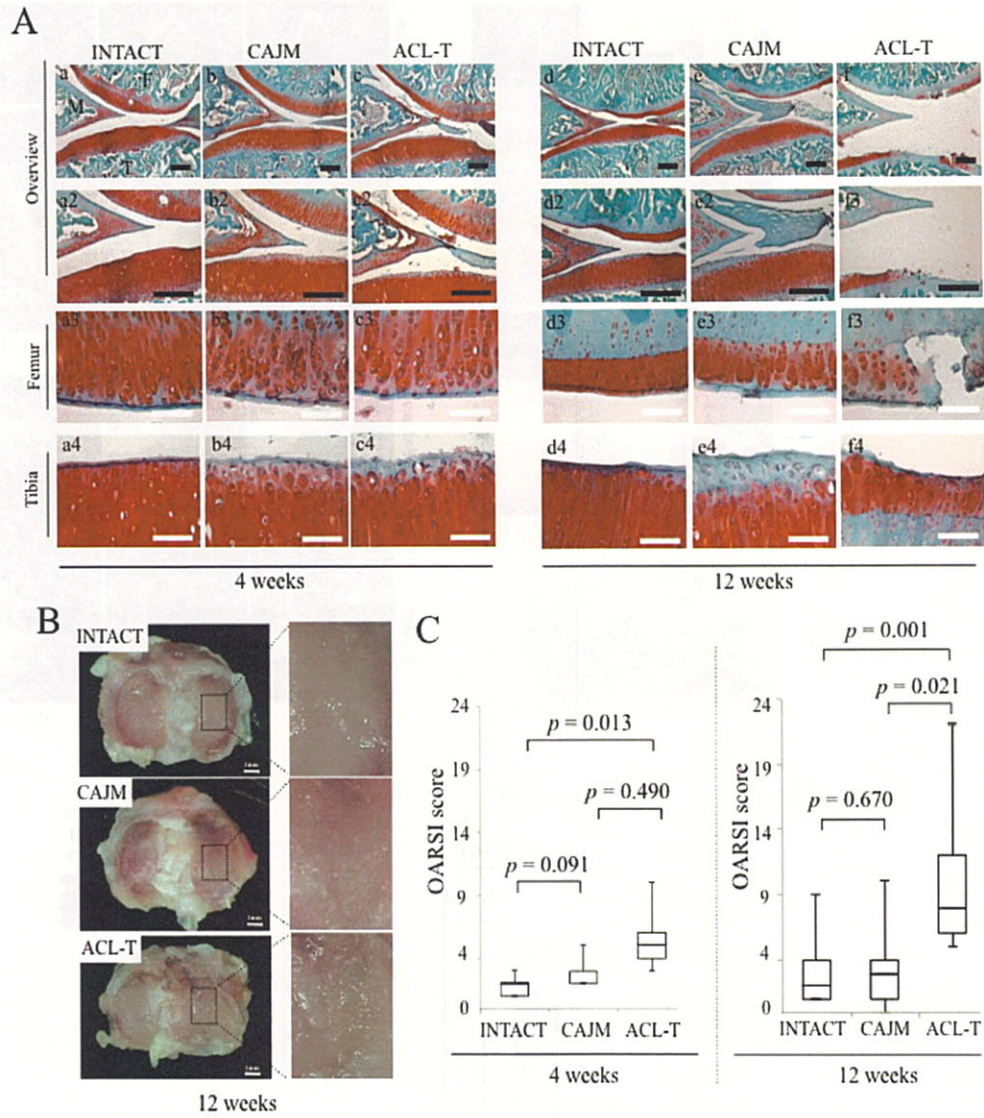


Fig.7. Cartilage histological findings and OARSI degeneration score comparison between groups at 4 weeks and 12 weeks (INTACT group; CAJM group; ACL-T group). (A) Cartilage sections stained with Safranin O and fast green from the INTACT (a and d), CAJM (b and e), and ACL-T (c and f) groups are shown at 5× (overview upper panels), 20× (overview lower panels), and 40× (femoral and tibial panels) magnification. Black scale bar, 100 μm; white scale bar, 50 μm. (B) Gross appearance of the tibial articular surface 12 weeks after surgery in the INTACT, CAJM, and ACL-T groups. The glossiness of the articular surface is preserved in the INTACT group. There is loss of glossiness over the medial portion of the CAJM joint and the tibial plateau of the ACL-T group. Severe osteophyte changes are visible on the surface of the articular cartilage in the ACL-T group. (C) Influence of controlling joint instability indicated by OARSI score. The INTACT group has a significantly lower score compared to the ACL-T group ( $p = 0.013$  with post-hoc Mann-Whitney U test with Bonferroni correction,  $n = 10$  knees) at 4 weeks. At 12 weeks, the ACL-T group had a significantly higher OARSI score compared to the INTACT group and the CAJM group (INTACT,  $p = 0.001$  with post-hoc Mann-Whitney U test with Bonferroni correction; CAJM,  $p = 0.021$  with post-hoc Mann-Whitney U test with Bonferroni correction, both  $n = 10$  knees). Data are presented as median and with interquartile range.

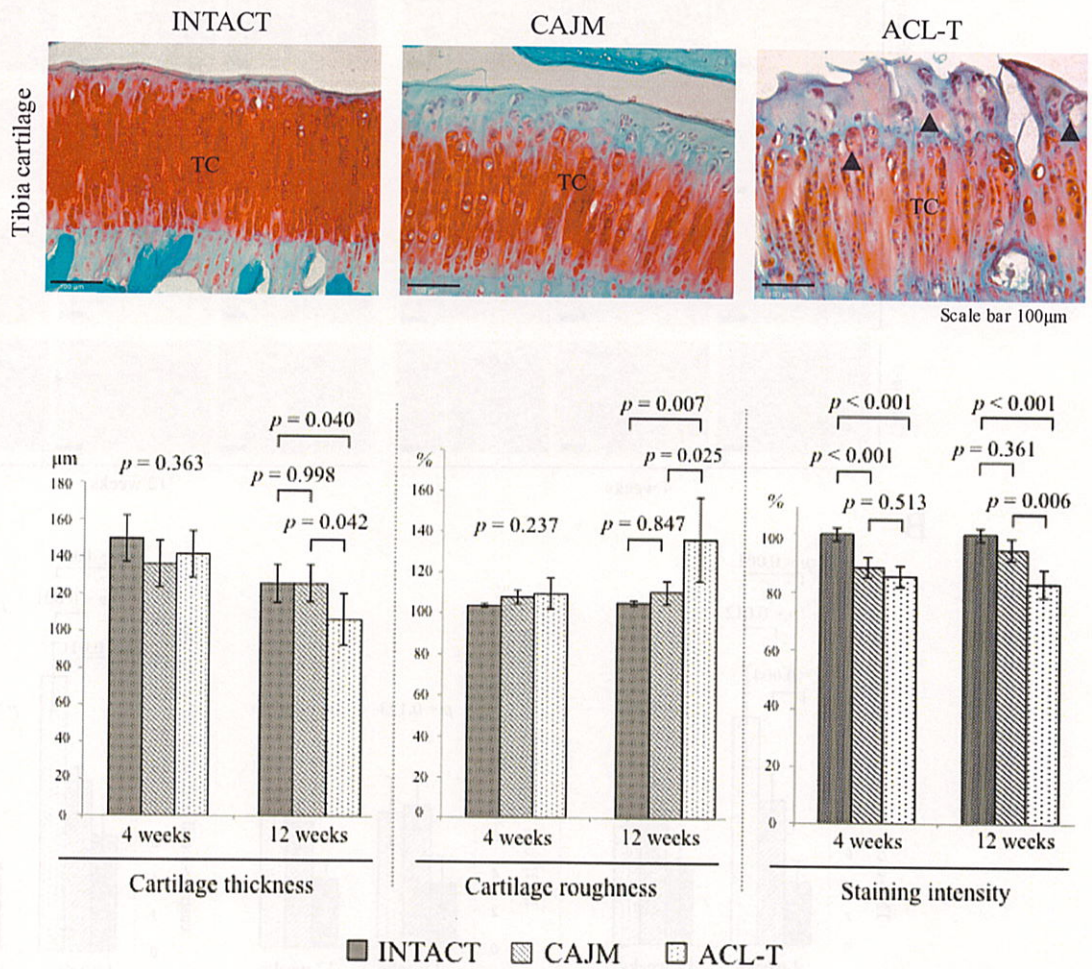


Fig.8. Influence of controlling joint instability for articular cartilage. Cartilage thickness, roughness, and relative staining intensity were compared across the three groups (INTACT group; CAJM group; ACL-T group). Statistical evaluation of inter-group differences in cartilage thickness, roughness, and stainability at 4 weeks and 12 weeks is shown. Cartilage thickness was significantly lower in the ACL-T group compared to the INTACT and CAJM groups (INTACT,  $p = 0.040$  with post-hoc Tukey test; CAJM,  $p = 0.040$  with post-hoc Tukey test; both  $n = 10$  knees) at 12 weeks. Cartilage toughness was also greater in the ACL-T group compared to the INTACT and CAJM groups at 12 weeks (INTACT,  $p = 0.007$  with post-hoc Tukey test; CAJM,  $p = 0.025$  with post-hoc Tukey test; both  $n = 10$  knees). Moreover, relative staining intensity was greater in the INTACT group compared to the CAJM and ACL-T groups at 4 weeks (CAJM,  $p < 0.001$  with post-hoc Tukey test; ACL-T,  $p < 0.001$  with post-hoc Tukey test; both  $n = 10$  knees). Data are presented as mean with 95% confidence interval

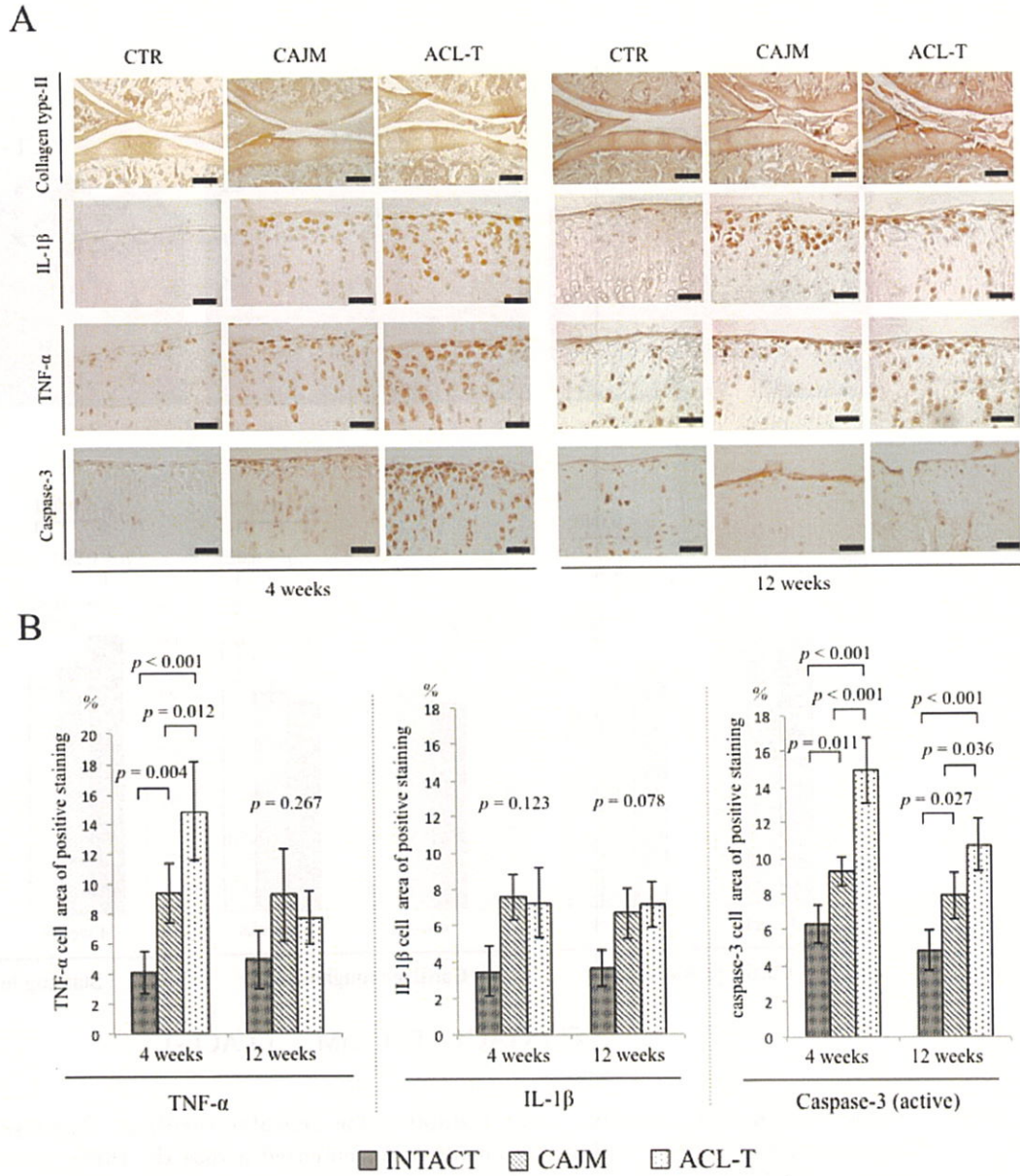


Fig.9. Controlling joint instability inhibits inflammatory factors observed using immunohistochemical analysis at 4 weeks and 12 weeks between groups (INTACT group; CAJM group; ACL-T group). (A) Immunohistochemical staining sections for collagen type II, IL-1 $\beta$ , TNF- $\alpha$ , and active caspase-3 at 4 weeks and 12 weeks. Microscope objective lens, 10 $\times$  (Collagen type II), 40 $\times$  (IL-1 $\beta$ , TNF- $\alpha$ , and caspase-3); scale bar, 100  $\mu$ m or 50  $\mu$ m. (B) The proportion of chondrocyte staining for TNF- $\alpha$ , IL-1 $\beta$ , and caspase-3 was calculated and expressed as a percentage of the total area of chondrocytes within each region. TNF- $\alpha$  significantly differed across the three groups ( $p < 0.001$  with ANOVA test,  $n = 15$  knees) at 4 weeks. Specifically, the INTACT group had a significantly smaller TNF- $\alpha$ -positive staining area compared to the CAJM group and ACL-T group (CAJM,  $p = 0.004$  with post-hoc Tukey test; ACL-T,  $p < 0.001$  with post-hoc Tukey test; both  $n = 10$  knees). The CAJM group had a significantly

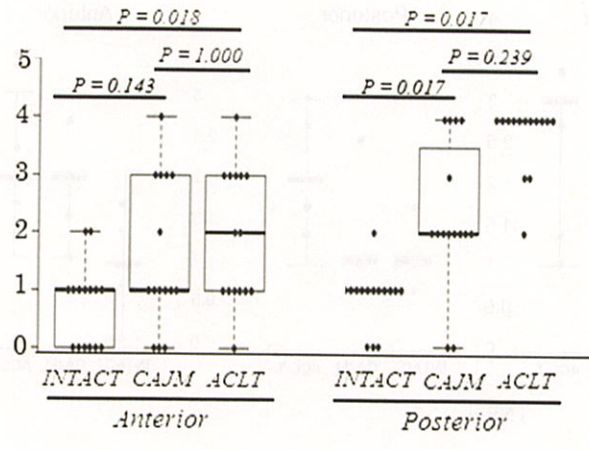
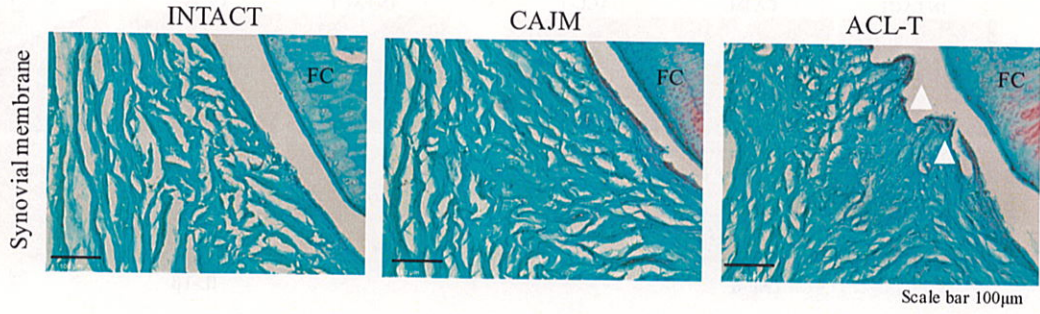


Fig.10. Synovial membrane histological findings and synovial membrane inflammation score comparison between groups at 12 weeks (INTACT group; CAJM group; ACL-T group). Anterior synovial membrane sections stained with Safranin O and fast green at 12 weeks. Below indicated influence of controlling abnormal joint movement indicated by synovial membrane inflammation score. About anterior synovial membrane, the INTACT group has a significantly lower score compared to the ACL-T group ( $p = 0.018$  with post-hoc Mann-Whitney U test with Bonferroni correction,  $n = 5$  knees) at 12 weeks. In posterior area, the CAJM group and ACL-T group had a significantly higher score compared to the INTACT group (CAJM,  $p = 0.017$  with post-hoc Mann-Whitney U test with Bonferroni correction; CAJM,  $p = 0.017$  with post-hoc Mann-Whitney U test with Bonferroni correction, both  $n = 5$  knees). Data are presented as median and with interquartile range.

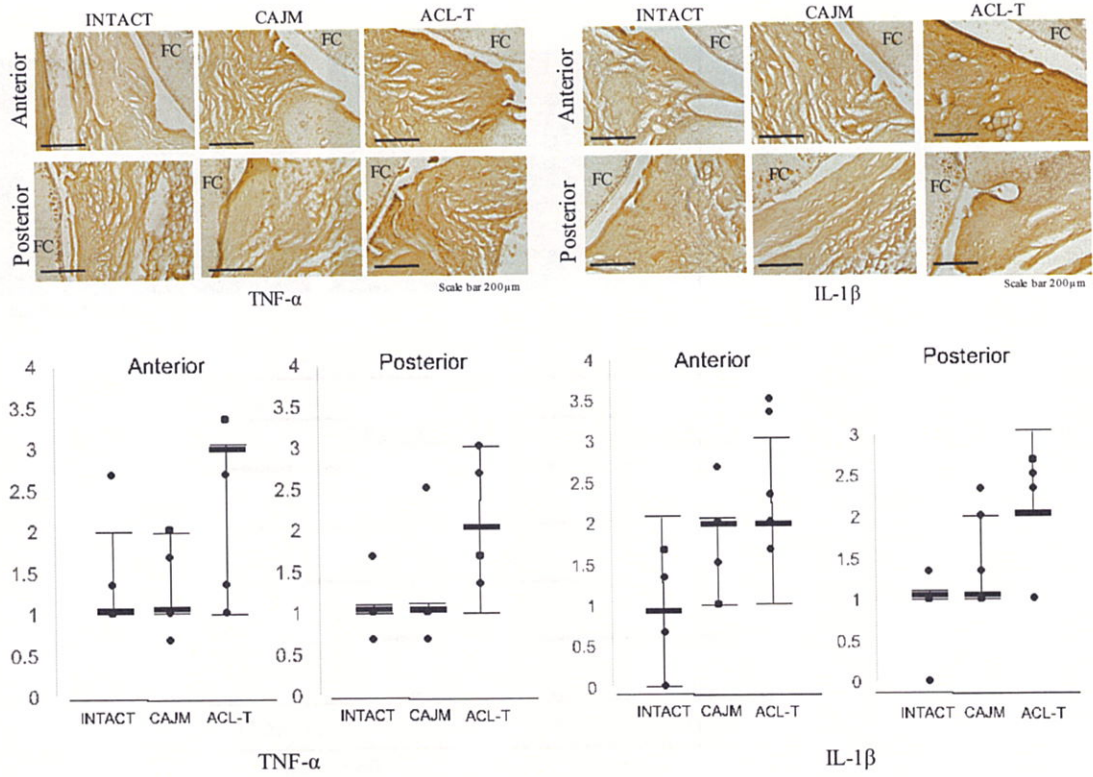


Fig.11. Controlling abnormal joint movement inhibits inflammatory factors observed using immunohistochemical observation at 12 weeks between groups and IHC staining score (INTACT group; CAJM group; ACL-T group). Immunohistochemical staining sections for IL-1 $\beta$  and TNF- $\alpha$ .

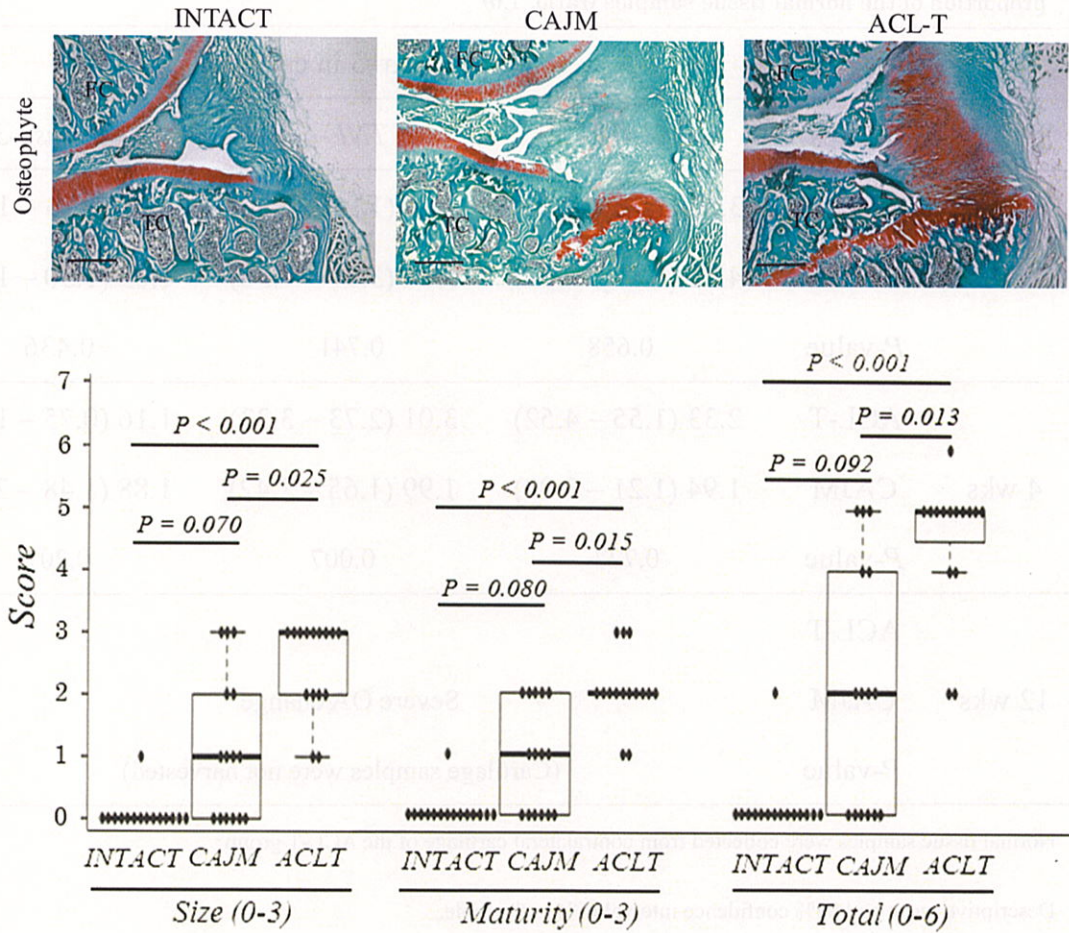


Fig.12. Histological osteophyte formation scoring system (HOFSS) comparison between groups at 12 weeks (INTACT group; CAJM group; ACL-T group). Posterior cartilage sections stained with Safranin O and fast green. Black scale bar, 100  $\mu\text{m}$ ; white scale bar, 50  $\mu\text{m}$ . Below indicated influence of controlling abnormal joint movement indicated by HOFSS. The INTACT and CAJM group has a significantly lower size score compared to the ACL-T group (INTACT,  $p < 0.001$  with post-hoc Mann-Whitney U test with Bonferroni correction; CAJM,  $p = 0.013$  with post-hoc Mann-Whitney U test with Bonferroni correction,  $n = 5$  knees). Data are presented as median and with interquartile range.

Table.3. Controlling joint instability inhibits mRNA expression of inflammatory factors as a proportion of the normal tissue samples (ratio, 1.0)

Cartilage (n=5 in each group)				
	Groups	<i>IL-1<math>\beta</math></i>	<i>TNF-<math>\alpha</math></i>	<i>Caspase-3</i>
2 wks	ACL-T	3.81 (1.78 – 8.20)	3.59 (1.98 – 6.50)	1.57 (1.43 – 1.88)
	CAJM	4.22 (3.87 – 4.61)	5.84 (3.57 – 9.56)	1.63 (1.30 – 1.91)
	<i>P</i> -value	0.658	0.741	0.436
4 wks	ACL-T	2.33 (1.55 – 4.52)	3.01 (2.73 – 3.33)	1.16 (0.75 – 1.78)
	CAJM	1.94 (1.21 – 3.99)	1.99 (1.65 – 2.42)	1.88 (1.48 – 2.40)
	<i>P</i> -value	0.727	0.007	0.201
12 wks	ACL-T			
	CAJM		Severe OA change	
	<i>P</i> -value		(Cartilage samples were not harvested)	

Normal tissue samples were collected from contralateral cartilage of the ACL-T group

Descriptive mean and 95% confidence interval (CI) in the table.

*P*-values for paired comparison: CAJM vs ACL-T (Mann-Whitney U test).

## 5. 考察

本研究では、動物モデルを用いて前十字靭帯断裂によって生じた関節不安定性とその制動効果について、関節軟骨を対象に組織学的解析、免疫組織学的解析、生化学的解析を行った。組織学解析では、関節不安定性を制動することで、脛骨後方の骨棘形成を抑制し、滑膜細胞の増殖抑制や滑膜線維層の肥厚が軽減、結果として関節軟骨変性の進行を遅延させた。また、関節軟骨変性メディエータである TNF- $\alpha$  やアポトーシス誘導因子の一つである Caspase-3 は、関節不安定性を制動することで発現量が減少した。これらの結果は、関節不安定性に伴う脛骨と大腿骨の関節運動の変化が関節軟骨変性の進行に関与する一要因あることを明らかにしたと同時に、関節不安定性の抑制が軟骨の変性を遅延させる予防法となり得ることを示している。

ヒトの関節運動は、骨の自動的ならびに他動的運動に伴って起こる構成運動と関節包内で生じる副運動で構成される。これらは、関節を構成する骨形態、関節周囲に付着する筋組織や靭帯などの軟部組織によって変化し、関節自体がその機能を最大限発揮するために周囲組織を含めた機能的な適合性が保たれている。しかしながら、関節を安定化させる靭帯の損傷や筋力低下によって関節自体の不安定性が引き起こされた場合、正常から逸脱した関節運動が惹起され、発揮できる関節機能の低下や関節自体へ力学的ストレスが増加することが明らかにされている<sup>73),74),75)</sup>。特に、膝関節を構成する脛骨と大腿骨の関節面は、骨構造的に不安定であるため、その安定性を靭帯や半月板に依存していることは関節運動学と OA 発症との関連性を検証する上で非常に重要な視点である<sup>76)</sup>。具体的には、前十字靭帯や後十字靭帯は脛骨の前後方向、内側側副靭帯や外側側副靭帯は脛骨の側方方向への安定性、半月板は大腿骨顆部の彎曲と脛骨関節面に対する安定性ならびにショックアブソ

ーバーとして機能し、各々の組織は矢状面や前額面のみならず水平面の回旋方向における静的ならびに動的安定性にも寄与している。このため、靭帯が損傷した場合、正常である関節運動が困難となるケースが存在し、代表的な例として、前十字靭帯損傷後に生じる脛骨の過度な前方引出しは関節接触面が狭小化することが報告されている<sup>77)</sup>。また、高齢者に多い膝関節の屈曲位では、大腿骨顆部の曲率半径が小さくなることから大腿骨顆部と脛骨関節面の接触面積が減少し、機能的な適合性の低下から荷重時の機械的ストレスが増大する<sup>78),79)</sup>。特に、高齢者の OA 患者に観察される外側スラストは、屈曲拘縮に伴う機能的な適合性の低下から関節の不安定性が惹起され、荷重時に膝関節が外側へ振れる現象として OA 進行の重症度の関連することが報告されている<sup>80)</sup>。OA 患者は膝関節の不安定性を自覚的に訴えることが報告されているが<sup>62),63),64),65)</sup>、外側スラストのような異常な関節運動に伴う脛骨や大腿骨の相対的な回旋については、三次元動作解析を用いても解析することは難しい。すなわち、外側スラストのような膝関節の不安定性に伴って生じる異常な関節運動は関節軟骨を進行させる機械的ストレスの一要因であることは経験的に理解されているが、その直接的な作用については明らかにされていない。動物モデルでは、膝関節前十字靭帯を損傷させることで、矢状方向の不安定性が惹起される ACL-T モデル<sup>81)</sup>において軟骨変性が進行することは一般的であるものの、従来 ACL-T モデルでは靭帯損傷による関節内への影響が変性へ関与する一次的要因か、靭帯損傷後に生じた関節不安定性に伴う異常関節運動による二次的な機械的ストレスによる軟骨変性の進行であるかは明確ではなかった。この異常関節運動に着目した近年の報告として、Kokubun らは異常関節運動を制動する新たなモデルを提唱した<sup>66)</sup>。このモデルは、前十字靭帯損傷後に生じた前方引出しを関節包外で制動するモデルであり、本モデルによって前十字靭帯が治癒したことから、異常関節運

動の有無が関節内のメカノバイオロジーに何らかの変化を及ぼす可能性を報告した。このモデルは、先述した問題点に対して、OA の発症や進行における関節不安定性という機械的ストレスについて、明確にする一つの解決策となり得ると考えられた。

関節軟骨の変性は、生理的限界を超過した強い衝撃に伴う関節軟骨の変性か、破壊まで至らないまでも継続した機械的ストレスの蓄積によって関節軟骨の変性が進行する。前十字靭帯損傷後に大腿骨に対して脛骨の過度な前方引出しが生じることで脛骨と大腿骨との間に生じる圧縮ストレスならびに剪断ストレスを増大させると報告されていることから<sup>82)</sup>、本研究における CAJM モデルはこの前方向の異常関節運動を制動することで軟骨組織に対する圧縮ストレスならびに剪断ストレスを軽減させ、表層 Roughness や染色性の低下、表層の菲薄化といった関節軟骨への変性を遅延させる結果に至った可能性が示唆された。このことは、機械的ストレスのなかでも脛骨と大腿骨との間で生じる異常関節運動が軟骨変性メカニズムの一端に関与し、異常関節運動を制動することで関節軟骨を予防できる可能性が本研究で示された。関節軟骨変性に関する進行の目安として、X 線を用いた検査による骨棘は一般的に用いられる分類方法である。1950 年代頃に提唱された Kellgren-Lawrence 分類<sup>83)</sup>は、現在の診療でも用いられ、骨棘の増加は軟骨変性の重症度と関連する（疼痛が軟骨の重症度と比例するかは明確でない）。骨棘は、関節軟骨辺縁部に形成されることが多く、骨棘形成シグナルには滑膜組織が大きく関与することが報告されている。この過程において、膝関節への機械的ストレスによって滑膜や滑液に発現した炎症性サイトカインは、関節の軟骨細胞を異常分化および肥大化させ、軟骨構成組織の II 型コラーゲンではなく、X 型コラーゲンを分泌が進んでいく<sup>84)</sup>。X 型コラーゲンは、BMP とともに内軟骨性骨化過程において軟骨石灰化に重要な役割を果たし、硬骨化されてい

く。しかしながら、骨への置換へは血管栄養が必須であることから、滑膜から栄養が供給される必要があり、血管流入する関節軟骨辺縁部では骨棘が形成される。一方、関節軟骨の中央部は無血行分野であり、その栄養を滑液や滑膜に依存している。このため、関節軟骨の部位は肥大軟骨細胞から細胞死が進行していくが<sup>85),86)</sup>、その過程によって形成された骨棘は力学的に虚弱であり、機械的ストレスによって破壊された微細組織は貧食作用による関節内炎症の長期化につながる。また、ヒトは何らかの身体的異常を感知した場合、それらによる影響を最小限に留める生体反応が機能するが、関節不安定性に伴う異常な関節運動を感知した場合、骨増殖体による膝関節の再安定化を得ようとすることが報告されている<sup>87),88),89)</sup>。すなわち、関節不安定性に伴う異常関節運動は生体内ではネガティブな機械的ストレスと探知され、骨棘を形成することで再安定化を得ようとする生体反応が生じていることと推測できる。この一連の反応は、異常な関節力学に起因する増加した接触応力は骨の成長を促進するというウルフの法則<sup>90)</sup>とよばれ、本研究結果では、滑膜組織の TNF- $\alpha$  や IL-1 $\beta$  の陽性反応が異常関節運動によって強かったこと、滑膜組織の細胞増殖や肥厚が観察できること、さらに Caspase-3 の発現によりアポトーシスへの影響を確認できることを示した。この結果は、異常な関節運動に伴う大腿骨と脛骨との部分的な軟骨接触圧の増加していたことを間接的に示唆しているものと考えられる。一方、関節制動を施した CAJM モデルにおいても、関節軟骨の変性が部分的に進行していることを確認した。先述したように、ACL の損傷に伴う関節内炎症によって誘発された炎症性サイトカインが滑膜や滑液を介して軟骨組織へ働きかけることでプロテオグリカンやコラーゲンの分解作用を有するタンパク質分解酵素 やアグリカナナーゼの分泌に関与した可能性がある。本研究でも INTACT モデルに比較して ACL-T モデルのみならず CAJM モデルにおいても TNF- $\alpha$  や IL-1 $\beta$  の発現が確

認められたことから、これらがメディエータとして軟骨細胞へ MMP-13 や ADAMTS-4、ADAMTS-5 といった軟骨構成組織を分解する因子の発現に寄与している可能性が示唆された。特に、免疫組織化学染色では軟骨表層のみならず軟骨中間層や深層でのサイトカインの発現が確認されており、ACL-T モデルと CAJM モデルとの機械的ストレスの違いとなる表層のせん断力だけでは説明がつかないことから、サイトカイン、タンパク質分解酵素、成長因子を介した複雑な細胞内伝達機構が関与していた可能性を示唆している<sup>91)</sup> (Fig.1)。現在、OA の治療や予防は社会的ニーズの一つでもあることは周知の事実であるが、軟骨変性に起因する OA の発症には、機械的ストレスに伴って生じる軟骨細胞のネクロシスや滑膜・滑液から産生される様々な因子が関与している。しかし、その作用は独立せず相互的に機能し、関節軟骨の分解と合成の不均衡は軟骨組織の変性を導くことからその全ては解明されていない。その背景には、機械的ストレスが存在することは過去の研究から明らかになっているが、本研究の重要な視点は機械的ストレスなかでも異常関節運動に着目したことである。その結果、異常関節運動の制動は関節軟骨の変性を遅延させる結果を得たことから、機械的ストレスの具体性を示した研究であるといえる。

## 6. 研究の限界と今後の展望

本研究の結果の解釈には、いくつかの考慮すべき点がある。一つ目は、異常関節運動に関して、運動学的解析ならびに運動力学的解析は実施できていない。このことは異常関節運動の制動した効果を数値として客観的に示すことが困難であることを示唆している。しかしながら、前述のごとく、限度を超えた生理的な強い衝撃だけではなく、関節軟骨の破壊まで至らないケースにおいても、慢性的な機械的ストレスが蓄積された場合、関節軟骨は徐々に変性し、分解が進んでいくことが報告されている。すなわち、本研究は三次元動作解析装置を用いた解析には至ってはいないが、運動学的な変化が少なくとも関節包内運動のレベルでは異常な関節運動が惹起されている可能性がある。今後、異常な関節運動を三次元動作解析装置や床反力計等を用い、運動学的ならびに運動力学的に影響を及ぼしているか更なる解析が必要である。

二つ目は、CAJM モデルでは骨孔を開口している点について解釈に注意が必要となる。CAJM モデルでは、前方引出を制動するために骨孔にナイロン糸を通過させる方法を採用していることから、骨孔の影響を否定することはできなかったが、本研究では骨孔の影響を考慮しなかった。しかしながら、軟骨下骨を解析対象とする場合は、ACL を切断した後に骨孔のあるモデルを Sham モデルとして準備する必要があった。後の検証（参考論文 2: Murata et al. Cartilage 2017）では、脛骨を開孔させた Sham モデルを用いたが、関節軟骨の変性について同様の結果を得ている。

最後に、OA 進行に関わる因子について炎症性サイトカインのみの分析に留まり、その下流における MMP や ADAMTS といった軟骨構成組織の破壊に関与する因子の検討までは至っていない点である。このことは、異常関節運動が軟骨変性に関与し、その抑制が軟骨変性を予防するという結論に至る

には不十分であり、軟骨変性過程における更なる解析が必要である。しかしながら、本研究におけるこれらの研究限界を考慮しても、関節軟骨が関節運動という力学的情報を探知していることは明白であるといえる。しかし、関節軟骨が力学的情報をどのように探知し、細胞内への情報伝達を司るのか、そのメカノバイオリジカル機構について未だ不明な点が多く、明らかにされていない。

今後、関節運動の違いによって変化する要因を生化学的に探索し、その作用を検証することで、関節環境の重要性を語るエビデンスとして構築していく必要がある。これまでの多くの研究が OA の病態解明や OA に対する薬理効果の検証に着目している中、今回の研究により得られた知見のように OA の発症メカニズムに異常関節運動のような具体的な機械的ストレスの関与を示すことは、ヒトの治療方針や予防方法としての提案が可能となり、健康寿命の延伸やリハビリテーション分野における科学的根拠の確立が期待できる。

## 7. 結語

異常関節運動を制動することは関節軟骨の変性を遅延させたことから、関節不安定性の制御は OA の発症と進行に重要な役割を果たす。

## 8. 謝辞

本博士論文の主査、副査として、ご指導ならびにご鞭撻いただきました 埼玉県立大学 保健医療福祉学部 共通教育科 原元彦教授、埼玉県立大学 保健医療福祉学部 看護科 鈴木幸子教授、北海道大学大学院 保健科学研究院機能回復学分野 前島洋教授 に心より感謝申し上げます。

本研究を進めるにあたり、実験に関する基礎的な知識や解析手法をご教授頂きました 埼玉県立大学 保健医療福祉学部 共通教育科 田中健一准教授、埼玉県立大学 保健医療福祉学部 共通教育科 林弘之准教授 に、深謝申し上げます。

研究方針ならびに研究環境の整備にあたり、埼玉県立大学 保健医療福祉学部 理学療法学科 高柳清美教授には、多くの御協力を頂きました。本研究の議論や検討にあたり、埼玉県立大学 保健医療福祉学部 理学療法学科 国分貴徳助教には、実験結果の解釈ならびに国際雑誌投稿の際に熱心にご指導いただきました。ここに深く感謝いたしますとともに、御礼申し上げます。また、本研究にご協力頂きました東京女子医科大学八千代医療センター 鬼塚勝哉先生、春日部厚生病院 清水大介先生、大学院生である藤野努氏、森下佑里氏、藤原秀平氏、中島彩氏には、共同研究者として研究にご協力頂きまして、感謝いたします。

最後に、本研究の過程において、終始懇切なるご指導ならびにご鞭撻を賜りました 埼玉県立大学大学院 保健医療福祉学研究科 金村尚彦教授 に心より感謝申し上げます。

## 9. 引用文献

- 1) Muraki S, Oka H, Akune T, Mabuchi A, En-yo Y, Yoshida M, Saika A, Suzuki T, Yoshida H, Ishibashi H, Yamamoto S, Nakamura K, Kawaguchi H, Yoshimura N. Prevalence of radiographic knee osteoarthritis and its association with knee pain in the elderly of Japanese population-based cohorts: the ROAD study. *Osteoarthritis and Cartilage* 2009; 17:1137-43.
- 2) Felson DT. Osteoarthritis as a disease of mechanics. *Osteoarthritis and Cartilage* 2013; 21:10-15.
- 3) Kyriacos AA, Eric MD, Grayson DD, Jerry CH, A. Hari R. *Articular Cartilage*. CRC Press 2013.
- 4) Sophia FAJ, Bedi A, Rodeo SA. The basic science of articular cartilage: structure, composition, and function. *Sports health* 2009; 1(6): 461-468.
- 5) Buckwalter JA, Anderson DD, Brown TD, Tochigi Y, Martin JA. The Roles of Mechanical Stresses in the Pathogenesis of Osteoarthritis: Implications for Treatment of Joint Injuries. *Cartilage* 2013; 4(4):286-294.
- 6) Gabay O, Hall DJ, Berenbaum F, Henrotin Y, Sanchez C. Osteoarthritis and obesity: experimental models. *Joint Bone Spine* 2008; 75:675-9.
- 7) Tchetina EV. Developmental mechanisms in articular cartilage degradation in osteoarthritis. *Arthritis* 2011; 683970.
- 8) Rojas-Ortega M, Cruz R, Vega-López MA, Cabrera-González M, Hernández-Hernández JM, Lavalle-Montalvo C, Kouri JB. Exercise modulates the expression of IL-1 $\beta$  and IL-10 in the articular cartilage of normal and osteoarthritis-induced rats. *Pathology-Research and Practice* 2015; 211(6): 435-443.

- 9) Woodell-May J, Matuska A, Oyster M, Welch Z, O'shaughnessey K, Hoepfner J. Autologous protein solution inhibits MMP-13 production by IL-1 $\beta$  and TNF- $\alpha$  stimulated human articular chondrocytes. *Journal of Orthopaedic Research* 2011; 29(9): 1320-1326.
- 10) Stannus O, Jones G, Cicuttini F, Parameswaran V, Quinn S, Burgess J, Ding C. Circulating levels of IL-6 and TNF- $\alpha$  are associated with knee radiographic osteoarthritis and knee cartilage loss in older adults. *Osteoarthritis and Cartilage* 2010; 18(11):1441-1447
- 11) Franciozi CE, Tarini VA, Reginato RD, Gonçalves PR, Medeiros VP, Ferretti M, Dreyfuss JL, Nader HB, Faloppa F. Gradual strenuous running regimen predisposes to osteoarthritis due to cartilage cell death and altered levels of glycosaminoglycans. *Osteoarthritis and Cartilage* 2013; 21(7):965-972.
- 12) Little CB, Barai A, Burkhardt D, Smith SM, Fosang AJ, Werb Z, Shah M, Thompson EW. Matrix metalloproteinase 13 deficient mice are resistant to osteoarthritic cartilage erosion but not chondrocyte hypertrophy or osteophyte development. *Arthritis & Rheumatism* 2009; 60(12): 3723-3733.
- 13) Sandell LJ, Aigner T. Articular cartilage and changes in arthritis: cell biology of osteoarthritis. *Arthritis Research Therapy* 2001; 3(2):107.
- 14) Van der Kraan PM, Van den Berg WB. Chondrocyte hypertrophy and osteoarthritis: role in initiation and progression of cartilage degeneration? *Osteoarthritis and Cartilage* 2012; 20(3):223-232.
- 15) Hamamura K, Zhang P, Zhao L, Shim JW, Chen A, Dodge TR, Wan Q, Shih H, Na S, Lin CC, Sun HB, Yokota H. Knee loading reduces MMP13 activity in the mouse cartilage. *BMC musculoskeletal disorders*

2013;14(1):312.

16) Robertson CM, Pennock AT, Harwood FL, Pomerleau AC, Allen RT, Amiel D. Characterization of pro-apoptotic and matrix-degradative gene expression following induction of osteoarthritis in mature and aged rabbits.

*Osteoarthritis and cartilage* 2006; 14(5):471-476.

17) 福井尚志. 早期 OA における滑膜病変. *JOINT BONE NERVE* 2016; 6(3):511-518.

18) Nelson F, Billingham RC, Pidoux I, Reiner A, Langworthy M, McDermott M, Malogne T, Sitler DF, Kilambi NR, Lenczner E, Poole AR. Early post-traumatic osteoarthritis-like changes in human articular cartilage following rupture of the anterior cruciate ligament. *Osteoarthritis and Cartilage* 2006; 14:114-119.

19) Harkey MS, Luc BA, Golightly YM, Thomas AC, Driban JB, Hackney AC, Pietrosimone B. Osteoarthritis-related biomarkers following anterior cruciate ligament injury and reconstruction: a systematic review. *Osteoarthritis and Cartilage* 2015; 23(1):1-12.

20) Pelletier JP, Martel-Pelletier J, Abramson SB. Osteoarthritis, an inflammatory disease: potential implication for the selection of new therapeutic targets. *Arthritis & Rheumatism* 2001; 44(6):1237-1247.

21) Scanzello CR, Goldring SR. The role of synovitis in osteoarthritis pathogenesis. *Bone* 2012; 51(2):249-257.

22) Partsch G, Steiner G, Leeb BF, Dunky A, Bröll H, Smolen JS. Highly increased levels of tumor necrosis factor-alpha and other proinflammatory cytokines in psoriatic arthritis synovial fluid. *The Journal of Rheumatology* 1997; 24(3):518-23.

- 23) Smith MD, Triantafillou S, Parker A, Youssef PP, Coleman M. Synovial membrane inflammation and cytokine production in patients with early osteoarthritis. *The Journal of Rheumatology* 1997; 24(2):365-71.
- 24 ) Vignon E, Balblanc JC, Mathieu P, Louisot P, Richard M. Metalloprotease activity, phospholipase A2 activity and cytokine concentration in osteoarthritis synovial fluids. *Osteoarthritis and Cartilage* 1993; 1(2):115-20.
- 25) Egloff C, Hart DA, Hewitt C, Vavken P, Valderrabano V, Herzog W. Joint instability leads to long-term alterations to knee synovium and osteoarthritis in a rabbit model. *Osteoarthritis and Cartilage* 2016; 24:1054-60.
- 26) Furman BD, Mangiapani DS, Zeitler E, Bailey KN, Horne PH, Huebner JL, Kraus VB, Guilak F, Olson SA. Targeting pro-inflammatory cytokines following joint injury: acute intra-articular inhibition of interleukin-1 following knee injury prevents post-traumatic arthritis. *Arthritis research therapy* 2014; 16(3):R134.
- 27) Haslauer CM, Elsaid KA, Fleming BC, Proffen BL, Johnson VM, Murray MM. Loss of extracellular matrix from articular cartilage is mediated by the synovium and ligament after anterior cruciate ligament injury. *Osteoarthritis and Cartilage* 2013; 21(12):1950-1957.
- 28) Hashimoto S, Creighton-Achermann L, Takahashi K, Amiel D, Cooutts RD, Lotz M. Development and regulation of osteophyte formation during experimental osteoarthritis. *Osteoarthritis and Cartilage* 2002;10: 180-187.
- 29) Pickarski M, Hayami T, Zhuo Y, Duong LT. Molecular changes in articular cartilage and subchondral bone in the rat anterior cruciate

ligament transection and meniscectomized models of osteoarthritis. *BMC musculoskeletal disorders* 2011; 12(1):197.

30) Saetan N, Honsawek S, Tanavalee A, Yuktanandana P, Meknavin S, Ngarmukos S, Tanpowpong T, Parkpian V. Relationship of plasma and synovial fluid vascular endothelial growth factor with radiographic severity in primary knee osteoarthritis. *International orthopaedics* 2014; 38(5):1099-1104.

31) Jian-Lin Z, Hong-Song F, Hao P, Shuang D, Shen C, Jian-Ping L, Qiu B, Weng J, Feng L. The relationship between HIF-2 $\alpha$  and VEGF with radiographic severity in the primary osteoarthritic knee. *Yonsei medical journal* 2016; 57(3):735-740.

32) Liu Y, Hou R, Yin R, Yin W. Correlation of bone morphogenetic protein-2 levels in serum and synovial fluid with disease severity of knee osteoarthritis. *Medical Science Monitor* 2015; 21: 363–370.

33) Davidson EB, Vitters EL, Van Der Kraan PM, van den Berg WB. Expression of transforming growth factor- $\beta$  (TGF- $\beta$ ) and the TGF- $\beta$  signaling molecule SMAD-2P in spontaneous and instability-induced osteoarthritis: role in cartilage degradation, chondrogenesis and osteophyte formation. *Annals of the Rheumatic Diseases* 2006;65: 1414-1421.

34) Chen R, Mian M, Fu M, Zhao JY, Yang L, Li Y, Xu L. Attenuation of the progression of articular cartilage degeneration by inhibition of TGF- $\beta$ 1 signaling in a mouse model of osteoarthritis. *American Journal of Pathology* 2015; 185(11): 2875-2885.

35) Gerber HP, Vu TH, Ryan AM, Kowalski J, Werb Z, Ferrara N. VEGF

- couples hypertrophic cartilage remodeling, ossification and angiogenesis during endochondral bone formation. *Nature medicine* 1999; 5(6):623-628.
- 36) van der Kraan PM, van den Berg WB. Osteophytes: relevance and biology. *Osteoarthritis and Cartilage* 2007; 15:237-244.
- 37) Iijima H, Aoyama T, Ito A, Tajino J, Yamaguchi S, Nagai M, Kiyon W, Zhang X, Kuroki H. Exercise intervention increases expression of bone morphogenetic proteins and prevents the progression of cartilage-subchondral bone lesions in a post-traumatic rat knee model. *Osteoarthritis and Cartilage* 2016; 24(6):1092-1102.
- 38) Iijima H, Aoyama T, Ito A, Yamaguchi S, Nagai M, Tajino J, Zhang X, Kuroki H. Effects of short-term gentle treadmill walking on subchondral bone in a rat model of instability-induced osteoarthritis. *Osteoarthritis and Cartilage* 2015; 23(9):1563-1574.
- 39) He Y, Siebuhr AS, Brandt-Hansen NU, Wang J, Su D, Zheng Q, Simonsen O, Petersen KK, Arendt-Nielsen L, Eskehave T, Hoeck HC, Karsdal MA, Bay-Jensen AC. Type X collagen levels are elevated in serum from human osteoarthritis patients and associated with biomarkers of cartilage degradation and inflammation. *BMC musculoskeletal disorders* 2014; 15(1):309.
- 40) TE McAlindon, RR Bannuru, MC Sullivan, NK Arden, F Berenbaum, SM Bierma-Zeinstra, GA Hawker, Y Henrotin, DJ Hunter, H Kawaguchi, K Kwok, S Lohmander, F Rannou, EM Roos, M Underwood. OARSI guidelines for the non-surgical management of knee osteoarthritis. *Osteoarthritis and Cartilage* 2014; 22:363-388.
- 41) Ozeki N, Muneta T, Koga H, Nakagawa Y, Mizuno M, Tsuji K, Mabuchi

Y, Akazawa C, Kobayashi E, Matsumoto K, Futamura K, Saito T, Sekiya I. Not single but periodic injections of synovial mesenchymal stem cells maintain viable cells in knees and inhibit osteoarthritis progression in rats. *Osteoarthritis and Cartilage* 2016; 24(6):1061-1070.

42) Greene MA, Loeser RF. Aging-related inflammation in osteoarthritis. *Osteoarthritis and Cartilage* 2015; 23:1966-71.

43) Matsui Y, Iwasaki N, Kon S, Takahashi D, Morimoto J, Matsui Y, Denhardt DT, Rittling S, Minami A, Uede T. Accelerated development of aging - associated and instability - induced osteoarthritis in osteopontin - deficient mice. *Arthritis Rheumatism* 2009; 60(8): 2362-2371.

44) Pennock AT, Robertson CM, Emmerson BC, Harwood FL, Amiel D. Role of apoptotic and matrix-degrading genes in articular cartilage and meniscus of mature and aged rabbits during development of osteoarthritis. *Arthritis Rheumatology* 2007; 56(5):1529-1536.

45) Bay-Jensen AC, Slagboom E, Chen-An P, Alexandersen P, Qvist P, Christiansen C, Meulenbelt I, Karsdal MA. Role of hormones in cartilage and joint metabolism: understanding an unhealthy metabolic phenotype in osteoarthritis. *Menopause* 2013; 20(5):578-586.

46) Sluka KA, Berkley KJ, O'Connor MI, Nicoletta DP, Enoka RM, Boyan BD, Hart DA, Resnick E, Kwok CK, Tosi LL, Coutts RD, Kohrt WM. Neural and psychosocial contributions to sex differences in knee osteoarthritic pain. *Biology of sex differences* 2012; 3(1):26.

47) Chen R, Mian M, Fu M, Zhao JY, Yang L, Li Y, Xu L. Attenuation of the progression of articular cartilage degeneration by inhibition of TGF- $\beta$ 1 signaling in a mouse model of osteoarthritis. *The American journal of*

pathology 2015;185(11):2875-2885.

48) Collins KH, Reimer RA, Seerattan RA, Leonard TR, W. Herzog. Using diet-induced obesity to understand a metabolic subtype of osteoarthritis in rats. *Osteoarthritis and Cartilage* 2015; 23:957-65.

49) Collins KH, Reimer RA, Seerattan RA, Leonard TR, Herzog W. Using diet-induced obesity to understand a metabolic subtype of osteoarthritis in rats. *Osteoarthritis and Cartilage* 2015; 23(6):957-965.

50) Steultjens MP, Dekker J, van Baar ME, Oostendorp RA, Bijlsma JW. Muscle strength, pain and disability in patients with osteoarthritis. *Clinical Rehabilitation* 2001; 15:331-41.

51) Egloff C, Sawatsky A, Leonard T, Hart DA, Valderrabano V, Herzog W. Effect of muscle weakness and joint inflammation on the onset and progression of osteoarthritis in the rabbit knee. *Osteoarthritis and Cartilage* 2014; 22:1886-93.

52) Fischenich KM, Button KD, Coatney GA, Fajardo RS, Leikert KM, Haut RC, Haut Donahue TL. Chronic changes in the articular cartilage and meniscus following traumatic impact to the lapine knee. *Journal of biomechanics* 2015; 48(2):246-253.

53) Drogset JO, Grøntvedt T, Robak OR, Mølster A, Viset AT, Engebretsen L. A sixteen-year follow-up of three operative techniques for the treatment of acute ruptures of the anterior cruciate ligament. *The Journal of bone and joint surgery. American volume* 2006;88(5):944-952.

54) Tochigi Y, Vaseenon T, Heiner AD, Fredericks DC, Martin JA, Rudert MJ, Hillis SL, Brown TD, McKinley TO. Instability dependency of osteoarthritis development in a rabbit model of graded anterior cruciate

ligament transection. *The Journal of bone and joint surgery. American* volume 2011; 93:640-7.

55) Kamekura S, Kawasaki Y, Hoshi K, Shimoaka T, Chikuda H, Maruyama Z, Komori T, Sato S, Takeda S, Karsenty G, Nakamura K, Chung UI, Kawaguchi H. Contribution of runt-related transcription factor 2 to the pathogenesis of osteoarthritis in mice after induction of knee joint instability. *Arthritis Rheumatology* 2006; 54:2462-70.

56) Kamekura S, Hoshi K, Shimoaka T, Chung U, Chikuda H, Yamada T, Uchida M, Ogata N, Seichi A, Nakamura K, Kawaguchi H. Osteoarthritis development in novel experimental mouse models induced by knee joint instability. *Osteoarthritis and Cartilage* 2005; 13:632-41.

57) Onur TS, Wu R, Chu S, Chang W, Kim HT, Dang AB. Joint instability and cartilage compression in a mouse model of posttraumatic osteoarthritis. *Journal of Orthopedic Research* 2014; 32:318-23.

58) Glasson SS, Blanchet TJ, Morris EA. The surgical destabilization of the medial meniscus (DMM) model of osteoarthritis in the 129/SvEv mouse. *Osteoarthritis and Cartilage* 2007; 15(9):1061-1069.

59) Lewek MD, Rudolph KS, Snyder-Mackler L. Control of frontal plane knee laxity during gait in patients with medial compartment knee osteoarthritis. *Osteoarthritis and Cartilage* 2004; 12:745-51.

60) Cammarata ML, Dhaher YY. Associations between frontal plane joint stiffness and proprioceptive acuity in knee osteoarthritis. *Arthritis Care Research* 2012; 64:735-43.

61) Cammarata ML, Dhaher YY. The differential effects of gender, anthropometry, and prior hormonal state on frontal plane knee joint

stiffness. *Clinical Biomechanics* 2008; 23:937-45.

62) Sharma L, Hayes KW, Felson DT, Buchanan TS, Kirwan-Mellis G, Lou C, Pai YC, Dunlop DD. Does laxity alter the relationship between strength and physical function in knee osteoarthritis? *Arthritis and Rheumatism* 1999; 42:25-32.

63) Gustafson JA, Gorman S, Fitzgerald GK, Farrokhi S. Alterations in walking knee joint stiffness in individuals with knee osteoarthritis and self-reported knee instability. *Gait and Posture* 2016; 43:210-5.

64) Knoop J, van der Leeden M, van der Esch M, Thorstensson CA, Gerritsen M, Voorneman RE, Lems WF, Roorda LD, Dekker J, Steultjens MP. Association of lower muscle strength with self-reported knee instability in osteoarthritis of the knee: results from the Amsterdam Osteoarthritis cohort. *Arthritis Care Research* 2012; 64:38-45.

65) Lewek MD, Rudolph KS, Snyder-Mackler L. Control of frontal plane knee laxity during gait in patients with medial compartment knee osteoarthritis. *Osteoarthritis and Cartilage* 2004;12(9):745-751

66) Kokubun T, Kanemura N, Murata K, Moriyama H, Morita S, Jinno T, Ihara H, Takayanagi K. Effect of changing the joint kinematics of knees with a ruptured anterior cruciate ligament on the molecular biological responses and spontaneous healing in a rat model. *The American Journal of Sports Medicine* 2016; 44(11):2900-2910.

67) Kilkenny C, Browne WJ, Cuthill IC, Emerson M, Altman DG. Improving bioscience research reporting: the ARRIVE guidelines for reporting animal research. *Osteoarthritis and Cartilage* 2012; 20:256-60.

68) Ranstam J. Repeated measurements, bilateral observations and

pseudoreplicates, why does it matter? *Osteoarthritis and Cartilage* 2012;20:473-5.

69) Gerwin N, Bendele AM, Glasson S, Carlson CS. The OARSI histopathology initiative - recommendations for histological assessments of osteoarthritis in the rat. *Osteoarthritis and Cartilage* 2010; 21:24-34.

70) Pritzker KPH, Gay S, Jimenez SA, Ostergaard K, Pelletier JP, Revell PA, Salter D, van den Berg WB. Osteoarthritis cartilage histopathology: grading and staging. *Osteoarthritis and Cartilage* 2006; 14:13-29.

71) Kaneko H, Ishijima M, Futami I, Tomikawa N, Kosaki K, Sadatsuki R, Yamada Y, Kurosawa H, Kaneko K, Arikawa-Hirasawa E. Synovial perlecan is required for osteophyte formation in knee osteoarthritis. *Matrix Biology* 2013; 32: 178-187.

72) Schultz M, Molligan J, Schon L, Zhang Z. Pathology of the calcified zone of articular cartilage in post-traumatic osteoarthritis in rat knees. *PLoS One* 2015; 10:e0120949.

73) Hurd WJ, Snyder-Mackler L. Knee instability after acute ACL rupture affects movement patterns during the mid - stance phase of gait. *Journal of Orthopaedic Research* 2007; 25(10):1369-1377.

74) Georgoulis AD, Papadonikolakis A, Papageorgiou CD, Mitsou A, Stergiou N. Three-dimensional tibiofemoral kinematics of the anterior cruciate ligament-deficient and reconstructed knee during walking. *The American Journal of Sports Medicine* 2003; 31(1):75-79.

75) Mikesky AE, Meyer A, Thompson KL. Relationship between quadriceps strength and rate of loading during gait in women. *Journal of Orthopaedic Research* 2000; 18(2):171-175.

- 76) Kapandji AI. 塩田悦仁, 訳. カラー版 カパンジー機能解剖学 II (2) 下肢原著第 6 版. 医歯薬出版, 東京(2010).
- 77 ) Anderson DD, Iyer KS, Segal NA, Lynch JA, Brown TD. Implementation of discrete element analysis for subject-specific, population-wide investigations of habitual contact stress exposure. *Journal of applied biomechanics* 2010;26(2):215-223
- 78) 森山英樹, 木藤伸宏, 編. 奈良勲, 監. 運動器疾患の病態と理学療法. 医歯薬出版, 東京(2015).
- 79) Harato K, Nagura T, Matsumoto H, Otani T, Toyama Y, Suda Y. Knee flexion contracture will lead to mechanical overload in both limbs: a simulation study using gait analysis. *The knee* 2008; 15(6):467-472.
- 80) Iijima H, Fukutani N, Aoyama T, Fukumoto T, Uritani D, Kaneda E, Ota K, Kuroki H, Matsuda S. Clinical phenotype classifications based on static varus alignment and varus thrust in Japanese patients with medial knee osteoarthritis. *Arthritis Rheumatology* 2015; 67(9):2354-2362.
- 81) Yoshioka M, Coutts RD, Amiel D, Hacker SA. Characterization of a model of osteoarthritis in the rabbit knee. *Osteoarthritis and Cartilage* 1996; 4(2): 87-98.
- 82) Yeow CH, Cheong CH, Ng KS, Lee PVS, Goh JCH. Anterior cruciate ligament failure and cartilage damage during knee joint compression a preliminary study based on the porcine model. *The American journal of sports medicine* 2008; 36(5):934-942.
- 83) Kellegren JH, Lawrence JS. Radiological assessment of osteoarthritis. *Annals of the Rheumatic Diseases* 1957; 16(4):494-502.
- 84) Dreier R. Hypertrophic differentiation of chondrocytes in osteoarthritis:

the developmental aspect of degenerative joint disorders. *Arthritis research therapy* 2010; 12(5):216.

85) Kühn K, D'Lima DD, Hashimoto S, Lotz M. Cell death in cartilage. *Osteoarthritis and Cartilage* 2004; 12(1):1-16.

86) Hwang HS, Kim HA. Chondrocyte apoptosis in the pathogenesis of osteoarthritis. *International journal of molecular sciences* 2015; 16(11): 26035-26054.

87) Hsia AW, Anderson MJ, Heffner MA, Lagmay EP, Zavodovskaya R, Christiansen BA. Osteophyte formation after ACL rupture in mice is associated with joint restabilization and loss of range of motion. *Journal of Orthopaedic Research* 2016 (In press)

88) Dayal N, Chang A, Dunlop D, Hayes K, Chang R, Cahue S, Song J, Torres L, Sharma L. The natural history of anteroposterior laxity and its role in knee osteoarthritis progression. *Arthritis Rheumatology* 2005; 52: 2343-2349.

89) Mansour JM, Wentorf FA, Degoede KM. In vivo kinematics of the rabbit knee in unstable models of osteoarthrosis. *Annals of biomedical engineering* 1998; 26(3):353-360.

90) Wolff J. The classic: on the inner architecture of bones and its importance for bone growth. *Clinical Orthopaedics and Related Research* 2010; 468(4):1056-1065.

91) Piotr W, ŁA Poniowski, D Szukiewicz. The Role of Inflammatory and Anti-Inflammatory Cytokines in the Pathogenesis of Osteoarthritis. *Mediators of Inflammation* 2014; Article ID 561459, 1

発表論文 (1)

**Controlling joint instability delays the degeneration of articular cartilage  
in a rat model**

Kenji Murata, Naohiko Kanemura, Takanori Kokubun, Tsutomu Fujino,  
Yuri Morishita, Katsuya Onistuka, Shuhei Fujiwara, Aya Nakashima,  
Daisuke Shimizu, Kiyomi Takayanagi.

*Osteoarthritis and Cartilage*, 25(2): 297–308, 2017.

Article history: Received 13 July 2016

Accepted 10 October 2016



# Osteoarthritis and Cartilage



## Controlling joint instability delays the degeneration of articular cartilage in a rat model

K. Murata †‡, N. Kanemura ‡\*, T. Kokubun ‡, T. Fujino †, Y. Morishita †, K. Onitsuka †, S. Fujiwara †, A. Nakajima †, D. Shimizu ‡, K. Takayanagi ‡

† Graduate Course of Health and Social Services, Graduate School of Saitama Prefectural University, Saitama, Japan

‡ Department of Physical Therapy, School of Health and Social Services, Saitama Prefectural University, Saitama, Japan

### ARTICLE INFO

#### Article history:

Received 13 July 2016

Accepted 10 October 2016

#### Keywords:

Osteoarthritis

Articular cartilage

Joint instability

Tumor necrosis factor alpha

Caspase-3

### SUMMARY

**Objective:** Joint instability induced by anterior cruciate ligament (ACL) transection is commonly considered as a predisposing factor for osteoarthritis (OA) of the knee; however, the influence of re-stabilization on the protection of articular cartilage is unclear. The aim of this study was to evaluate the effect of joint re-stabilization on articular cartilage using an instability and re-stabilization ACL transection model.

**Design:** To induce different models of joint instability, our laboratory created a controlled abnormal joint movement (CAJM) group and an anterior cruciate ligament transection group (ACL-T). Seventy-five Wistar male rats were randomly assigned to the CAJM ( $n = 30$ ), ACL-T ( $n = 30$ ), or no treatment (INTACT) group ( $n = 15$ ). Cartilage changes were assessed with soft X-ray analysis, histological and immunohistochemistry analysis, and real-time polymerase chain reaction (PCR) analysis at 2, 4, and 12 weeks.

**Results:** Joint instability, as indicated by the difference in anterior displacement between the CAJM and ACL-T groups ( $P < 0.001$ ), and cartilage degeneration, as evaluated according to the Osteoarthritis Research Society International (OARSIS) score, were significantly higher in the ACL-T group than the CAJM group at 12 weeks ( $P < 0.001$ ). Moreover, joint re-stabilization maintained cartilage structure (thickness [ $P < 0.001$ ], surface roughness [ $P < 0.001$ ], and glycosaminoglycan stainability [ $P < 0.001$ ]) and suppressed tumor necrosis factor-alpha (TNF- $\alpha$ ) and caspase-3 at 4 weeks after surgery.

**Conclusion:** Re-stabilization of joint instability may suppress inflammatory cytokines, thereby delaying the progression of OA. Joint instability is a substantial contributor to cartilage degeneration.

© 2016 Osteoarthritis Research Society International. Published by Elsevier Ltd. All rights reserved.

### Introduction

Osteoarthritis (OA) is a common cause of chronic pain, impairment in activities of daily living, and disability. Multiple factors have been identified as contributors to the development of knee OA, including aging, sex, obesity, trauma, muscle weakness, and inflammation<sup>1–7</sup>. In particular, mechanical stress has been proposed to play a critical role in the progression of articular cartilage degeneration. Recently, joint instability has been identified as one of the important factors for OA progression. Stability at the knee joint is provided by static structures, such as muscles, ligaments,

menisci, and the joint capsule, in combination with the coordinated activation of dynamic movement; together, these factors produce appropriate loading of the articular cartilage in response to knee movement. However, instability induced by anterior cruciate ligament (ACL) transection alters kinematics, resulting in abnormal loading during weight-bearing activities<sup>8–11</sup>. Therefore, the ACL transection model has been widely used as an animal model to investigate the pathomechanics of OA.

However, the influence of stability on OA remains unclear. Movement with adequate stability is a positive mechanical stress, and articular cartilage requires mechanical loading to maintain homeostasis. On the other hand, increases in joint instability are considered a negative mechanical stress in the pathogenesis of OA. Previously, animal studies have shown that OA progression increases at a rate proportional to instability, resulting in significant changes in knee joint loading and gait performance<sup>12–14</sup>. In a

\* Address correspondence and reprint requests to: N. Kanemura, Department of Physical Therapy, School of Health and Social Services, Saitama Prefectural University, Sannomiya 820, Koshigaya, Saitama, Japan. Fax: 81-48-973-4123.

E-mail address: kanemura-naohiko@spu.ac.jp (N. Kanemura).

human study, self-reported knee instability was associated with significant alterations in knee joint function during the stance phase of gait in patients with OA<sup>15,16</sup>. Moreover, high adduction moments during weight-bearing activities were associated with OA progression, and were noted to result in significant knee instability<sup>17–19</sup>. For this reason, joint instability is a major contributing factor to the progression of OA in both human and animal models, and results in abnormal mechanical loading on the affected knee.

Therefore, we hypothesized that providing biomechanical control following ACL transection may result in the inhibition of articular cartilage degradation. Intra-articular surgery, such as that performed in the ACL transection, is insufficient to evaluate the relationship between joint instability and OA progression. Because intra-articular surgery is invasive, it cannot be determined whether inflammation and secondary instability is a product of ACL transection or other mechanisms<sup>20</sup>. Thus, an animal model is required that can replicate the intra-articular instability condition of ACL transection and provide control over abnormal instability using an extra-articular bracing system.

The purpose of our study was to examine the effect of providing control of instability after ACL transection on the progression of OA. Consequently, it was necessary to develop a novel controlled abnormal joint movement (CAJM) rodent model. Histological and immunofluorescence analyses were performed as a means of examining cartilage structure and pro-inflammatory responses.

## Material and methods

### Animals and experimental design

For this study, a novel protocol was devised according to the Animal Research: Reporting of In Vivo Experiments (ARRIVE) guidelines<sup>21</sup>. In addition, all methods and procedures were approved by the Animal Research Committee of Saitama Prefectural University (approval number: 27-6). The experimental design is presented in Fig. 1. Wistar male rats (Clea Japan, Tokyo, Japan), aged 6 months and weighing 320–380 g, were used in our study. A total of 75 rats were randomized into three groups: no surgery group (INTACT,  $n = 15$ ; without intervention), CAJM group (CAJM,  $n = 30$ ; external support provided to stabilize the knee joint after ACL injury), and ACL transection group (ACL-T,  $n = 30$ ; the ACL was surgically transected). All rats were housed in polycarbonate cages, with two animals per cage. The room had a 12/12 h light–dark cycle and was maintained at a

constant temperature of 23°C. Rats were permitted unrestricted movement within the cage and had access to food and water freely.

### Surgical procedures

In the ACL-T and CAJM groups, ACL transection was performed to introduce joint instability. In the CAJM group, a second procedure was performed to restore biomechanical function following ACL transection using a nylon suture, placed on the outer aspect of the knee joint [Fig. 2(A)]. After a 1-week acclimatization period, animals in the CAJM and ACL-T groups underwent surgery. Under anesthesia with pentobarbital (1.0 ml/kg), the right knee joint was exposed via the medial capsule [Fig. 2(B-a)] without disruption of the patellar tendon, and the ACL was completely transected [Fig. 2(B-b)]. Transection caused excessive anterior translation of the tibia on the femur, resulting in abnormal joint kinematics, a defining feature of joint instability. To mitigate anterior translation of the tibia on the femur following ACL transection in the CAJM group, a bone tunnel was created in the anterior portion of the proximal tibia [Fig. 2(B-c)]. Subsequently, a nylon thread was passed through the tunnel [Fig. 2(B-d)], and secured to the posterior aspect of the distal femur [Fig. 2(B-e)]. The nylon thread, therefore, had the same orientation as the native ACL, providing a posteriorly directed traction force on the tibia to resist anterior motion over the condyles of the femur [Fig. 2(B-f,g)].

### Soft X-ray radiography

To evaluate knee instability and OA change, rats were sacrificed at 4 and 12 weeks after surgery. Joint instability was evaluated by anterior traction using a constant force spring (0.2 kgf) and soft-X ray radiography (M-60; Softex Co., Tokyo, Japan). To assess OA change, limbs were dissected free of all soft tissues and positioned with 90° of flexion at the knee joint. Frontal and sagittal radiographs were taken. Soft X-ray radiography was performed at 28 kV and 1 mA for 1 s, and imaged using a NAOMI digital X-ray sensor (RF Co. Ltd., Nagano, Japan).

### Histological analysis

Rats ( $n = 30$ , each group  $n = 10$ ) were sacrificed at 4 and 12 weeks, and the knee joints were fixed in a 4% paraformaldehyde/phosphate-buffered saline (PBS) solution for 48 h at 4°C. The knees were then

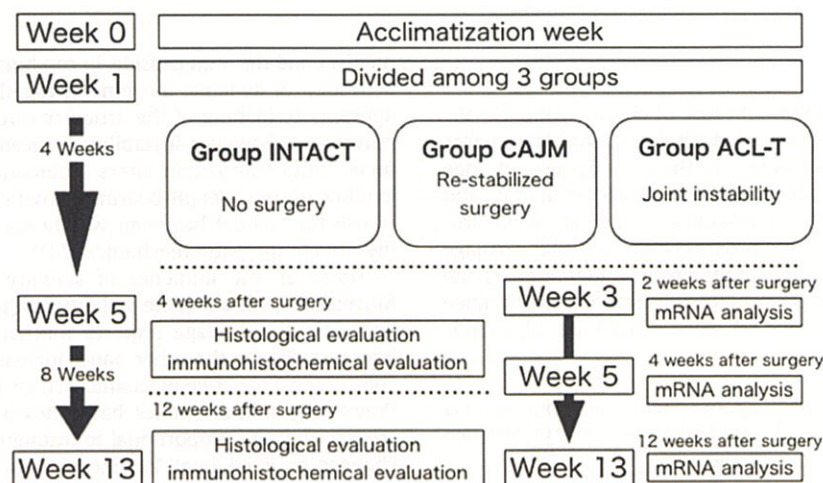
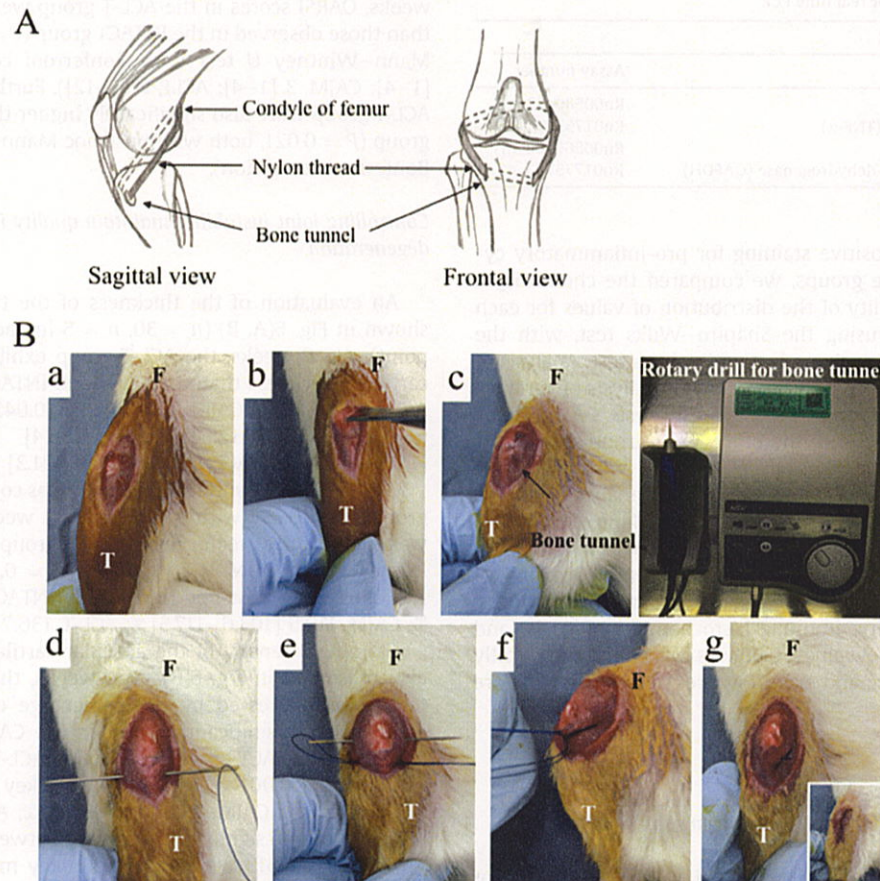


Fig. 1. Schematic of the experimental protocol.



**Fig. 2.** Surgery for the CAJM model. (A) Schematic of the surgical procedure. The CAJM group underwent a second procedure that was performed to restore biomechanical function following ACL transection using a nylon suture placed on the outer aspect of the knee joint. (B) Detailed surgery overview. The medial capsule of the right knee joint is exposed (a), and the ACL is transected (b). A bone tunnel is created in the anterior portion of the proximal tibia using a rotary drill (c), and a 3-0 nylon thread is passed through the tunnel (d) and secured to the posterior aspect of the distal femur (e). The nylon thread (f), therefore, provides a posteriorly directed traction force on the tibia to resist anterior motion over the femoral condyles (g). F, femur; T, tibia.

placed in a 10% EDTA-based solution (Sigma–Aldrich, MO, USA) for decalcification, at a pH of 7.4, for approximately 60 days. The decalcifying solution was renewed twice a week. After complete decalcification, the knee joint was immersed in sucrose solutions of different concentrations (10% for 4 h, 15% for 4 h, and 20% for 8 h). The knee joint was then embedded in an optimal cutting temperature compound (O.C.T., Sakura Finetek Japan, Tokyo, Japan), and 14- $\mu$ m sections were cut along the sagittal plane using a Leica CM 3050 S cryostat (Leica Microsystems AG, Wetzlar, Germany). Every six sections of the medial and lateral compartments were prepared according to previously reported methods<sup>22,23</sup>. All slides were then stained with Safranin O, fast green, and toluidine blue. Sections were evaluated using the osteoarthritis cartilage histopathology assessment system (OARSI score) established by Pritzker *et al.*<sup>24</sup>. The OARSI score ranges from 0 to 24, with higher values indicating more advanced cartilage degeneration. Sample scores were evaluated by two independent observers. Moreover, we performed an analysis of histological characteristics, including cartilage thickness, roughness, and relative staining intensity, using Safranin O and fast green<sup>25</sup>. For details see [Supplementary material and methods](#).

#### Immunohistochemical analysis

Tumor necrosis factor- $\alpha$  (TNF- $\alpha$ ), interleukin 1-beta (IL-1 $\beta$ ), active-caspase-3 were visualized using immunohistochemistry.

The streptavidin–biotin–peroxidase complex technique was subsequently performed using an ABC kit (Vector Laboratories, CA, USA). Sections were stained using diaminobenzidine (Agilent Technologies, CA, USA). For details see [Supplementary material and method](#).

#### Real-time polymerase chain reaction (PCR)

Articular cartilage samples from the ACL-T and CAJM groups were evaluated for mRNA expression using real-time PCR at 2, 4, and 12 weeks post-surgery ( $n = 30$ , each group  $n = 15$ ). The ACL-T group's contralateral articular cartilage (left side) was used for standardization ( $n = 15$ , normal tissue samples). Real-time PCR was performed with a StepOne-Plus real-time system (Applied Biosystems, CA, USA). The primers used are listed in [Table 1](#) (TaqMan Gene Expression Assay, Applied Biosystems, CA, USA). For details see [Supplementary material and method](#).

#### Statistical analysis

All analyses were performed using SPSS 21.0J for Windows (IBM Corp., NY, USA). To evaluate the influence of joint instability on articular cartilage, we compared joint instability displacement, OARSI cartilage degeneration scores, and thickness, roughness, and stainability from the histological analysis among the three groups.

**Table 1**  
Gene expression assays used for real time PCR

Primer used in Real time PCR	
Gene	Assay number
Interleukin 1-beta (IL-1 $\beta$ )	Rn00580432_m1
Tumor necrosis factor-alpha (TNF- $\alpha$ )	Rn01753871_m1
Caspase-3	Rn00563902_m1
Glyceraldehyde 3-phosphate dehydrogenase (GAPDH)	Rn01775763_g1

Moreover, to evaluate positive staining for pro-inflammatory cytokines among the three groups, we compared the chondrocyte density area. The normality of the distribution of values for each variable was evaluated using the Shapiro–Wilks test, with the homogeneity of variance evaluated using Levene's test. Analysis of parametric data was performed using a 1-way analysis of variance (ANOVA), applying Tukey's test for post-hoc analysis. OARSI scores were not normally distributed; therefore, inter-group differences were evaluated using the Kruskal–Wallis test, with the Mann–Whitney *U* test used for post-hoc analysis. For analysis of mRNA data between the CAJM and ACL-T models, the Mann–Whitney *U* test was used. Descriptive statistics were calculated as median with interquartile for OARSI score, as mean with 95% confidence interval (CI) for anterior displacements, cartilage thickness, roughness, relative staining intensity, immune-histochemical analysis, and mRNA expression data. A *P*-value < 0.05 was considered statistically significant in all analyses, and exact *P*-values between groups are shown in graphs.

## Results

### Evaluation of controlling joint instability using soft X-ray analysis

Sagittal plane stability was quantified in terms of anterior displacement, as determined using soft X-ray radiography with the drawer test ( $n = 15$ , each group  $n = 5$ ). Anterior displacement in the ACL-T group was significantly increased compared to the INTACT and CAJM group (INTACT, 0.23 [0.16–0.30] mm; CAJM, 1.26 [1.00–1.52] mm; ACL-T, 2.43 [2.32–2.54] mm). Exact *P*-values are given in Fig. 3.

### Characteristic change of osteophyte formation on soft X-ray observation

To evaluate OA change, knee radiographs were taken at 4 and 12 weeks (Fig. 4). Osteophyte formation along the tibial plateau was observed in the ACL-T group. Moreover, the degree of joint destruction was higher in the ACL-T group. Though joint deformation was observed in both groups following surgery, it appeared earlier in the ACL-T group.

### Controlling joint instability inhibit articular cartilage degeneration as seen on histological analysis

Histological characteristics at 4 and 12 weeks are presented in Fig. 5(A). Changes in the relative area of positive staining and the structure of the surface layer of cartilage were identified in all three groups at 4 weeks. At 12 weeks, clustering of cells, loss of cartilage structure, and tidemark degeneration were observed.

Evaluation of cartilage degeneration at 4 and 12 weeks using the OARSI score is shown in Fig. 5(C) ( $n = 30$ ,  $n = 5$  in each group at each time point). The OARSI scores were significantly higher for the ACL-T group, when compared to the INTACT group at 4 weeks ( $P = 0.013$  with post-hoc Mann–Whitney *U* test with Bonferroni

correction) (INTACT, 2 [1–2]; CAJM, 2 [2–3]; ACLT, 5 [4–6]). At 12 weeks, OARSI scores in the ACL-T group were significantly higher than those observed in the INTACT group ( $P = 0.001$ , with post-hoc Mann–Whitney *U* test with Bonferroni correction) (INTACT, 2 [1–4]; CAJM, 3 [1–4]; ACLT, 8 [6–12]). Furthermore, scores in the ACL-T group were also significantly higher than those in the CAJM group ( $P = 0.021$ , both with post-hoc Mann–Whitney *U* test with Bonferroni correction).

### Controlling joint instability maintain quality in articular cartilage degeneration

An evaluation of the thickness of the tibial cartilage layer is shown in Fig. 6(A, B) ( $n = 30$ ,  $n = 5$  in each group at each time point). At 12 weeks, the ACL-T group exhibited significantly less cartilage thickness than the CAJM and INTACT groups ([INTACT vs ACL-T]  $P = 0.040$ , [CAJM vs ACL-T]  $P = 0.042$  with post-hoc Tukey test) (INTACT, 125.6 [114.8–136.4]  $\mu\text{m}$ ; CAJM, 126.5 [115.1–137.1]  $\mu\text{m}$ ; ACL-T, 106.6 [91.8–121.3]  $\mu\text{m}$ ).

At 4 weeks, the surface roughness was comparable between the groups ( $P = 0.237$  with ANOVA). At 12 weeks, surface roughness was significantly greater in the ACL-T group than in the CAJM and INTACT groups ([INTACT vs ACL-T]  $P = 0.007$ , [CAJM vs ACL-T]  $P = 0.025$  with post-hoc Tukey test) (INTACT, 105.4 [103.4–107.4] %; CAJM, 110.5 [103.6–117.5] %; ACL-T, 136.7 [111.8–161.5] %).

Staining intensity of the articular cartilage with Safranin O is also presented in Fig. 6(B). At 4 weeks, the average staining intensity, as expressed by the percentage of Safranin O positive staining, was significantly lower in the CAJM and ACL-T groups, than in the INTACT group ([INTACT vs ACL-T]  $P < 0.001$ , [CAJM vs ACL-T]  $P < 0.001$  with post-hoc Tukey test) (INTACT, 100.0 [97.6–102.4] %; CAJM, 88.5 [85.1–92.0] %; ACL-T, 85.5 [81.7–89.3] %). There was no significant difference between the CAJM and ACL-T groups ( $P = 0.513$  with post-hoc Tukey methods). At 12 weeks, staining intensity was lower in the ACL-T group than in either the CAJM or INTACT group ([INTACT vs ACL-T]  $P < 0.001$ , [CAJM vs ACL-T]  $P = 0.006$  with post-hoc Tukey test) ( $P < 0.001$ ; INTACT, 100.0 [102.4–97.6] %; CAJM, 94.9 [91.1–98.6] %; ACL-T 83.1 [78.4–87.8] %). Moreover, the staining intensity of ACL-T group was also significantly lower than in the CAJM group ( $P = 0.361$  with post-hoc Tukey test).

### Controlling joint instability inhibit inflammation factors as seen on immune-histochemical analysis

Representative TNF- $\alpha$ , IL-1 $\beta$ , and caspase-3 immunostaining of cartilage specimens is shown in Fig. 7 ( $n = 30$ ,  $n = 5$  in each group at each time point). At 4 weeks, the area of positive staining in pre-determined rectangular area was significantly increased in the ACL-T group, compared to the CAJM and INTACT groups ([INTACT vs ACL-T]  $P < 0.001$ , [INTACT vs CAJM]  $P = 0.004$ , [CAJM vs ACL-T]  $P = 0.012$  with post-hoc Tukey test) (INTACT, 4.09 [2.69–5.48] %; CAJM, 9.40 [7.39–11.40] %; ACL-T, 14.83 [11.55–18.11] %). Active-caspase-3, when evaluated at 4 weeks, exhibited a significantly greater staining area in the ACL-T group than in the INTACT and CAJM groups ([INTACT vs ACL-T]  $P < 0.001$ , [INTACT vs CAJM]  $P = 0.011$ , [CAJM vs ACL-T]  $P < 0.001$  with post-hoc Tukey test) (INTACT, 6.30 [5.17–7.43] %; CAJM, 9.24 [8.40–10.09] %; ACL-T, 14.39 [12.61–16.17] %). At 12 weeks, the relatively higher staining area in the ACL-T group persisted, when compared to the CAJM and INTACT groups ([INTACT vs ACL-T]  $P < 0.001$ , [INTACT vs CAJM]  $P = 0.027$ , [CAJM vs ACL-T]  $P = 0.036$  with post-hoc Tukey test) (INTACT, 4.81 [3.70–5.91] %; CAJM, 7.89 [6.49–9.28] %; ACL-T, 10.71 [9.25–12.17] %). In contrast, the area of positive staining for IL-1 $\beta$  cells was comparable among the groups at 4 weeks and 12 weeks.

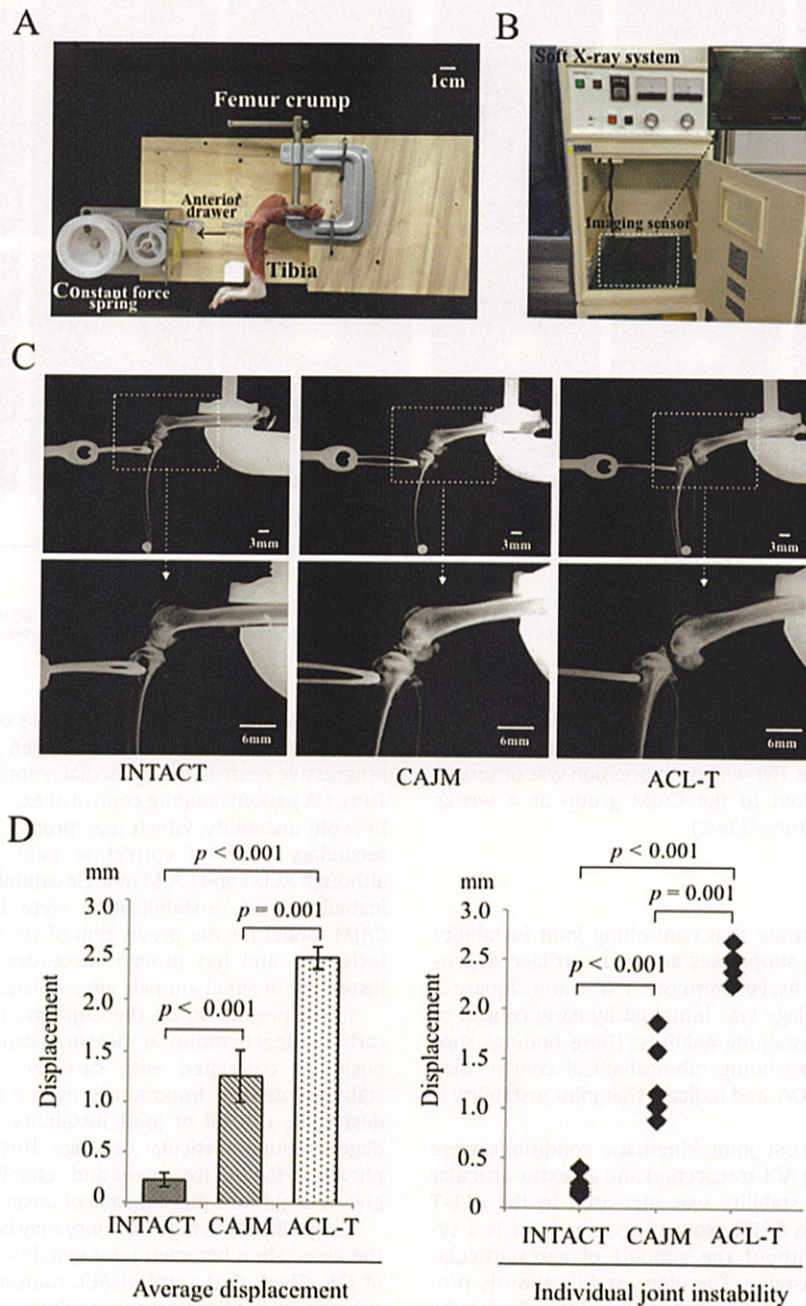


**Fig. 3.** Influence of controlling joint instability by CAJM surgery. (A) System for examination of joint instability. The femur was set into the examination system, and knee instability was maintained by anterior traction using a 0.2 kgf constant force spring. Soft X-ray radiographs were taken using a soft radiogram M-60. (B) Soft X-ray radiography was performed at 28 kV and 1 mA for 1.5 s, and imaged using a NAOMI digital X-ray image sensor. (C) Radiographs were used to assess the degree of joint instability. Differences in joint instability were compared across the INTACT, CAJM, and ACL-T groups. The ACL-T model is shown with the tibia positioned such that the resulting abnormality can be observed. The CAJM model is shown with external bracing of the anterior motion of the tibia, as provided by the nylon thread. (D) Anterior displacement was quantified on digital images and compared across the three groups. Anterior displacement significantly differed across the three groups ( $P < 0.001$  with ANOVA test,  $n = 15$  knees). Specifically, a significant influence of controlling joint instability was detected, with the INTACT group demonstrating significantly lower displacement compared to the CAJM group and ACL-T group (both  $P < 0.001$  with post-hoc Tukey test,  $n = 10$  knees). Moreover, anterior displacement was significantly increased in the ACL-T group compared to the CAJM group ( $P = 0.001$  with post-hoc Tukey test,  $n = 10$  knees). Data are presented as mean with 95% CI.

#### Controlling joint instability inhibit mRNA expression of inflammation factors as seen on real-time PCR analysis

Cartilage samples were not harvested at 12 weeks as a means of avoiding bone contamination due to degeneration. Macroscopic changes on the surface of the tibial articular cartilage were obvious

in both experimental groups (CAJM and ACL-T) compared to the INTACT group [Fig. 5(B)]. Articular surface glossiness, which was present in the INTACT group, was not observed in the CAJM or ACL-T groups. Between experimental groups, articular cartilage differences became obvious at 12 weeks, with increased roughness and degeneration of the articular surface observed in the ACL-T group.

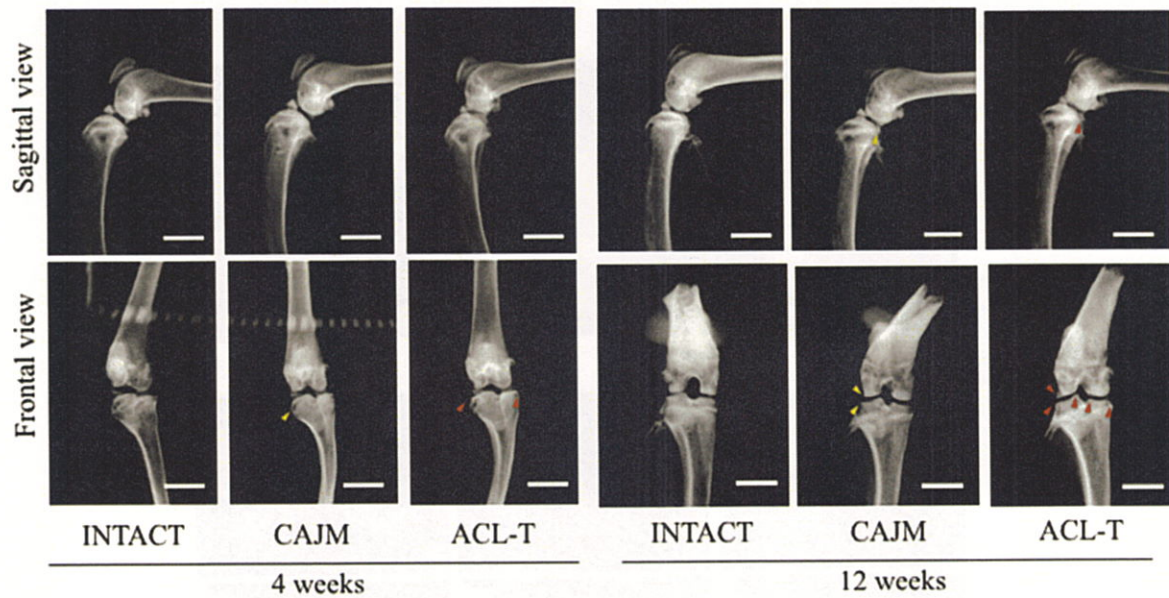


**Fig. 4.** Frontal and sagittal osteophyte formation by soft X-ray observation of the knee 4 weeks and 12 weeks following surgery in each group. In the ACL-T group, osteophyte formation was observed at the 4-week and 12-week time points (red triangle). CAJM also led to osteophyte formation (yellow triangle); however, the ACL-T group demonstrated the most severe change. Scale bar indicates 1000  $\mu$ m.

Cartilage mRNA expression of TNF- $\alpha$ , IL-1 $\beta$ , and caspase-3 are presented in Table II ( $n = 30$ ,  $n = 5$  in each group at each time point). A 3.01-fold increase of TNF- $\alpha$  gene expression was observed in the ACL-T group compared to the CAJM group at 4 weeks ( $P = 0.007$  with Mann–Whitney  $U$  test).

## Discussion

Our data clearly demonstrate that controlling joint instability induced by ACL transection suppresses articular cartilage degeneration on histological analysis. Furthermore, TNF- $\alpha$  and caspase-3 expression in articular cartilage was inhibited by early control of joint instability on immunostaining analysis. These findings support the hypothesis that providing biomechanical control may suppress the progression of OA, and indicate that joint instability is a factor in OA progression.

In this study, two different joint kinematic conditions were created in a rat model, using ACL transection and an extra-articular bracing system. Anterior instability was increased in the ACL-T group, in comparison to the CAJM group. The knee joint is a synovial hinge joint that, without the support of extra-articular structures, is inherently unstable. Therefore, stabilization is provided by ligaments, tendons, menisci, and capsule. In particular, the ACL plays a prominent role in joint stability during static and dynamic motion; consequently, ACL transection has been identified as a major risk factor for cartilage degeneration. Previous studies have shown that joint instability resulting from ACL transection increases the rate of progression to OA in rabbit<sup>8,9</sup>, mouse<sup>10,11</sup>, and rat<sup>13</sup> models. These studies have shown that the degree of joint instability is correlated with OA progression<sup>9</sup>, and have demonstrated significant changes in rodent gait as a consequence<sup>13</sup>. Thus, joint instability is an important factor for the progression of OA.

Clinically, high adduction moments contribute to degenerative changes through greater compression of the medial component of the joint, and have been proposed to induce lateral thrust<sup>17–19</sup>. The OA patient exhibits overall frontal plane joint instability, and some authors have confirmed that such instability is associated with high adduction moments<sup>26</sup>. High medial compartment loads induced by

joint instability occur along the line of force acting as the foot passes medial to the knee joint center, and may contribute to the progressive destruction of medial compartment articular cartilage. Thus, OA patients require control of excessive medial laxity in order to avoid instability, which may protect the articular cartilage as a secondary effect of correcting joint instability. In this study, although ACL-T and CAJM models exhibited sagittal instability, joint instability and re-stabilization were faithfully reproduced. Our CAJM model for the prevention of OA uses a similar stabilization technique and has proven successful in controlling knee joint instability in small animals after ACL transection.

In the present study, the CAJM group exhibited suppression of cartilage degeneration, as measured using the OARSI score, which is positively correlated with cartilage thickness, roughness, and staining intensity. Importantly, even if the structure of the joint is destroyed, control of joint instability may be able to delay the degeneration of articular cartilage. This finding has important implications for the treatment and rehabilitation of OA patients, and gives insight into mechanisms of onset and prevention.

Surgically inducing ACL injury may be insufficient to understand the association between joint instability and the pathophysiology of OA. Given that surgical ACL transection causes intra-articular damage, pro-inflammatory cytokines might be increased in the synovial fluid or synovial membrane<sup>13,27–30</sup>. The pathogenesis of OA is not completely understood, but is strongly associated with a number of inflammatory factors<sup>31,32</sup>. Levels of pro-inflammatory cytokines, such as IL-1 $\beta$  and TNF- $\alpha$ , have been shown to elevate acutely during early OA progression. These cytokines induce caspase-3, which is associated with chondrocyte apoptosis, matrix metalloproteinases, and A disintegrin and metalloproteinase with thrombospondin motifs (ADAMTS), which break down the extracellular matrix, such as glycosaminoglycan and collagen fibers in articular cartilage. Therefore, cytokines have been postulated to play a role in the development of OA<sup>33–35</sup>. Indeed, the CAJM group exhibited reduced, but not completely inhibited, cartilage degradation, indicating that inflammatory factors may have continued to contribute to pathogenic changes. However, more importantly, the two intervention models (CAJM and ACL-T) exhibited differing

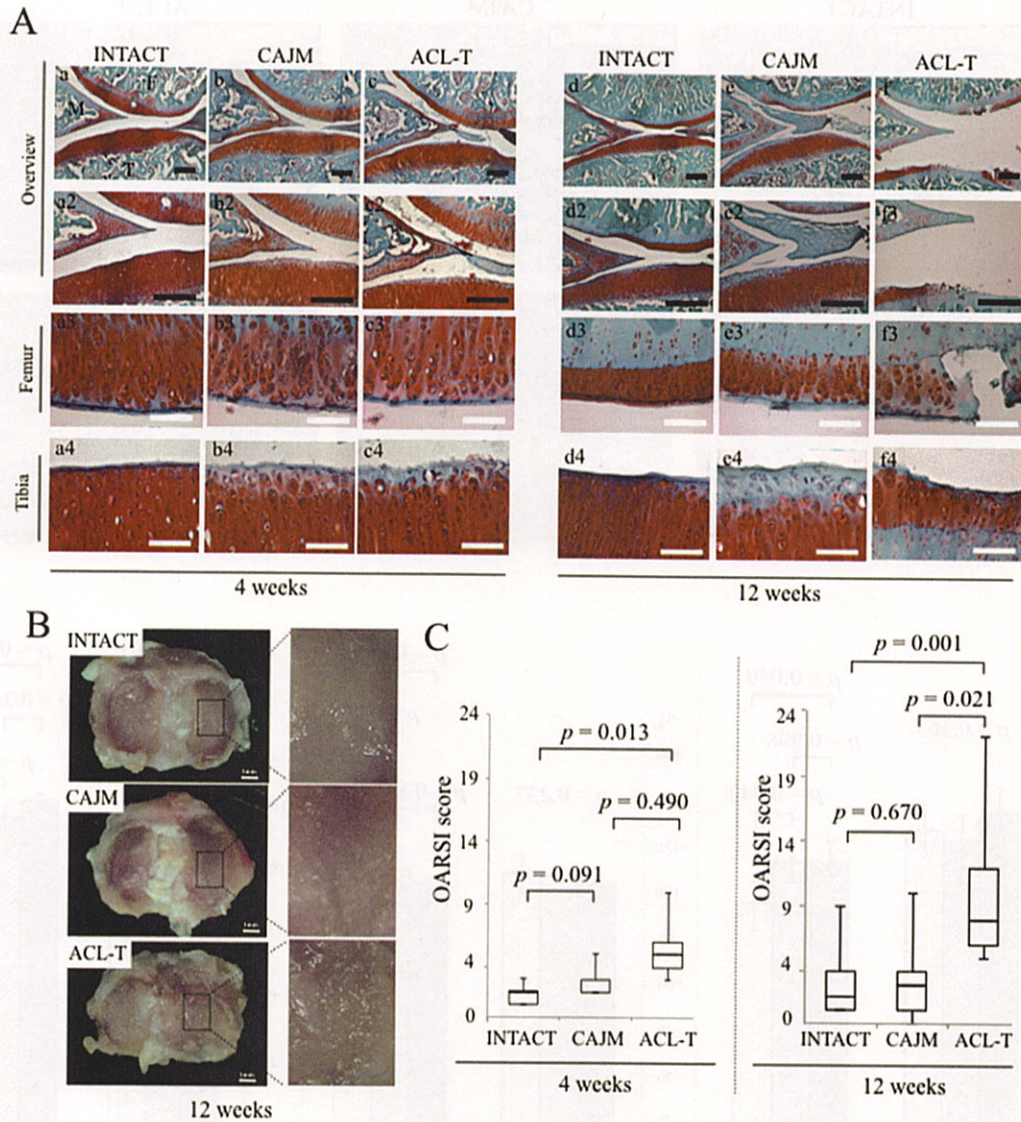


**Fig. 5.** Cartilage histological findings and OARSJ degeneration score comparison between groups at 4 weeks and 12 weeks (INTACT group; CAJM group; ACL-T group). (A) Cartilage sections stained with Safranin O and fast green from the INTACT (a and d), CAJM (b and e), and ACL-T (c and f) groups are shown at 5 $\times$  (overview upper panels), 20 $\times$  (overview lower panels), and 40 $\times$  (femoral and tibial panels) magnification. Black scale bar, 100  $\mu$ m; white scale bar, 50  $\mu$ m. (B) Gross appearance of the tibial articular surface 12 weeks after surgery in the INTACT, CAJM, and ACL-T groups. The glossiness of the articular surface is preserved in the INTACT group. There is loss of glossiness over the medial portion of the CAJM joint and the tibial plateau of the ACL-T group. Severe osteophyte changes are visible on the surface of the articular cartilage in the ACL-T group. (C) Influence of controlling joint instability indicated by OARSJ score. The INTACT group has a significantly lower score compared to the ACL-T group ( $P = 0.013$  with post-hoc Mann–Whitney  $U$  test with Bonferroni correction,  $n = 10$  knees) at 4 weeks. At 12 weeks, the ACL-T group had a significantly higher OARSJ score compared to the INTACT group and the CAJM group (INTACT,  $P = 0.001$  with post-hoc Mann–Whitney  $U$  test with Bonferroni correction; CAJM,  $P = 0.021$  with post-hoc Mann–Whitney  $U$  test with Bonferroni correction, both  $n = 10$  knees). Data are presented as median and with interquartile range.

expressions of TNF- $\alpha$  and caspase-3. In particular, there are two major types of caspase-3 activity involved in articular cartilage degeneration<sup>36,37</sup>. First, apoptotic signals are initiated by cell surface death receptors, exemplified by Fas, leading to caspase-3 activation. Second, the granzyme/perforin-mediated pathway is associated with chondrocyte apoptosis. Perforin is vital to cytotoxic effector function and is able to induce apoptosis in target cells. Granzyme delivery into the cytoplasm by perforin mediates caspase-3 activation and leads to apoptosis of chondrocytes. Thus, caspase-3 is in the downstream part of the apoptotic cascade, and TNF is present in the upstream part. In this study, although CAJM reflected the same condition as ACL-T with regard to intra-articular injury, the degree of instability differed. Consequently, the changes

indicate that differences in joint instability were a product of the model itself, with the extra-articular bracing system implemented in the CAJM group reducing relative instability.

However, there was no significant difference between the ACL-T and CAJM groups in the expression of IL-1 $\beta$ . The cartilage degeneration cascade is very complex, with many factors, including inflammatory mediators, proteases, and prostaglandins, all of which interact amongst themselves. IL-1 $\beta$  is a pro-inflammatory cytokine that has been associated with OA progression<sup>38</sup>; however, it remains unclear whether up- or down-regulation of IL-1 $\beta$  underpins this association. Previous research has identified the possibility that IL-1 $\beta$  and TNF- $\alpha$  may be differentially regulated in activating the apoptotic pathway in human chondrocytes, with this

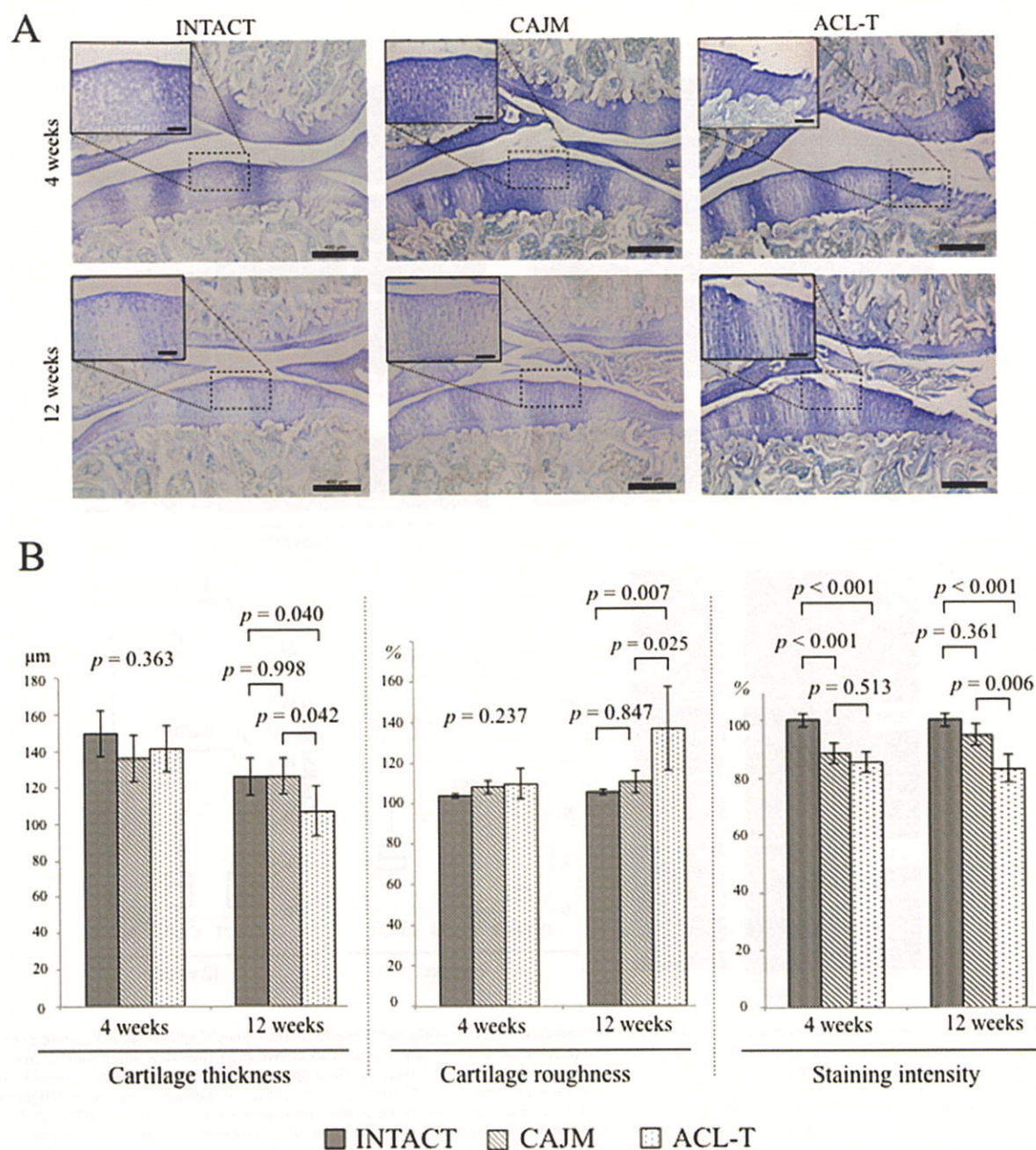


**Fig. 6.** Influence of controlling joint instability for articular cartilage. Cartilage thickness, roughness, and relative staining intensity were compared across the three groups (INTACT group; CAJM group; ACL-T group). (A) Cartilage sections stained with toluidine blue. Scale bar indicates 100 µm. (B) Statistical evaluation of inter-group differences in cartilage thickness, roughness, and stainability at 4 weeks and 12 weeks is shown. Cartilage thickness was significantly lower in the ACL-T group compared to the INTACT and CAJM groups (INTACT,  $P = 0.040$  with post-hoc Tukey test; CAJM,  $P = 0.040$  with post-hoc Tukey test; both  $n = 10$  knees) at 12 weeks. Cartilage roughness was also greater in the ACL-T group compared to the INTACT and CAJM groups at 12 weeks (INTACT,  $P = 0.007$  with post-hoc Tukey test; CAJM,  $P = 0.025$  with post-hoc Tukey test; both  $n = 10$  knees). Moreover, relative staining intensity was greater in the INTACT group compared to the CAJM and ACL-T groups at 4 weeks (CAJM,  $P < 0.001$  with post-hoc Tukey test; CAJM,  $P < 0.001$  with post-hoc Tukey test; both  $n = 10$  knees). Data are presented as mean with 95% CI.

difference being dependent on the levels of nitric oxide<sup>39–41</sup>. Chemical responses to injury can alter the balance between anabolic and catabolic activities, which are crucial for maintaining the integrity of cartilage tissue and for enabling repair at a molecular level.

The limitations of this study must be acknowledged when interpreting and applying our findings. First, experimental measurements were only taken at two points (4 and 12 weeks) for

histological analysis after surgery; therefore, the mechanism underpinning cartilage degeneration are unknown. Intra-articular reactions following ACL transection occur relatively early after surgery, often within the first 2 weeks following injury, as shown in previous studies<sup>23</sup>. Moreover, ACL transection alone results in less severe cartilage degeneration and slower OA progression than the combined ACL transection and medial meniscus destabilization model by Gerwin *et al.*<sup>23</sup>. Therefore, it was assumed that the CAJM

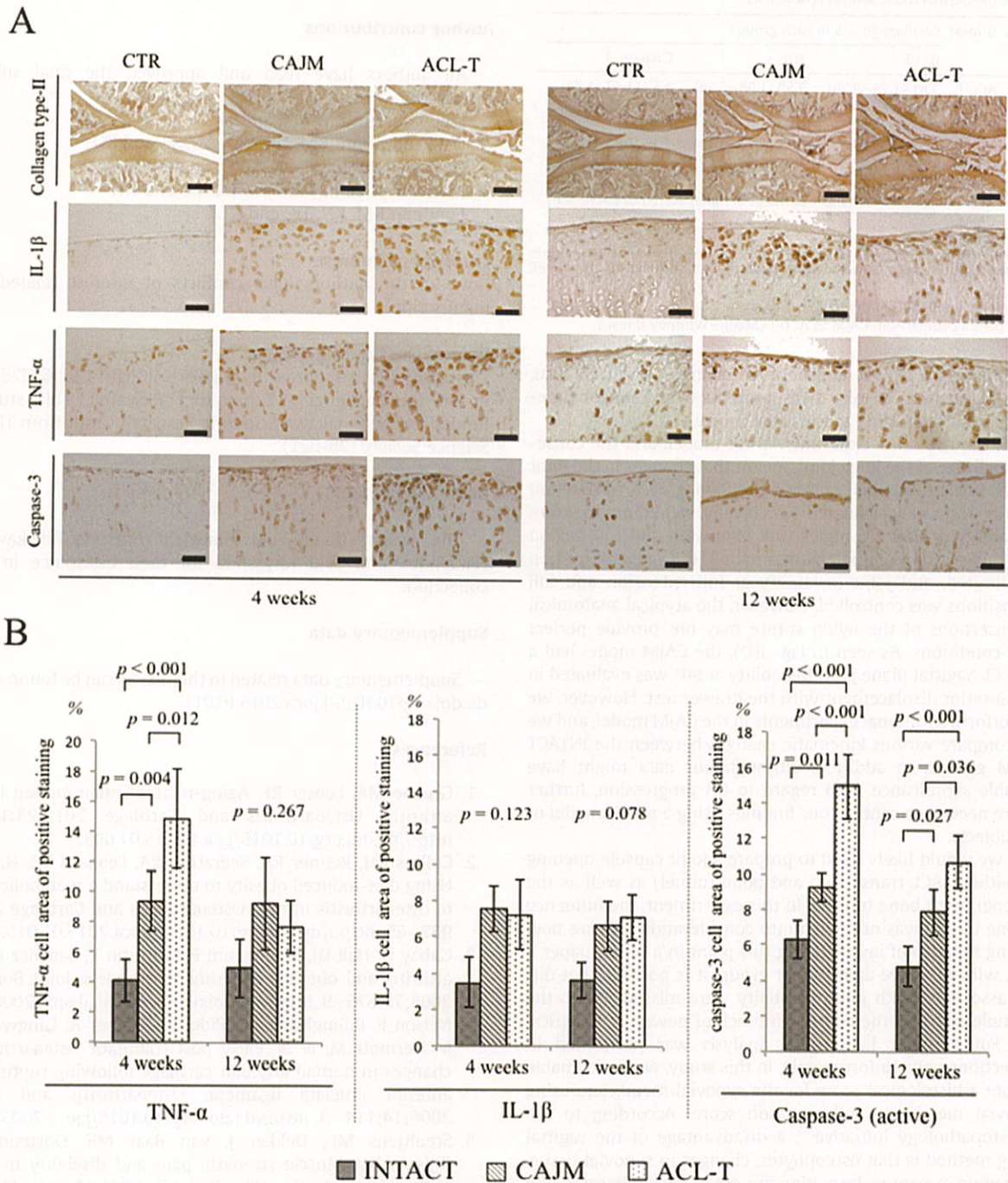


**Fig. 7.** Controlling joint instability inhibits inflammatory factors observed using immunohistochemical analysis at 4 weeks and 12 weeks between groups (INTACT group; CAJM group; ACL-T group). (A) Immunohistochemical staining sections for collagen type II, IL-1 $\beta$ , TNF- $\alpha$ , and active caspase-3 at 4 weeks and 12 weeks. Microscope objective lens, 10 $\times$  (Collagen type II), 40 $\times$  (IL-1 $\beta$ , TNF- $\alpha$ , and caspase-3); scale bar, 100  $\mu$ m or 50  $\mu$ m. (B) The proportion of chondrocyte staining for TNF- $\alpha$ , IL-1 $\beta$ , and caspase-3 was calculated and expressed as a percentage of the total area of chondrocytes within each region. TNF- $\alpha$  significantly differed across the three groups ( $P < 0.001$  with ANOVA test,  $n = 15$  knees) at 4 weeks. Specifically, the INTACT group had a significantly smaller TNF- $\alpha$ -positive staining area compared to the CAJM group and ACL-T group (CAJM,  $P = 0.004$  with post-hoc Tukey test; ACL-T,  $P < 0.001$  with post-hoc Tukey test; both  $n = 10$  knees). The CAJM group had a significantly smaller TNF- $\alpha$ -positive staining area compared to the ACL-T group ( $P = 0.012$  with post-hoc Tukey test,  $n = 10$ ). Active caspase-3 also significantly differed across the three groups ( $P < 0.001$  with ANOVA test,  $n = 15$  knees) at 4 and 12 weeks. The INTACT group had a significantly smaller caspase-3-positive staining area compared to the CAJM group and ACL-T group at 4 weeks (CAJM,  $P = 0.011$  with post-hoc Tukey test; ACL-T,  $P < 0.001$  with post-hoc Tukey test; both  $n = 10$  knees). The CAJM group had a significantly smaller caspase-3-positive staining area compared to the ACL-T group ( $P = 0.012$  with post-hoc Tukey test,  $n = 10$ ). Moreover, at 12 weeks, the INTACT group had a significantly smaller caspase-3-positive staining area compared to the CAJM group and ACL-T group at 4 weeks (CAJM,  $P = 0.027$  with post-hoc Tukey test; ACL-T,  $P < 0.001$  with post-hoc Tukey test; both  $n = 10$  knees). Data are presented as mean with 95% CI.

**Table II**  
Controlling joint instability inhibits mRNA expression of inflammatory factors as a proportion of the normal tissue samples (ratio, 1.0)

Time point	Groups	Cartilage (n = 5 in each group)		
		IL-1 $\beta$	TNF- $\alpha$	Caspase-3
2 Weeks	ACL-T	3.81 (1.78–8.20)	3.59 (1.98–6.50)	1.57 (1.43–1.88)
	CAJM	4.22 (3.87–4.61)	5.84 (3.57–9.56)	1.63 (1.30–1.91)
	P-value	0.658	0.741	0.436
4 Weeks	ACL-T	2.33 (1.55–4.52)	3.01 (2.73–3.33)	1.16 (0.75–1.78)
	CAJM	1.94 (1.21–3.99)	1.99 (1.65–2.42)	1.88 (1.48–2.40)
	P-value	0.727	0.007	0.201
12 Weeks	ACL-T	Severe OA change (Cartilage samples were not harvested)		
	CAJM			
	P-value			

Normal tissue samples were collected from contralateral cartilage of the ACL-T group.

Descriptive mean and 95% CI in the table.

P-values for paired comparison: CAJM vs ACL-T (Mann–Whitney *U* test).

model represents a slower degenerative change, which, in turn, informed the decision to take measurements over a longer time-period than that pertaining to the acute injury.

Second, the use of an experimental rat model, and the consequently small size of the knee joint, meant that changes in the joint kinematics (including tibial rotation) following ACL transection could not be accurately evaluated. Specifically, we did not measure joint instability at various angles (full extension and full flexion positions). As we show [Supplemental data 2](#), the range of motion was not limited, and joint instability at full extension and full flexion positions was controlled. However, the atypical anatomical femoral insertions of the nylon suture may not provide perfect isometric conditions. As seen in [Fig. 3\(D\)](#), the CAJM model had a wide 95% CI. Sagittal plane joint instability at 90° was evaluated in terms of anterior displacement with the drawer test. However, we need to perform additional experiments in the CAJM model, and we need to compare various kinematic changes between the INTACT and CAJM groups. In addition, although our data might have considerable significance with regard to OA progression, further studies are needed to confirm our findings using a rabbit model or human subjects.

Third, we would likely need to prepare a joint capsule opening model (without ACL transection and bone tunnel) as well as the ACL-T model (with bone tunnel). In this experiment, the influence of the bone tunnel was not taken into consideration. We are now considering the idea of investigating this point in a future paper.

Lastly, with only five animals per group, it is possible that differences associated with joint instability were missed due to the small sample size and the consequent lack of power in statistical analysis. Furthermore, histological analysis was performed in sagittal sections only. Unfortunately, in this study, we were unable to compute a histological score for the synovial membrane using the synovial membrane inflammation score. According to the OARSI histopathology initiative<sup>24</sup>, a disadvantage of the sagittal sectioning method is that osteophytes, changes in synovial tissue, and thickening or pannus formation are not as easily detectable in sagittal sections as in frontal or coronal sections. However, we performed not only histological analysis, but also showed data supporting immunostaining and radiography, including the mRNA of the data.

In conclusion, our study provides level IV evidence regarding the protective role of knee stability in the progression of articular cartilage degeneration. Indeed, it appears that joint stability is related to OA, with instability hastening and re-stabilization delaying the progression thereof. However, further research is needed to fully characterize the features of mechanical stress that are associated with the development of OA, and to gather

information to direct the development of interventions that will optimize cartilage health in the knee joint.

#### Author contributions

All authors have read and approved the final submitted manuscript.

Study design: KM, NK, and TK.

Data collection: KM, NK, YM, AN, SF, and KO.

Histological analysis: KM, KO, SF, and DS.

Manuscript composition: KM, NK, and KT.

Funding: KM, KN, TK, and KT.

#### Conflicts of interest

None of the authors have conflicts of interest related to the manuscript.

#### Role of the funding source

This study was supported by a JSPS KAKENHI (26560278) Grant-in-Aid for Challenging Exploratory Research. This study was funded by the Sasakawa Scientific Research Grant from The Japan Science Society (28-621).

#### Acknowledgments

The authors thank Yuki Minegishi, Natsuna Takekawa, Kota Nakamoto, and Saki Miyashita for their assistance in sample collection.

#### Supplementary data

Supplementary data related to this article can be found at <http://dx.doi.org/10.1016/j.joca.2016.10.011>.

#### References

- Greene MA, Loeser RF. Aging-related inflammation in osteoarthritis. *Osteoarthritis and Cartilage* 2015;23:1966–71, <http://dx.doi.org/10.1016/j.joca.2015.01.008>.
- Collins KH, Reimer RA, Seerattan RA, Leonard TR, Herzog W. Using diet-induced obesity to understand a metabolic subtype of osteoarthritis in rats. *Osteoarthritis and Cartilage* 2015;23:957–65, <http://dx.doi.org/10.1016/j.joca.2015.01.015>.
- Gabay O, Hall DJ, Berenbaum F, Henrotin Y, Sanchez C. Osteoarthritis and obesity: experimental models. *Joint Bone Spine* 2008;75:675–9, <http://dx.doi.org/10.1016/j.jbspin.2008.07.011>.
- Nelson F, Billingham RC, Pidoux I, Reiner A, Langworthy M, McDermott M, et al. Early post-traumatic osteoarthritis-like changes in human articular cartilage following rupture of the anterior cruciate ligament. *Osteoarthritis and Cartilage* 2006;14:114–9, <http://dx.doi.org/10.1016/j.joca.2005.08.005>.
- Steultjens MP, Dekker J, van Baar ME, Oostendorp RA, Bijlsma JW. Muscle strength, pain and disability in patients with osteoarthritis. *Clin Rehabil* 2001;15:331–41, <http://dx.doi.org/10.1191/026921501673178408>.
- Egloff C, Sawatsky A, Leonard T, Hart DA, Valderrabano V, Herzog W. Effect of muscle weakness and joint inflammation on the onset and progression of osteoarthritis in the rabbit knee. *Osteoarthritis and Cartilage* 2014;22:1886–93, <http://dx.doi.org/10.1016/j.joca.2014.07.026>.
- Felson DT. Osteoarthritis as a disease of mechanics. *Osteoarthritis and Cartilage* 2013;21:10–5, <http://dx.doi.org/10.1016/j.joca.2012.09.012>.
- Egloff C, Hart DA, Hewitt C, Vavken P, Valderrabano V, Herzog W. Joint instability leads to long-term alterations to

- knee synovium and osteoarthritis in a rabbit model. *Osteoarthritis and Cartilage* 2016;24:1054–60, <http://dx.doi.org/10.1016/j.joca.2016.01.341>.
9. Tochigi Y, Vaseenon T, Heiner AD, Fredericks DC, Martin JA, Rudert MJ, et al. Instability dependency of osteoarthritis development in a rabbit model of graded anterior cruciate ligament transection. *J Bone Joint Surg* 2011;93:640–7, <http://dx.doi.org/10.2106/JBJSJ.00150>.
  10. Kamekura S, Kawasaki Y, Hoshi K, Shimoaka T, Chikuda H, Maruyama Z, et al. Contribution of runt-related transcription factor 2 to the pathogenesis of osteoarthritis in mice after induction of knee joint instability. *Arthritis Rheumatol* 2006;54:2462–70, <http://dx.doi.org/10.1002/art.22041>.
  11. Kamekura S, Hoshi K, Shimoaka T, Chung U, Chikuda H, Yamada T, et al. Osteoarthritis development in novel experimental mouse models induced by knee joint instability. *Osteoarthritis and Cartilage* 2005;13:632–41, <http://dx.doi.org/10.1016/j.joca.2005.03.004>.
  12. Allen KD, Mata BA, Gabr MA, Huebner JL, Adams Jr SB, Kraus VB, et al. Kinematic and dynamic gait compensations resulting from knee instability in a rat model of osteoarthritis. *Arthritis Res Ther* 2012;14:R78, <http://dx.doi.org/10.1186/ar3801>.
  13. Sharma L, Hayes KW, Felson DT, Buchanan TS, Kirwan-Mellis G, Lou C, et al. Does laxity alter the relationship between strength and physical function in knee osteoarthritis? *Arthritis Rheum* 1999;42:25–32, [http://dx.doi.org/10.1002/1529-0131\(199901\)](http://dx.doi.org/10.1002/1529-0131(199901)).
  14. Frank CB, Beveridge JE, Huebner KD, Heard BJ, Tapper JE, O'Brien EJ, et al. Complete ACL/MCL deficiency induces variable degrees of instability in sheep with specific kinematic abnormalities correlating with degrees of early osteoarthritis. *J Orthop Res* 2012;30:384–92, <http://dx.doi.org/10.1002/jor.21549>.
  15. Gustafson JA, Gorman S, Fitzgerald GK, Farrokhi S. Alterations in walking knee joint stiffness in individuals with knee osteoarthritis and self-reported knee instability. *Gait Posture* 2016;43:210–5, <http://dx.doi.org/10.1016/j.gaitpost.2015.09.025>.
  16. Knoop J, van der Leeden M, van der Esch M, Thorstensson CA, Gerritsen M, Voorneman RE, et al. Association of lower muscle strength with self-reported knee instability in osteoarthritis of the knee: results from the Amsterdam Osteoarthritis cohort. *Arthritis Care Res* 2012;64:38–45, <http://dx.doi.org/10.1002/acr.20597>.
  17. Lewek MD, Rudolph KS, Snyder-Mackler L. Control of frontal plane knee laxity during gait in patients with medial compartment knee osteoarthritis. *Osteoarthritis and Cartilage* 2004;12:745–51, <http://dx.doi.org/10.1016/j.joca.2004.05.005>.
  18. Cammarata ML, Dhaher YY. Associations between frontal plane joint stiffness and proprioceptive acuity in knee osteoarthritis. *Arthritis Care Res* 2012;64:735–43, <http://dx.doi.org/10.1002/acr.21589>.
  19. Cammarata ML, Dhaher YY. The differential effects of gender, anthropometry, and prior hormonal state on frontal plane knee joint stiffness. *Clin Biomech* 2008;23:937–45, <http://dx.doi.org/10.1016/j.clinbiomech.2008.03.071>.
  20. Onur TS, Wu R, Chu S, Chang W, Kim HT, Dang AB. Joint instability and cartilage compression in a mouse model of posttraumatic osteoarthritis. *J Orthop Res* 2014;32:318–23, <http://dx.doi.org/10.1002/jor.22509>.
  21. Kilkenny C, Browne WJ, Cuthill IC, Emerson M, Altman DG. Improving bioscience research reporting: the ARRIVE guidelines for reporting animal research. *Osteoarthritis and Cartilage* 2012;20:256–60, <http://dx.doi.org/10.1016/j.joca.2012.02.010>.
  22. Ranstam J. Repeated measurements, bilateral observations and pseudoreplicates, why does it matter? *Osteoarthritis and Cartilage* 2012;20:473–5, <http://dx.doi.org/10.1016/j.joca.2012.02.011>.
  23. Gerwin N, Bendele AM, Glasson S, Carlson CS. The OARSI histopathology initiative - recommendations for histological assessments of osteoarthritis in the rat. *Osteoarthritis and Cartilage* 2010;21:24–34, <http://dx.doi.org/10.1016/j.joca.2010.05.030>.
  24. Pritzker KPH, Gay S, Jimenez SA, Ostergaard K, Pelletier JP, Revell PA, et al. Osteoarthritis cartilage histopathology: grading and staging. *Osteoarthritis and Cartilage* 2006;14:13–29, <http://dx.doi.org/10.1016/j.joca.2005.07.014>.
  25. Schultz M, Molligan J, Schon L, Zhang Z. Pathology of the calcified zone of articular cartilage in post-traumatic osteoarthritis in rat knees. *PLoS One* 2015;10:e0120949, <http://dx.doi.org/10.1371/journal.pone.0120949>.
  26. Haslauer CM, Proffen BL, Johnson VM, Murray MM. Expression of modulators of extracellular matrix structure after anterior cruciate ligament injury. *Wound Repair Regen* 2014;22:103–10, <http://dx.doi.org/10.1111/wrr.12130>.
  27. Kiapour AM, Murray MM. Basic science of anterior cruciate ligament injury and repair. *Bone Joint Res* 2014;3:20–31, <http://dx.doi.org/10.1302/2046-3758.32.2000241>.
  28. Tang Z, Yang L, Zhang J, Xue R, Wang Y, Chen PC, et al. Coordinated expression of MMPs and TIMPs in rat knee intra-articular tissues after ACL injury. *Connect Tissue Res* 2009;50:315–22, <http://dx.doi.org/10.1080/03008200902741463>.
  29. Tang Z, Yang L, Wang Y, Xue R, Zhang J, Huang W, et al. Contributions of different intraarticular tissues to the acute phase elevation of synovial fluid MMP-2 following rat ACL rupture. *J Orthop Res* 2009;27:243–8, <http://dx.doi.org/10.1002/jor.20763>.
  30. Zhang J, Yang L, Tang Z, Xue R, Wang Y, Luo Z, et al. Expression of MMPs and TIMPs family in human ACL and MCL fibroblasts. *Connect Tissue Res* 2009;50:7–13, <http://dx.doi.org/10.1080/03008200802376139>.
  31. Van der Kraan PM, van den Berg WB. Chondrocyte hypertrophy and osteoarthritis: role in initiation and progression of cartilage degeneration? *Osteoarthritis and Cartilage* 2012;20:223–32, <http://dx.doi.org/10.1016/j.joca.2011.12.003>.
  32. Sandell LJ, Aigner T. Articular cartilage and changes in arthritis. An introduction: cell biology of osteoarthritis. *Arthritis Res Ther* 2001;3:107–13, <http://dx.doi.org/10.1186/ar148>.
  33. Smith MD, Triantafyllou S, Parker A, Youssef PP, Coleman M. Synovial membrane inflammation and cytokine production in patients with early osteoarthritis. *J Rheumatol* 1997;24:365–71.
  34. Wang P, Guan PP, Guo C, Zhu F, Konstantopoulos K, Wang ZY. Fluid shear stress-induced osteoarthritis: roles of cyclooxygenase-2 and its metabolic products in inducing the expression of proinflammatory cytokines and matrix metalloproteinases. *FASEB J* 2013;27:4664–77, <http://dx.doi.org/10.1096/fj.13-234542>.
  35. Guilak F. Biomechanical factors in osteoarthritis. *Best Pract Res Clin Rheumatol* 2011;25:815–23, <http://dx.doi.org/10.1016/j.berh.2011.11.013>.
  36. Hwang HS, Kim HA. Chondrocyte apoptosis in the pathogenesis of osteoarthritis. *Int J Mol Sci* 2015;16(11):26035–54, <http://dx.doi.org/10.3390/ijms161125943>.
  37. Kühn K, D'Lima DD, Hashimoto S, Lotz M. Cell death in cartilage. *Osteoarthritis and Cartilage* 2004;12:1–16, <http://dx.doi.org/10.1016/j.joca.2003.09.015>.
  38. Lee AS, Ellman MB, Yan D, Kroin JS, Cole BJ, van Wijnen AJ, et al. A current review of molecular mechanisms regarding osteoarthritis and pain. *Gene* 2013;527:440–7, <http://dx.doi.org/10.1016/j.gene.2013.05.069>.
  39. Fan Z, Söder S, Oehler S, Fundel K, Aigner T. Activation of interleukin-1 signaling cascades in normal and osteoarthritic

- articular cartilage. *Am J Pathol* 2007;171:938–46, <http://dx.doi.org/10.2353/ajpath.2007.061083>.
40. Lopez-Armada MJ, Carames B, Lires-Dean M, Cillero-Pastor B, Ruiz-Romero C, Galdo F, et al. Cytokines, tumor necrosis factor- $\alpha$  and interleukin-1, differentially regulate apoptosis in osteoarthritis cultured human chondrocytes. *Osteoarthritis and Cartilage* 2006;14:660–9, <http://dx.doi.org/10.1016/j.joca.2006.01.005>.
41. Franciozi CE, Tarini VA, Reginato RD, Gonçalves PR, Medeiros VP, Ferretti M, et al. Gradual strenuous running regimen predisposes to osteoarthritis due to cartilage cell death and altered levels of glycosaminoglycans. *Osteoarthritis and Cartilage* 2013;21:965–72, <http://dx.doi.org/10.1016/j.joca.2013.04.007>.

## Supplementary data 1

### Controlling joint instability delays the degeneration of articular cartilage in a rat model

Kenji Murata †‡, Naohiko Kanemura ‡, Takanori Kokubun ‡  
Tsutomu Fujino †, Yuri Morishita †, Katsuya Onitsuka †, Shuhei Fujiwara †  
Aya Nakashima †, Daisuke Shimizu ‡, Kiyomi Takayanagi ‡

#### Histological analysis for cartilage thickness, roughness, and stainability

The articular cartilage thickness of each region was evaluated using the average thickness, calculated from 5× microscope objective lens images using WinROOF software version 7.0.0 (Mitani Corporation, Tokyo, Japan). To evaluate the surface roughness of the articular cartilage, images of sections within the anterior and posterior areas were obtained at 10× magnification and processed using ImageJ software (<http://rsb.info.nih.gov/ij/>). Lines were drawn as an approximation of straight tangential length for the standard calculation of tidemark roughness. The true length of the cartilage surface was also determined and used to normalize the degree of surface roughness, expressed as the true length/approximation of the straight length.

Glycosaminoglycan content (relative staining intensity with Safranin O stain) of the articular cartilage was evaluated on Safranin O/fast-green stained sections using digital densitometry and proprietary imaging software (WinROOF version 7.0.0, Mitani Corporation, Tokyo, Japan). Initially, digital images were acquired to quantify the staining intensity of areas staining red in sections from the tibial articular cartilage using the 10x microscope objective lens. Color images were then converted to grayscale images using digital densitometry. Random areas were selected, and the scale of staining intensity for the cartilage tissue was calculated by averaging the measurements taken at 9 points for each section from the anterior, middle, and posterior regions of the tibial cartilage. Staining intensity was normalized INTACT group as 100% in each time point.

#### Immunohistochemical analysis

Sections were air-dried for 10 min and washed twice for 5 min with a PBS solution. Endogenous peroxidase was inactivated by incubating the sections in 0.3% hydrogen peroxide/ethanol solution for 30 min. Sections were blocked with 0.1% bovine serum albumin/PBS solution, and were incubated overnight at 4°C with rabbit polyclonal anti-tumor necrosis factor-alpha (TNF- $\alpha$ ) antibody (dilution 1:250; Bioss, MA, USA), anti-interleukin 1-beta (IL-1 $\beta$ ) antibody (dilution 1:250; Bioss, MA, USA), rabbit polyclonal antibody active-caspase-3 (dilution 1:250; Bioss, MA, USA), and type-II

collagen (dilution 1:400; Abcam, MA, USA). The streptavidin-biotin-peroxidase complex technique was then performed at room temperature, using an ABC kit (Vector Laboratories, CA, USA). Sections for immunohistochemical analysis were stained using diaminobenzadine (Agilent Technologies, CA, USA). To evaluate the area of positive pro-inflammatory cells, 3 images of the chondrocytes were obtained at 20x magnification within the tibial cartilage. Images were converted to grayscale, and the staining chondrocytes within a predetermined rectangular area of 10000  $\mu\text{m}^2$  were counted. The proportion of chondrocyte staining for TNF- $\alpha$ , IL-1 $\beta$ , and caspase-3 was calculated and expressed as a percentage of the total number of chondrocytes within each area using WinROOF software version 7.0.0 (Mitani Corporation, Tokyo, Japan).

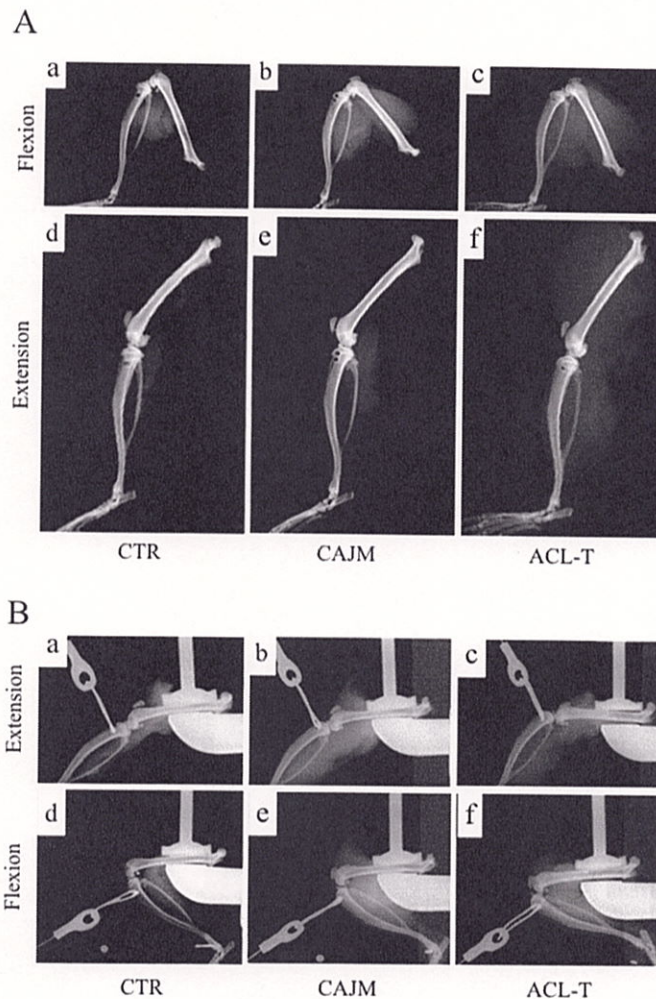
### **Real-time polymerase chain reaction**

Cartilage specimens were carefully collected using a surgical knife, and submerged in an RNA stabilizing solution (Ambion, TX, USA) at 4°C for 48 h. Whole RNA was extracted with the RNeasy Lipid Tissue Mini Kit (Qiagen, CA, USA) using QIAzol reagent and chloroform, according to manufacturer instructions. Synthesis of cDNA was conducted using a high-capacity cDNA reverse transcription kit (Applied Biosystems, CA, USA). cDNA was synthesized under the following conditions: 10 min at 25°C, 120 min at 37°C, and 10 min at 85°C. Real-time PCR was performed with a StepOne-Plus real-time system (Applied Biosystems, CA, USA), using 2  $\mu\text{L}$  of cDNA in the presence of TaqMan primers (Applied Biosystems, CA, USA). PCR was performed under the following conditions: 20 s at 95°C and 20 s at 60°C, with the cycle repeated 40 times. The primers used are *TNF- $\alpha$* , *IL-1 $\beta$* , and *caspase-3* (TaqMan Gene Expression Assay, Applied Biosystems, CA, USA). The relative value of expression for each gene was normalized to the expression of *glyceraldehyde 3-phosphate dehydrogenase (GAPDH)*, using the  $2^{-\Delta\Delta C_t}$  method to calculate relative levels of mRNA expression.

## Supplementary data 2

### Controlling joint instability delays the degeneration of articular cartilage in a rat model

Kenji Murata †‡, Naohiko Kanemura ‡, Takanori Kokubun ‡  
Tsutomu Fujino †, Yuri Morishita †, Katsuya Onitsuka †, Shuhei Fujiwara †  
Aya Nakashima †, Daisuke Shimizu ‡, Kiyomi Takayanagi ‡



Influence of the controlled abnormal joint movement (CAJM) and anterior cruciate ligament transection (ACL-T) surgery. (A) Difference of range of motion among three groups. Flexion and extension range was not limited.

However, ACLT group was confirmed little excessive extension angle. The excessive range seems to be the influence of joint instability with ACL injury. (B) Examination systems of joint instability evaluation at flexion and extension angle. CAJM model was braced anterior instability compared to ACL-T group at both angles (flexion and extension angle).

発表論文 (2)

**Acute chondrocyte response to controlling joint instability in an osteoarthritis model**

Kenji Murata, Naohiko Kanemura, Takanori Kokubun, Tsutomu Fujino, Yuri Morishita, Kiyomi Takayanagi.

*Sport Sci Health*, 13(1):113-119, 2017.

Article history: Received 12 April 2016

Accepted 20 September 2016



## Acute chondrocyte response to controlling joint instability in an osteoarthritis rat model

Kenji Murata<sup>1,2\*</sup>, Naohiko Kanemura<sup>1</sup>, Takanori Kokubun<sup>1</sup>,  
Yuri Morishita<sup>2</sup>, Tsutomu Fujino<sup>2</sup>, Kiyomi Takayanagi<sup>1</sup>

<sup>1</sup> Department of Physical Therapy, School of Health and Social Services, Saitama Prefectural University, Saitama, Japan

<sup>2</sup> Department of Health and Social Services, Graduate School of Saitama Prefectural University, Saitama, Japan

**Corresponding author:** Kenji Murata, MSc., Department of Physical Therapy, School of Health and Social Services, Saitama Prefectural University. Sannomiya 820, Koshigaya, Saitama, Japan  
Tel: +81-489-73-4123 Fax: +81-489-73-4123 E-mail: murata-kenji@spu.ac.jp

### Abbreviations<sup>1</sup>

---

<sup>1</sup>OA, osteoarthritis; ACL, anterior cruciate ligament; ECM, extracellular matrix; ACL-T, ACL transection with joint instability; CAJM, controlled abnormal joint movement with ACL transection

## **Abstract**

**Objective:** Osteoarthritis is a common consequence of anterior cruciate ligament (ACL) injury. Joint instability induced by ACL transection is involved in the chondrocyte response in the articular cartilage degeneration process. The aim of this study was to confirm the effect of controlling joint instability after ACL injury by investigating the chondrocyte reaction in the early osteoarthritic disease process.

**Methods:** For inducing different joint conditions (stability and instability), 15 Wistar rats were randomized into three groups: ACL transection with joint instability (ACL-T, n =5), controlled abnormal joint movement with ACL transection (CAJM, n =5), and control (n =5). One week after surgery, all rats were euthanized and their knees removed. Histological analysis was performed on the knee cartilages, which involved evaluation of cell numbers and density.

**Results:** There were no significant differences in chondrocyte numbers among the three groups within each articular cartilage zone (surface, middle, and deep zones) nor between zones ( $p > 0.05$ ). In contrast, the chondrocyte cell density area was significantly suppressed in the CAJM compared to the ACL-T group in each zone (deep zone,  $p = 0.032$ ; middle zone,  $p = 0.029$ ; surface zone,  $p = 0.019$ ).

**Conclusions:** Early control of joint instability induced by ACL injury inhibited chondrocyte hypertrophy in articular cartilage. This result indicates that knee joint instability increases mechanical stress, and the controlling of these joint movements might provide a new treatment approach for the long-term prevention of osteoarthritis.

**Keywords:** osteoarthritis, articular cartilage, joint instability, animal study, acute chondrocyte response

## **Introduction**

Multiple factors are involved in the pathogenesis of osteoarthritis (OA) [1, 2]. Knee OA is a common chronic joint disease with painful joint movement during daily activities. Knee joint stability is provided by the ligaments, meniscus, and articular capsule. The anterior cruciate ligament (ACL) is the primary structural contributor to joint stability. However, injuries to the ACL produce anterior-posterior knee instability, and lead to the development of articular cartilage degeneration within a relatively short time in humans and animals [3-5]. Commonly, joint instability induced by ACL injury causes abnormal mechanical loading on the articular cartilage [6]. Therefore, an ACL transection model has been used widely as a model of joint instability to investigate the pathogenesis of knee OA.

Ihara et al. provided evidence of the effectiveness of conservative treatment for ACL using a knee brace with a coil spring traction system to allow early protection from joint instability [7]. Kokubun et al. showed that inhibition of abnormal joint movement had a favorable influence on the intra-articular condition, and stimulated an ACL healing response [8]. These findings highlight the need to validate the influence of controlling joint instability in terms of articular cartilage degeneration.

Generally, the reaction patterns of chondrocytes during the progression of OA can be categorized in three ways: proliferation and hypertrophy, cartilage degradation, and osteophyte formation [9]. Sandell et al. [10] showed that normal cartilage cells were small and uniform, and characterized by low levels of proliferation. However, activated chondrocytes showed high levels of proliferation and hypertrophy in articular cartilage [10]. Controlling joint instability during the acute phase of injury delays the degeneration of articular cartilage; however, the acute cellular response to controlling joint instability is unclear. Therefore, we hypothesized that controlling the joint instability induced by an ACL injury leads to low levels of chondrocyte proliferation and hypertrophy during the early cellular responses. The purpose of this study was to use histomorphometry to determine any differences of early chondrocyte responses between controlled, and uncontrolled joint instability models.

## **Methods**

### *Animals*

All methods and procedures were approved by the Animal Research Committee of Saitama Prefectural University. Fifteen 12-week-old male Wistar rats (Clea Japan, Tokyo, Japan) were randomized into three groups: ACL transection with joint instability (ACL-T, n = 5), controlled abnormal joint movement with ACL transection (CAJM, n = 5), and control (CTR, n = 5; without surgery). The ACL-T and CAJM groups received different surgical treatments on the right knee according to the protocols described below. The animals were allowed unrestricted activity and were housed at 23°C under a 12/12-h light/dark cycle.

### *Surgical procedures*

As described previously [8], the CAJM rat model is designed to restore biomechanical function following ACL transection by using a nylon suture placed along an orientation similar to the original cruciate ligament on the outer side of the joint. In this model, anterior instability is dampened through traction in a posterior direction. Unlike in ACL reconstruction, abnormal joint movements can be dampened, although intra-articular suturing of the ligament is not possible.

Under pentobarbital anesthesia, the right knee joint was exposed to the medial capsule without disrupting the patellar tendon, and the ACL was transected completely. The transection caused excessive anterior drawing of the tibia on the femur, resulting in abnormal joint kinematics. A defining feature of joint instability is the induction of abnormal joint movement because of ligament transection. This model shows the inability to perform kinesiologically normal joint movements. The joint stability group involved animals in which the anterior drawing of the tibia caused by complete ACL transection was dampened. To achieve a damping force in the knee joint after ACL transection, we created a bone tunnel to the anterior proximal tibia, passed a nylon thread through the bone tunnel, and tied and secured it to the posterior distal femur, thus dampening the anterior drawing force of the femur on the tibia.

To evaluate joint condition between CAJM and ACL-T groups, right lower limbs including knee joint underwent radiographic examination. Femur was set to original examination systems, and knee instability was evaluated by anterior traction using 0.2kgf constant force spring (Sunco spring Corp., Kanagawa, Japan), and take

radiographs using soft radiogram M-60 (Softex, Kanagawa, Japan). X-ray radiography was performed at 28 kV and 1 mA for 1.5 second, and imaged using a NAOMI digital X-ray sensor (RF Corp., Nagano, Japan).

### *Histomorphometry*

Rats were anesthetized with pentobarbital and the knee collected one week after surgery. As described previously [11], specimens were fixed at 4°C for 48 h in a 4% paraformaldehyde solution at pH 7.4. Samples were then decalcified for 45 days in 10% ethylenediaminetetraacetic acid (Sigma-Aldrich, Tokyo, Japan) at pH 7.4. After decalcification, samples were immersed in a 10% sucrose solution for 4 h, 15% sucrose for 4 h, and 20% sucrose for 8 h, and embedded in OCT compound (Sakura Finetek, Torrance, CA, USA). Serial 14- $\mu\text{m}$ -thick sagittal sections were stained with hematoxylin and eosin [12,13].

At one week, hematoxylin and eosin stained sections were subjected to histomorphometric analysis using WinROOF ver.7.0.0 image analysis software (Mitani, Tokyo, Japan). Three images were captured for each specimen at 20-fold magnification, and the number of chondrocytes and cell density area were determined. Three different regions (surface, middle, and deeper zones) of the cartilage at the contact area with the femur were measured with a standardized area of approximately 10,000  $\mu\text{m}^2$ .

### *Statistical analysis*

SPSS ver. 21 software for Windows (IBM, Chicago, IL, USA) was used for statistical analysis. Statistical significance among the 3 groups was estimated using one-way ANOVA and Tukey's method for post-hoc analysis. Data are expressed as the means  $\pm$  SD. Differences were considered significant at  $p < 0.05$ .

## **3. Results**

Histological characteristics of the cartilage are presented in Figure 3. There was no difference between the groups in the total cell number in any zone (deep zone: CTR,  $19.9 \pm 5.1$ ; CAJM,  $20.2 \pm 1.6$ ; ACL-T,  $17.6 \pm 3.0$ ;  $P = 0.558$ ; middle zone: CTR,  $21.6 \pm 4.8$ ; CAJM,  $15.9 \pm 3.4$ ; ACL-T,  $17.0 \pm 4.8$ ;  $P = 0.089$ ; surface zone: CTR,  $21.9 \pm 4.5$ ; CAJM,  $19.3 \pm 3.8$ ; ACL-T,  $19.6 \pm 6.0$ ;  $P = 0.644$ ) (Figure 4). In contrast,

the chondrocyte density area was significantly suppressed in the CAJM compared to the ACL-T group (deep zone: CTR,  $6.7 \pm 2.6\%$ ; CAJM,  $13.6 \pm 2.0\%$ ; ACL-T,  $12.0 \pm 7.6\%$ ;  $P = 0.032$ ; middle zone: CTR,  $14.3 \pm 2.7\%$ ; CAJM,  $13.6 \pm 4.9\%$ ; ACL-T,  $21.8 \pm 3.6\%$ ;  $P = 0.029$ ; surface zone: CTR,  $20.0 \pm 5.0\%$ ; CAJM,  $20.9 \pm 7.1\%$ ; ACL-T,  $33.4 \pm 14.9\%$ ;  $P = 0.019$ ) (Figure 5).

#### 4. Discussion

The ACL plays a prominent role in knee joint stability, and joint instability induced by injury to the ACL is a major risk factor for cartilage degeneration. Moreover, joint instability is a factor for the progression of OA in humans and animals [14-16]. Several researchers have used animal models of ACL injury to elucidate the pathophysiology of OA. Kamekura et al. showed that joint instability-induced ligament and meniscus injury was accelerated in a mouse knee model [5]. Tochigi et al. showed that the progression of OA increased at a rate proportional to the joint instability induced by ACL injury [4].

The current study investigated the effects of joint stability on the acute chondrocyte response following ACL injury. The responses described here at one week post-surgery might reflect the early phase of OA progression. In the acute phase, the CAJM model was able to suppress chondrocyte hypertrophy, as demonstrated by histological analysis. This result shows that joint instability is a factor in the chondrocyte response during the early phase. Together with prior work, it is apparent that joint instability caused by ACL injury is an important factor in cartilage degeneration.

Ihara et al. provided evidence of the effectiveness of conservative treatment of ACL injury by using the Kyuro knee brace with a coil spring traction system to allow early protective joint stability and promote ACL healing [7]. However, details of the influence of stabilizing the knee after ACL injury are not clear. Our laboratory created the CAJM model as a different model of joint instability where biomechanical function is restored by using a nylon suture. Our experimental model for preventing OA used a similar stabilization technique and has proven successful in controlling knee joint kinematics in small animals after ACL injury [8].

Because joint instability is a substantial contributor to cartilage degeneration, and to assess any difference of the acute cartilage cell response between joint instability and our novel model, we evaluated cartilage, using histomorphometry. Joint re-stabilization after ACL injury may suppress inflammatory cytokines, thereby delaying the progression of OA in the long term. However, some studies have indicated joint re-stabilization using surgical ACL reconstruction does not necessarily decrease the risk of developing OA [17]. Since intra-articular responses are induced by intra-articular surgery, it cannot be determined whether inflammation and secondary instability is a product of ACL transection or other mechanisms [18,19]. In our study, since an extra-articular bracing system was performed after ACL injury, intra-articular condition was same at both CAJM group and ACL-T group. A published study suggested that joint instability induced by ACL injury resulted in the formation of osteophytes that caused joint re-stabilization and decreased the joint range of motion [20]. Osteophytes can grow from any bone, but are most often found in the knee in OA patient [9]. Furthermore, chondrocyte proliferation and hypertrophy are associated with the process of osteophyte formation [9, 10]. Therefore, our model stabilizes the joint at an early stage, the density area was significantly decreased in the CAJM group.

Articular cartilage consists mainly of chondrocytes and extracellular matrix (ECM) (i.e.; type 2 collagen and proteoglycan). Therefore, the decreased density we observed indicated a loss of ECM as chondrocytes underwent necrosis via hypoxia. The reaction pattern of chondrocytes in osteoarthritic disease can be classified into categories. In particular, proliferation and hypertrophy of chondrocytes are involved in the main cellular response during the progression of OA. Sandell et al. showed that normal cartilage cells are small and uniform with low levels of proliferation [10]; however, activated chondrocytes showed high levels of proliferation. Cell proliferation may lead to chondrocyte clustering. These cells incorporate ECM proteins and differentiate into hypertrophic chondrocytes. The proliferation and hypertrophy of chondrocytes leads to the up-regulation of pro-inflammatory cytokines such as interleukin-1 $\beta$  and tumor necrosis factor- $\alpha$ , leading to a significant breakdown of cartilage [21]. These cytokines also inhibit anabolic factors, resulting in ECM degradation. In the present study, there was a significant reduction of

chondrocytes density in the CAJM compared to the ACL-T group. This result indicated that treatments that maintain joint stability in the acute phase, such as using a knee brace and ACL reconstruction, might be important in the prevention of knee OA.

Limitations of our study include the interpretation and application of our findings. First, we did not grade the degree of knee joint instability in our ACL model and, therefore, the relationship between the magnitude of joint instability and the extent of OA development could not be evaluated. The relevance of the degree of joint instability that initiates and allows the progression of OA should be considered in future studies. Second, one week after injury is very early to make conclusions about effects on cartilage. However, our previous study indicated a protective role of controlling abnormal joint kinematics after ACL transection in delaying the long-term degeneration of articular cartilage. Therefore, the current study focused on the response to acute lesions, although we recommend that future studies examine much later time points. Overall, further research is needed to fully characterize the features of mechanical stress that are associated with the development of OA after ACL injury. This information is required to guide the design of interventions that will optimize knee joint cartilage health after ACL injury.

### **Acknowledgements**

This research was supported partially by a Japan Society for the Promotion of Science KAKENHI Grant-in-Aid for Challenging Exploratory Research, 2014-2016 (26560278, Kiyomi Takayanagi).

### **Conflict of interest**

The authors have no conflicts of interest to declare.

### **Ethical approval**

The Animal Research Committee of Saitama Prefectural University approved all experiments in this study.

## References

- [1] Greene MA, Loeser RF (2015) Aging-related inflammation in osteoarthritis. *Osteoarthritis and Cartilage* 23:1966-71
- [2] Felson DT (2013) Osteoarthritis as a disease of mechanics. *Osteoarthritis and cartilage* 21;10-15
- [3] Nelson F, Billingham RC, Pidoux I, Reiner A, Langworthy M, McDermott M, Malogne T, Sitler DF, Kilambi NR, Lenczner E, Poole AR (2016) Early post-traumatic osteoarthritis-like changes in human articular cartilage following rupture of the anterior cruciate ligament. *Osteoarthritis Cartilage* 14:114-19
- [4] Tochigi Y, Vaseenon T, Heiner AD, Fredericks DC, Martin JA, Rudert MJ, Hillis SL, Brown TD, McKinley TO (2011) Instability dependency of osteoarthritis development in a rabbit model of graded anterior cruciate ligament transection. *J Bone Joint Surg Am* 93:640–647
- [5] Kamekura S, Hoshi K, Shimoaka T, Chung U, Chikuda H, Yamada T, Uchida M, Ogata N, Seichi A, Nakamura K, Kawaguchi H (2005) Osteoarthritis development in novel experimental mouse models induced by knee joint instability. *Osteoarthritis and cartilage* 13:632-641
- [6] Allen KD, Mata BA, Gabr MA, Huebner J., Adams Jr SB, Kraus VB, Schmitt DO, Setton LA. Kinematic and dynamic gait compensations resulting from knee instability in a rat model of osteoarthritis. *Arthritis Research & Therapy* 2012;14:R78
- [7] Ihara H, Miwa M, Takayanagi K, Nakayama A. (1994) Acute torn meniscus combined with acute cruciate ligament injury: second look arthroscopy after 3-month conservative treatment. *Clinical Orthopaedics and Related Research* 307:146-54.
- [8] Kokubun T, Kanemura N, Murata K, Moriyama H, Morita S, Jinno T, Ihara H, Takayanagi K (2016) Effect of Changing the Joint Kinematics of Knees With a Ruptured Anterior Cruciate Ligament on the Molecular Biological Responses and Spontaneous Healing in a Rat Model. *The American Journal of Sports Medicine*, pii: 0363546516654687.
- [9] van der Kraan PM, van den Berg WB (2007) Osteophytes: relevance and biology. *Osteoarthritis Cartilage* 15:237-244
- [10] Sandell LJ, Aigner T (2001) Articular cartilage and changes in arthritis. An

introduction: cell biology of osteoarthritis. *Arthritis Res* 3:107–113.

- [11] Murata K, Kanemura N, Kokubun T, Fujino T, Matsumoto J, Yasui K, Takayanagi K (2014). Age-related changes in collagen degeneration of the rotator cuff in an animal model. *American Journal of Biomedical and Life Sciences* 2: 156-162.
- [12] Schmitz N, Laverty S, Kraus VB, Aigner T (2010). Basic methods in histopathology of joint tissues. *Osteoarthritis and cartilage* 18:113-116.
- [13] Gerwin N, Bendele AM, Glasson S, Carlson CS (2010). The OARSI histopathology initiative—recommendations for histological assessments of osteoarthritis in the rat. *Osteoarthritis and Cartilage* 18: 24-34.
- [14] Egloff C, Hart DA, Hewitt C, Vavken P, Valderrabano V, Herzog W. (2016) Joint instability leads to long-term alterations to knee synovium and osteoarthritis in a rabbit model. *Osteoarthritis and Cartilage* 24:1054-60.
- [15] Gustafson JA, Gorman S, Fitzgerald GK, Farrokhi S. (2015) Alterations in walking knee joint stiffness in individuals with knee osteoarthritis and self-reported knee instability. *Gait Posture* 43:210-5.
- [16] Dayal N, Chang A, Dunlop D, Hayes K, Chang R, Song J, Torres L, Sharma L (2005) The natural history of anteroposterior laxity and its role in knee osteoarthritis progression. *Arthritis & Rheumatism* 52:2343-2349.
- [17] Simon D, Mascarenhas R, Saltzman BM, Rollins M, Bach BR, MacDonald P (2015) The relationship between anterior cruciate ligament injury and osteoarthritis of the knee. *Advances in orthopedics*, DOI:10.1155/2015/928301
- [18] Bigoni M, Sacerdote P, Turati M, Franchi S, Gandolla M, Gaddi D, Moretti S, Munegato D, Augusti CA, Bresciani E, Omeljaniuk RJ, Locatelli V, Torsello A (2013) Acute and late changes in intraarticular cytokine levels following anterior cruciate ligament injury. *Journal of Orthopaedic Research* 31:315-321.
- [19] Bigoni M, Turati M, Gandolla M, Sacerdote P, Piatti M, Castelnovo A, Franchi S, Gorla M, Munegato Daniele, Gaddi D, Pedrocchi A, Omeljaniuk RJ, Locatelli V, Pedrocchi, A. (2016) Effects of ACL Reconstructive Surgery on Temporal Variations of Cytokine Levels in Synovial Fluid. *Mediators of Inflammation*, DOI: 10.1155/2016/8243601
- [20] Hsia AW, Anderson MJ, Heffner MA, Lagmay EP, Zavodovskaya R, Christiansen BA (2016) Osteophyte formation after ACL rupture in mice is

associated with joint restabilization and loss of range of motion. Journal of Orthopaedic Research. DOI: 10.1002/jor.23252

- [21] Van der Kraan PM, van den Berg WB. (2012) Chondrocyte hypertrophy and osteoarthritis: role in initiation and progression of cartilage degeneration. Osteoarthritis and Cartilage 20:223-32.

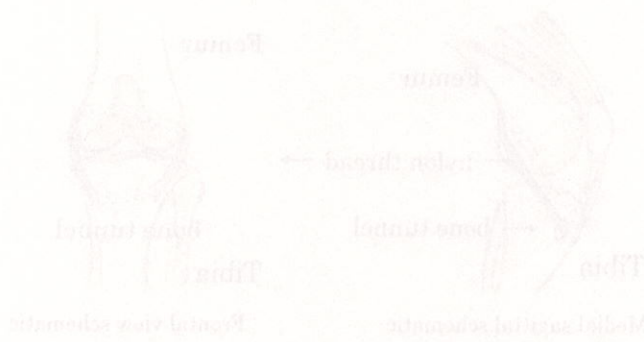
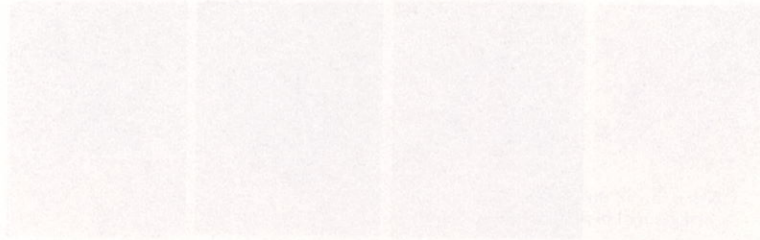


Figure 1

Controlled experiment joint movement model. The medial capsule of the right knee joint was exposed without damage the patellar tendon (A), and the ACL was completely transected (B). To relieve a damping force in the knee joint after ACL transection, a bone tunnel to the anterior proximal tibia was created and a tylon thread passed through the tunnel (C). The thread was tied and secured to the posterior distal femur (D), thus directing the anterior drawing force of the femur on the tibia (E). A schematic of the surgical procedure is shown in the bottom panel.

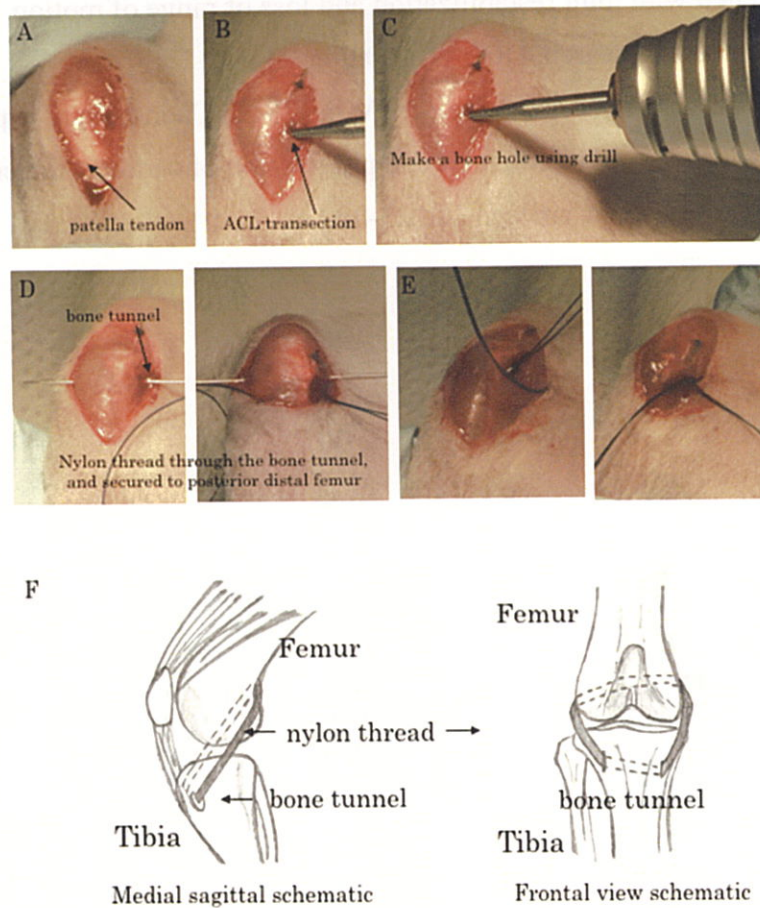


Figure 1

Controlled abnormal joint movement model. The medial capsule of the right knee joint was exposed without disrupting the patellar tendon (A), and the ACL was completely transected (B). To achieve a damping force in the knee joint after ACL transection, a bone tunnel to the anterior proximal tibia was created and a nylon thread passed through the tunnel (C). The thread was tied and secured to the posterior distal femur (D), thus dampening the anterior drawing force of the femur on the tibia (E). A schematic of the surgical procedure is shown in the bottom panel.

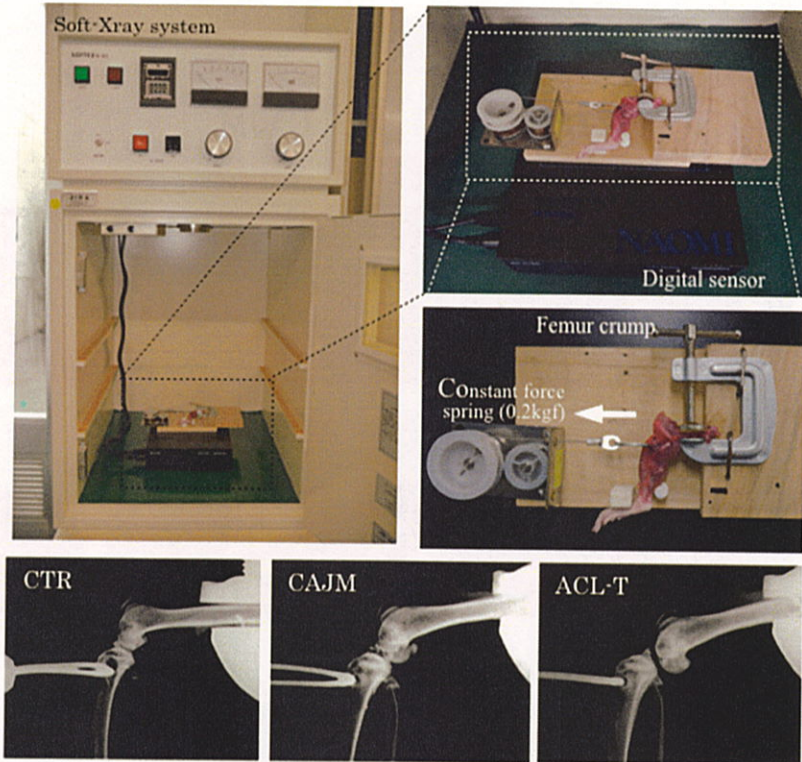


Figure 2

Influence of the controlled abnormal joint movement (CAJM) model. Joint instability was evaluated using soft x-ray radiography (M-60; Softex, Tokyo, Japan). Differences in joint instability between the CAJM and anterior cruciate ligament with abnormal joint movement (ACL-T) models are shown. CTR, control..

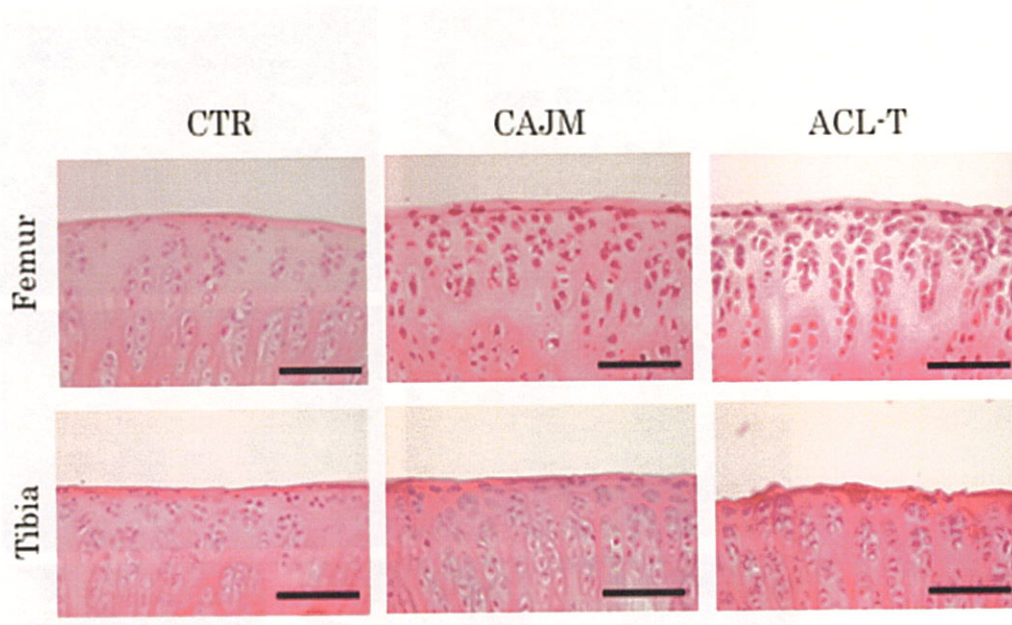


Figure 3

Histomorphometry results. One week post-surgery, articular cartilage from control (CTR), anterior cruciate ligament with abnormal joint movement (ACL-T), and controlled abnormal joint movement (CAJM) rats were sectioned sagittally and stained with hematoxylin and eosin. Scale bar, 50  $\mu$ m.

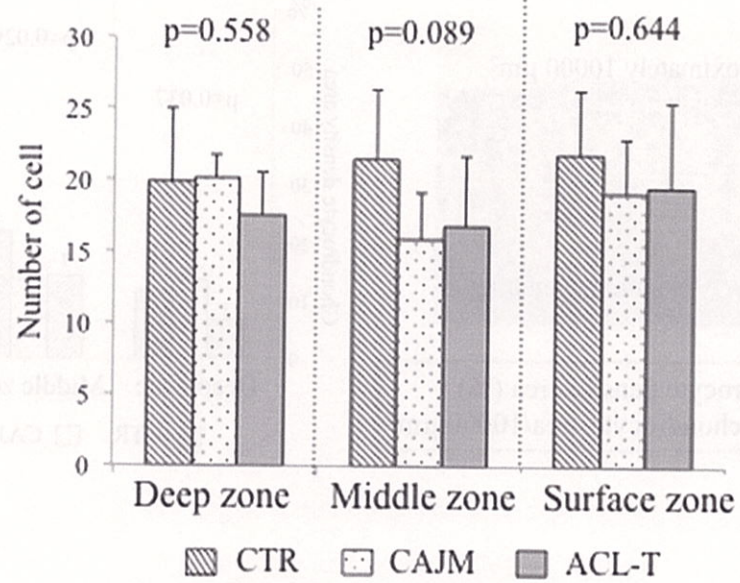


Figure 4  
 Number of chondrocyte in the surface, middle, and deep zones of the articular cartilage. CAJM, controlled abnormal joint movement group; ACL-T, anterior cruciate ligament with abnormal joint movement; CTR, control group. Data are expressed as means  $\pm$  SD. There were no significant differences between zones or treatments.

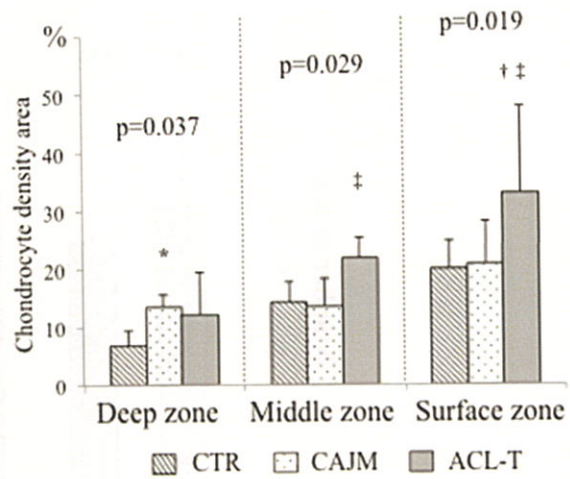
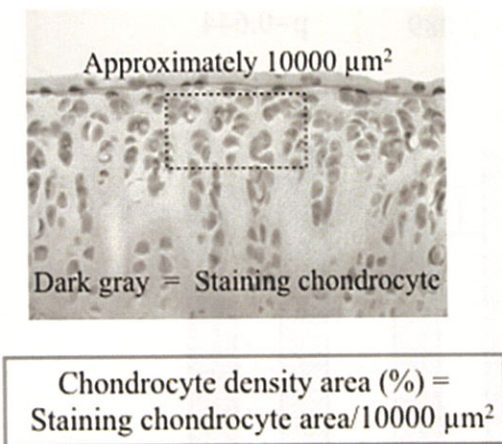


Figure 5

Chondrocyte density areas in the surface, middle, and deep zones of the articular cartilage.

Chondrocyte density area (%) = stained chondrocyte area ( $\mu\text{m}^2$ )/10,000  $\mu\text{m}^2 \times 100$ . CAJM, controlled abnormal joint movement group; ACL-T, anterior cruciate ligament with abnormal joint movement; CTR, control group. Data are expressed as means  $\pm$  SD. \*CTR vs. CAJM; †CTR vs. ACL-T; ‡CAJM vs. ACL-T.

発表論文 (3)

**Controlling abnormal joint movement inhibits response of osteophyte formation**

Kenji Murata, Takanori Kokubun, Yuri Morishita, Katsuya Onistuka, Shuhei Fujiwara, Aya Nakashima, Tsutomu Fujino, Kiyomi Takayanagi, Naohiko Kanemura.

*Cartilage*, First Published April 11, 2017.



## Controlling abnormal joint movement inhibits response of osteophyte formation

Kenji Murata MSc <sup>1</sup>, Takanori Kokubun, PhD <sup>1</sup>, Yuri Morishita, MSc <sup>2</sup>,  
Katsuya Onitsuka <sup>2</sup>, Shuhei Fujiwara <sup>2</sup>, Aya Nakajima <sup>2</sup>, Tsutomu Fujino, MSc <sup>2</sup>,  
Kiyomi Takayanagi PhD <sup>1</sup>, Naohiko Kanemura, PhD <sup>1\*</sup>

<sup>1</sup> Department of Physical Therapy, School of Health and Social Services, Saitama Prefectural University, Saitama, Japan

<sup>2</sup> Department of Health and Social Services, Course of Health and Social Services, Graduate School of Saitama Prefectural University, Saitama, Japan

**\* Corresponding author:**

Naohiko Kanemura, PhD.

Department of Physical Therapy, School of Health and Social Services, Saitama Prefectural University, Saitama, Japan

Tel: +81-489-73-4123 Fax: +81-489-73-4123 E-mail: kanemura-naohiko@spu.ac.jp

## Abstract

*Objective:* Osteoarthritis (OA) is induced by accumulated mechanical stress to joints; however little has been reported regarding the cause among detailed mechanical stress on cartilage degeneration. This study investigated the influence of the control of abnormal joint movement induced by anterior cruciate ligament (ACL) injury in the articular cartilage.

*Design:* The animals were divided into 3 experimental groups: CAJM group (n = 22: controlling abnormal joint movement), ACL-T group (n = 22: knee anterior instability increased), and INTACT group (n = 12: no surgery). After 2 and 4 weeks, the knees were harvested for digital microscopic observation, soft X-ray analysis, histological analysis, and synovial membrane molecular evaluation.

*Results:* The 4-week OARSI scores showed that cartilage degeneration was significantly inhibited in the CAJM group as compared with the ACL-T group ( $P < 0.001$ ). At 4 weeks, the osteophyte formation had also significantly increased in the ACL-T group ( $P < 0.001$ ). These results reflected the microscopic scoring and soft X-ray analysis findings at 4 weeks. Real-time synovial membrane PCR analysis for evaluation of the osteophyte formation-associated factors showed that the mRNA expression of *BMP-2* and *VEGF* in the ACL-T group had significantly increased after 2 weeks.

*Conclusions:* Typically, abnormal mechanical stress induces osteophyte formation; however, our results demonstrated that CAJM group inhibited osteophyte formation. Therefore, controlling abnormal joint movement may be a beneficial precautionary measure for OA progression in the future.

**Keywords:** Osteoarthritis; Articular cartilage; Osteophyte, Animal model

**Running title:** Effect of controlling joint movement

## **Introduction**

Knee osteoarthritis (OA) is a type of joint disease that results from cartilage degradation and osteophyte formation in joints, and believed to be caused by accumulated mechanical stress.<sup>1</sup> Generally, anterior cruciate ligament (ACL) transection model is widely used to elucidation of a mechanism of OA progression.<sup>2,3</sup> ACL transection promotes abnormal joint motion, such as anterior translation of tibia, and the abnormal mechanical stress may develop between the femur and tibia cartilage.

In our previous studies, to establish abnormal joint motion of the tibia and its controlled effect, we created a controlled abnormal joint movement (CAJM) model to restore the biomechanical function following ACL transection through a nylon suture placed on the outer aspect of the knee joint.<sup>4</sup> Using the CAJM model, we reported the controlled abnormal joint movement suppress inflammatory cytokines may help to delay the progression of OA.<sup>5</sup>

Moreover, other studies indicated that anterior translation of the tibia induced by ACL injury was related to osteophyte formation.<sup>6-8</sup> Anterior translation of the tibia causes abnormal joint mechanics by changes in contact stress. This change in contact stress results in an increase in concentration of various growth factors during osteophyte progression in the knee. In particular, the synovial membrane exhibits increased transforming growth factor beta (TGF- $\beta$ ), bone morphogenetic proteins (BMPs), and vascular endothelial growth factor (VEGF), which play an initial and terminal role in differentiation.<sup>9-11</sup> Although symptoms are not always present, various growth factors are expressed during the progression of osteophytes in the knees of patients with OA, and osteophytes are understood to be a result of abnormal mechanical stress.

We hypothesized that the abnormal joint movement is probably more from increased contact stresses on the joint, which the bone osteocytes will sense via Wolff's Law, and then the bone "senses" that it needs to "grow" osteophytes in order to limit the abnormal movement. The objective this study was to evaluate osteophyte formation and cartilage degeneration on controlled abnormal joint movement using histological and molecular biological analyses. These findings may help to understand the progression of OA and to provide new prevention methods for patients with OA.

## **Material and Methods**

## Animals and Experimental Design

All procedures were approved by the Ethics Committee of Saitama Prefectural University (approval number: 27-9). A new protocol was devised according to the “Animal Research: Reporting of in Vivo Experiments (ARRIVE)” guidelines.<sup>12</sup> A total of 56 ten-week-old Wistar rats (Sankyo Labo Service Corp., Tokyo, Japan) were obtained for use in this study (Fig. 1). The animals were divided into 3 experimental groups: an intact group (INTACT, n = 12: the rats did not undergo any surgery), a CAJM group (CAJM, n = 22: external support was provided to decrease anterior translation after complete ACL transection), and an ACL transection group (ACL-T, n = 22: bone tunnel with complete ACL transection, anterior translation increased). All rats were housed and maintained on a 12-hour light-dark cycle at a constant temperature of 23°C, with free access to food and tap water.

## Surgical Procedures

As described previously,<sup>4,5,13</sup> the ACL-T and CAJM models were established after anesthetization of the rats with pentobarbital (0.8 ml/kg) (Supplementary methods). The medial capsule of the right knee joint was exposed without disrupting the patellar tendon, and the ACL was completely transected. Both models were established by creating a bone tunnel along the anterior aspect of the proximal tibia. In the ACL-T group, the skin was closed with a 4-0 nylon suture and was disinfected. In the CAJM group, a nylon thread was passed through the bone tunnel and was tied to the posterior aspect of the distal femur. A reduction in abnormal joint movements was achieved without intra-articular suturing of the ligament.

## Functional Recovery and Anterior Translation Examination

The postoperative recovery of motor function was evaluated by placing rats randomly selected from different groups onto an accelerating rotarod (Muromachi Kikai Co., Japan) for rotarod analysis. To rule out differences in learning skills between the 3 groups of rats, each group was assessed over 3 trials (the rotation speed was adjusted to 10 rotations per minute). The motor function of each animal was determined by averaging the scores of 3 trials.

At 2 and 4 weeks, 6 rats from each group (n = 36) were sacrificed following anesthetization with pentobarbital, and their right lower limbs (including the knee joints) were examined radiographically. The femur was subjected to examination systems,<sup>4</sup> and the anterior translation of the tibia was evaluated with anterior traction using a 0.2 kgf constant force spring (Sunco Spring Corp., Kanagawa, Japan). Radiographs were

captured with a soft radiogram M-60 (Softex Corp., Kanagawa, Japan). X-ray radiography was performed at 28 kV and 1 mA for 1.5 seconds, and images were captured with a NAOMI digital X-ray sensor (RF Corp., Nagano, Japan). Digital images were used to quantify the anterior displacement relative to control rats under normal conditions using the ImageJ software (National Institutes of Health, Bethesda, MA, USA).

### Osteophyte Scoring from Radiographic Examination

To evaluate the changes in OA, the rats were positioned with their knee flexed at 90 degrees. Following scanning, the osteophyte score was evaluated based on a previous study<sup>14</sup> (Supplemental Table 1). The scoring comprised osteophyte, cyst, joint space, and sclerosis measurements.

### Histological Analysis

The rat knees were fixed in a 4% paraformaldehyde solution for 48 hours and were decalcified in a Super Decalcifier I solution (Polysciences Inc, Taipei, Taiwan) for 24 hours. They were subsequently washed with phosphate-buffered saline and were embedded in an optimal cutting temperature compound (Sakura Finetek Japan, Tokyo, Japan). The specimens were cut 16  $\mu\text{m}$  from the tibial plateau and femur on the frontal plane. Sections were stained with safranin-O/fast green staining and alizarin red/Alcian blue staining, and were rated according to the Osteoarthritis Research Society International (OARSI) scoring system for cartilage.<sup>15</sup> Every 3 sections of the 4 areas (i.e., the medial tibia, lateral tibia, medial femur, and lateral femur) were evaluated according to previously reported methods.<sup>16</sup> This scoring system consists of 2 subcategories: the grade (6 points) and the stage (4 points). The total OARSI scores were calculated as the “grade x stage.” A total score of 24 indicated severe OA, while a score of 0 indicated a normal joint. Four areas per section calculated the summed total score (0 to 96). According to a previous study,<sup>17</sup> the osteophytes were evaluated semi-quantitatively using osteophyte formation scores consisting of 2 dimensions: the size and maturity (Supplemental Table 2). Four areas per section (i.e., the medial tibia, lateral tibia, medial femur, and lateral femur) were evaluated to calculate the summed total score (0 to 24).

### Microscopic Examination

Five knee joints were harvested from each of the CAJM and ACL-T groups (n = 20) at 2 and 4 weeks after the surgery, and the samples were carefully separated from the tibia and femur. The contralateral articular

cartilage (left side) of the ACL-T group was used for INTACT. The tibia and femur were stained with Indian ink to visualize the damaged region. Microscopic pictures of the femur and tibia were captured with a digital microscopic system (Keyence, Tokyo, Japan). Based on a previous study,<sup>18</sup> the cartilage degeneration of the femur and the tibial surface was evaluated through macroscopic scoring on a scale of 0 to 5 points (Supplemental Table 3).

### Quantitative mRNA Expression

The *TGF- $\beta$* , *BMP-2*, and *VEGF* mRNA expression levels associated with bone marrow progression in the synovial membranes were evaluated with a real-time polymerase chain reaction (PCR) 2 weeks and 4 weeks after the surgery in the CAJM and ACL-T groups. The contralateral articular cartilage (left side) of the ACL-T group was used for standardization (normal tissue samples). The synovial membranes were isolated and immersed in an RNA-stabilizing solution (Ambion, TX, USA). The total RNA was extracted with an RNeasy Lipid Tissue Mini Kit (QIAGEN, CA, USA) according to the manufacturer's instructions. The synthesis of the cDNA was conducted with a high-capacity cDNA reverse transcription kit (Applied Biosystems, CA, USA). A real-time PCR was performed with a StepOne-Plus real-time system (Applied Biosystems, CA, USA) using 2  $\mu$ L of cDNA in the presence of the appropriate primers (TaqMan primers, NE, USA): *BMP-2*, *TGF- $\beta$* , and *VEGF* (Table 1). The relative expression levels of the genes were normalized to a housekeeping gene (*glyceraldehyde-3-phosphate dehydrogenase; GAPDH*) using the  $2^{-\Delta\Delta Ct}$  method to calculate the relative levels of mRNA expression.

### Statistical Analysis

Statistical analysis was performed with SPSS ver. 21.0 software (IBM Japan, Tokyo, Japan). The normality of the value distribution for each variable was evaluated with a Shapiro-Wilk test. A parametric statistical analysis of the 3 groups was performed with a one-way analysis of variance followed by a Tukey post-hoc analysis. A non-parametric statistical analysis was performed with a Kruskal-Wallis test followed by a Mann-Whitney U-test for pair-wise differences. The resulting p-values were compared with Bonferroni's corrected value ( $p = 0.017$ ), which was calculated based on the number of pair-wise comparisons made. To compare the 2 groups, a parametric statistical analysis was performed with the Student-t test. A non-parametric statistical analysis was performed with the Mann-Whitney U-test. Moreover, the correlation coefficient between the anterior translation and scores were calculated. *P*-values < 0.05 were considered significant.

## Results

There were no significant changes in the weight of the normal rats 2 weeks after surgery ( $p = 0.191$  with ANOVA; INTACT, 273 [252 to 293] g; CAJM, 279 [269 to 290] g; ACL-T, 287 [278 to 297] g) and 4 weeks after surgery: ( $p = 0.066$  with ANOVA; INTACT, 297 [277 to 316] g; CAJM, 282 [271 to 292] g; ACL-T, 299 [287 to 310] g) (Fig. 2A). The evaluation through the rotarod test after surgery demonstrated that the results did not differ between the 3 groups at 2 weeks ( $p = 0.586$  with ANOVA; INTACT, 14.1 [10.4 to 17.8] sec; CAJM, 13.3 [8.5 to 18.2] sec; ACL-T, 12.1 [7.4 to 16.7] sec) and 4 weeks ( $p = 0.989$  with ANOVA; INTACT, 15.3 [12.3 to 19.6] sec; CAJM, 15.6 [12.1 to 19.2] sec; ACL-T, 16.9 [12.3 to 20.1] sec) after surgery (Fig. 2B).

To evaluate the anterior translation after surgery, an X-ray was performed with our original anterior joint instability measurement system at 2 and 4 weeks. At 2 weeks, the anterior translation of the CAJM group had significantly decreased relative to the ACL-T group (INTACT, 0.301 [0.165 to 0.427] mm; CAJM, 0.556 [0.205 to 0.907] mm; ACL-T, 1.414 [0.959 to 1.868] mm). The anterior translation had also increased in the ACL-T group at four weeks (INTACT, 0.144 [0.114 to 0.173] mm; CAJM, 0.379 [0.122 to 0.636] mm; ACL-T, 0.876 [0.573 to 1.179] mm). Exact P-values are given in Fig. 2C.

### Osteophyte Scoring using Radiographic Examination

To evaluate the knee OA, soft X-ray digital scanning was performed at 2 and 4 weeks, respectively, and was graded with Oprenyeszki's score<sup>18</sup> (Fig. 3). At 2 weeks, the scores of the ACL-T groups were significantly higher than those of the INTACT groups (INTACT, 0 [0 to 1]; CAJM, 1 [1 to 2]; ACL-T, 1.5 [1 to 2]); however, no significant differences were detected between the CAJM and ACL-T groups ( $p = 0.233$  with post-hoc Mann-Whitney U-test; Bonferroni correction). At four weeks, the scores of the ACL-T groups were significantly lower than those of the CAJM and INTACT groups (INTACT, 0 [0 to 1]; CAJM, 1 [1 to 2]; ACL-T, 2.5 [2 to 3]). No significant differences were noted between the CAJM and ACL-T groups ( $p = 0.064$  with post-hoc Mann-Whitney U-test; Bonferroni correction).

### Microscopic Examination

The articular cartilage was graded according to the degeneration progression in the tibia and femur based on a macroscopic examination (Fig. 4). At 2 weeks, in the tibial cartilage, no significant differences were detected among the 3 groups ( $p = 0.536$  with ANOVA; INTACT, 0.4 [0.0 to 1.0]; CAJM, 1.2 [0.0 to 2.2]; ACL-T, 1.4 [0.8 to 2.0]). At four weeks, the ACL-T group had higher tibia scores than the CAJM group and the INTACT group (INTACT, 0.2 [0.0 to 0.7]; CAJM, 1.2 [0.7 to 1.6]; ACL-T, 3.6 [2.3 to 4.9]). In comparison with the INTACT group, the femoral cartilage was significantly increased in the CAJM and ACL-T groups at 2 weeks (INTACT, 0.4 [0.0 to 1.0]; CAJM, 2.0 [1.2 to 2.6]; ACL-T, 2.2 [1.3 to 3.1]) and 4 weeks (INTACT, 0.4 [0.0 to 1.0]; CAJM, 2.0 [0.2 to 3.4]; ACL-T, 2.8 [1.6 to 4.0]).

### Histological Analysis of Cartilage Degeneration

Histological characteristics at four weeks are presented in Fig. 5. The CAJM group exhibited enlargement of the cartilage lacuna and increased the number of chondrocytes. Moreover, the ACL-T group exhibited a confirmed cluster of chondrocytes and surface fibrillation.

To evaluate the articular cartilage at 2 and 4 weeks, the latter was graded based on the OARSI histological scoring system (Fig. 5). At 2 weeks, the total OARSI score was significantly higher in the ACL-T group and CAJM group than in the INTACT groups (INTACT, 0 [0 to 1]; CAJM, 1 [1 to 4]; ACL-T, 2.5 [0 to 3]). However, there were no differences between the CAJM and ACL-T groups ( $p = 0.502$ , with post-hoc Mann-Whitney U-test; Bonferroni correction). At 4 weeks, the total OARSI score was significantly higher in the ACL-T group than in the CAJM and INTACT groups (INTACT, 0 [0 to 2]; CAJM, 2 [0 to 4]; ACL-T, 9 [3 to 17]). Exact P-values are given in Fig. 5.

#### Histological Analysis of Osteophyte Formation

The total osteophyte formation score was significantly higher in the ACL-T group and CAJM group than in the INTACT groups (INTACT, 0 [0 to 9]; CAJM, 2 [0 to 4]; ACL-T, 3 [2 to 4]) at 2 weeks. However, there were no differences between the CAJM and ACL-T groups ( $p = 0.389$ , with post-hoc Mann-Whitney U-test; Bonferroni correction). The scores at 4 weeks were significantly higher in the ACL-T group than in the CAJM group or the INTACT group (INTACT, 2 [2 to 2]; CAJM, 4 [3 to 6]; ACL-T, 6 [4 to 6]). Moreover, the correlation coefficient between the anterior translation weight and score were significant ( $p < 0.001$ ,  $R^2 = 0.63$ ). Exact P-values are given in Fig. 6.

#### mRNA Expression Levels in Synovial Membranes

The synovial membrane of the rats in the CAJM and ACL-T groups was harvested 2 and 4 weeks after the surgery. A real-time PCR was used to assess the alterations in the expression levels of the genes associated with osteophyte progression, and the changes in the CAJM and ACL-T groups were compared with the expression levels of the normal tissues (i.e., normal tissue samples harvested from the opposite knee) at the baseline. As shown in Fig. 7, at 2 weeks, the *BMP-2*, *TGF- $\beta$* , and *VEGF* mRNA expression levels were approximately 3.80-fold, 1.01-fold, and 2.18-fold higher in the ACL-T group, and 1.29-fold, 1.37-fold, and 1.40-fold higher in the CAJM group, respectively. The mRNA expression levels of *BMP-2* and *VEGF* in the ACL-T group were aberrantly significantly upregulated as compared with those in the CAJM group. The *BMP-2*, *TGF- $\beta$* , and *VEGF* mRNA expression levels were approximately 4.46-fold, 1.00-fold, and 0.81-fold higher in the ACL-T group, and 3.11-fold, 1.00-fold, and 1.33-fold higher in the CAJM group, respectively. The mRNA expression levels of the *BMP-2* and *VEGF* in the CAJM group were aberrantly significantly upregulated as compared with those in the ACL-T group.

## Discussion

Based on a previous study,<sup>4,5,13</sup> the present study used the CAJM model to understand the relationship of abnormal joint movements to the progression of articular cartilage degeneration and osteophyte formation. This model used a nylon suture to induce normal joint movement. As a result, the histological data indicated that the CAJM model significantly decreased cartilage degeneration and limited osteophyte formation and certain mRNA expressions according to osteophyte growth factors in the synovial membrane.

The abnormal joint motion caused by knee injury is a predominant factor in OA progression.<sup>19</sup> In animal models, abnormal joint movement, such as joint instability, leads to long-term alterations of the knee articular cartilage, as evidenced in mouse,<sup>3,6,20</sup> rat,<sup>5,13</sup> and rabbit models.<sup>2,21</sup> In particular, in rabbit model, the degree of anterior translation induced by ACL transection model was associated with degeneration of the articular cartilage.<sup>2</sup> Our model was designed to induce a biomechanical change, such as anterior translation, with nylon sutures. The results demonstrated different anterior translation between the ACL-T and CAJM models at 2 and 4 weeks, and the CAJM model inhibited the degeneration of the articular cartilage more than the ACL-T model. These findings indicated that the control of anterior joint instability had a beneficial effect on the articular cartilage, our model has obtained an analogous result to the previous research.

On the other hand, osteophytes are small spurs that form in and around the knee joint as a result of chronic inflammation. Although the mechanism of osteophyte formation in OA remains unclear, the involvement of the synovial membrane in osteophyte formation appeared within 2 weeks of the induction of experimental OA. According to our hypothesis, abnormal anterior translation of the tibia probably results from increased contact stresses on the bone, which the bone osteocytes will sense via Wolff's Law, and then the bone will "sense" that it needs to "grow" osteophytes in order to limit the abnormal motion. In particular, in animal models, anterior translation at a relatively early stage has been reported to reduce the range of motion with osteophytes.<sup>7, 21</sup> As the present model was a method to reduce abnormal joint movement at an early stage, the formation of osteophytes may have been mild.

In addition, the synovial membrane is an important site of osteophyte formation. The edges of the cartilage, which receive appropriate nutrition from the synovial membrane, induce the formation of osteophytes. Various growth factors are expressed in the osteophytes of experimental models and clinical patients. Both the TGF-beta and BMP2 can induce major osteophytes in murine knee joints. Moreover, in animal models,<sup>9-11</sup> newborn blood vessel factors such as the VEGF, VEGF-

receptor, VCAM, and FGF-2 also contribute to the growth of osteophytes as they supply nutrition. In the present study, the ACL-T model exhibited osteophyte formation at 4 weeks, and the synovial membrane mRNA expression levels of the BMP-2 and VEGF were increased at the 2- and 4-week time points in the ACLT model. These results indicated that the control of anterior translation inhibited osteophyte formation. Previous research has shown that anterior translation at 4 weeks after surgery was reduced in an ACL transection rat model, as the recovery process for animal models was expedited compared to that for humans.<sup>22</sup> Moreover, anterior translation induced by ACL injury requires osteophyte formation, and the range of motion and joint mobility is subsequently reduced.<sup>20</sup> Considering these various findings, osteophytes are probably a result of instability and may limit joint motion, but they form as a result of bone growth due to increased contact stress resulting from abnormal joint mechanics. On the other hand, for articular cartilage, the factors associated with osteophyte formation have been shown to induce OA. These abnormal contact stresses play a crucial role in the physiology of various tissues: mechanical signals are critical determinants of tissue morphogenesis and maintenance; however, high-strain mechanotransduction by cartilage mechanical stress is relevant to the pathogenesis of OA. The present results indicate that the control of contact stress resulting from abnormal anterior instability suppressed cartilage degeneration, which was associated with osteophyte formation in the histological and real-time PCR analyses. These findings showed that an appropriate contact stress condition maintained cartilage formation, and re-stabilization of the joint provided a good mechanical condition for the knee after ACL injury.

In order to interpret and apply the findings of the study properly, its limitations should be acknowledged. First, the experimental period only included the 2- and 4-week points after surgery; the long-term effects of cartilage degeneration and osteophyte formation were not examined. However, one of our previous studies showed that the CAJM model induced lower cartilage degeneration than the ACL-T model 12 weeks after surgery. Therefore, this study focused on controlling abnormal joint movement of the knee in an early stage. Second, the use of an experimental rat model, which implied a small knee joint size, meant that changes in the joint kinematics (including the tibial rotation) following ACL transection could not be accurately evaluated. Although, anterior displacement was measured by the distance between the non-traction condition and the anterior traction condition at each sacrifice time point, the anterior displacement differences at the later postoperative times between the control, CAJM, and ACL-T knees may also be due to changes in the knee soft tissues resulting from the surgical procedures and tissue responses.

In conclusion, this study examined the association between anterior translation and osteophyte formation in the progression of articular cartilage degeneration. It appeared that the control of abnormal joint movement was indeed associated with the inhibition of cartilage degeneration and osteophyte formation, as evidenced with microscopic, histological, and biochemical analyses. However, further research is required to characterize the features of mechanical stress associated with the development of OA and to gather information to guide the development of interventions intended to optimize the cartilage health of the knee joint.

### **Abbreviations**

ACL: anterior cruciate ligament

ACL-T: ACL transection

BMP: bone morphogenetic protein

CAJM: controlled abnormal joint movement

OA: osteoarthritis

OARSI: Osteoarthritis Research Society International

PCR: polymerase chain reaction

TGF- $\beta$ : transforming growth factor beta

VEGF: vascular endothelial growth factor

### **Acknowledgments**

The authors would like to thank Yuki Minegishi (Koseikai Hospital, PT), Daisuke Shimizu (Kasukabe-kose Hospital, PT), Mitsuhiro Kameda (Kasukabe Chuo General Hospital), Namine Kiso, Kanae Mastui, Kaichi Ozone, Shiori Tsukamoto, Yuichiro Oka, Yoko Shirose, and Nozomi Kuwahara (students at Saitama Prefectural University) for their assistance with the surgery and sample collection.

### **Conflicts of interest**

None of the authors have conflicts of interest related to the manuscript.

### **Role of the funding source**

This study was supported by the Sasakawa Scientific Research Grant from The Japan Science Society (28-621).

## References

1. Buckwalter JA, Anderson DD, Brown TD, Tochigi Y, Martin JA. The roles of mechanical stresses in the pathogenesis of osteoarthritis: implications for treatment of joint injuries. *Cartilage*. 2013;4(4):286-294. doi: 10.1177/1947603513495889
2. Tochigi Y, Vaseenon T, Heiner AD, Fredericks DC, Martin JA, Rudert MJ, Hillis SL, Brown TD, McKinley TO. Instability dependency of osteoarthritis development in a rabbit model of graded anterior cruciate ligament transection. *J Bone Joint Surg Am*. 2011;93(7):640-647. doi: 10.2106/JBJS.J.00150.
3. Kamekura S, Hoshi K, Shimoaka T, Chung U, Chikuda H, Yamada T, Uchida M, Ogata N, Seichi A, Nakamura K, Kawaguchi H. Osteoarthritis development in novel experimental mouse models induced by knee joint instability. *Osteoarthritis Cartilage*. 2005;13(7):632-641.
4. Kokubun T, Kanemura N, Murata K, Moriyama H, Morita S, Jinno T, Ihara H, Takayanagi K. Effect of changing the joint kinematics of knees with a ruptured anterior cruciate ligament on the molecular biological responses and spontaneous healing in a rat model. *Am J Sports Med*. 2016;44(11):2900-2910.
5. Murata K, Kanemura N, Kokubun T, Fujino T, Morishita Y, Onitsuka K, Fujiwara S, Nakajima A, Shimizu D, Takayanagi K. Controlling joint instability delays the degeneration of articular cartilage in a rat model. *Osteoarthritis Cartilage*. 2017;25(2):297-308. doi: 10.1016/j.joca.2016.10.011.
6. Hsia AW, Anderson MJ, Heffner MA, Lagmay EP, Zavodovskaya R, Christiansen BA. Osteophyte formation after ACL rupture in mice is associated with joint restabilization and loss of range of motion. *J Orthop Res*. 2016. doi: 10.1002/jor.23252. [Epub ahead of print]
7. van der Kraan PM, van den Berg WB. Osteophytes: relevance and biology. *Osteoarthritis Cartilage*. 2007;15(3):237-244.
8. Dayal N, Chang A, Dunlop D, Hayes K, Chang R, Cahue S, Song J, Torres L, Sharma L. The natural history of anteroposterior laxity and its role in knee osteoarthritis progression. *Arthritis Rheum*. 2005;52(8):2343-2349.
9. Davidson EB, Vitters EL, Van Der Kraan PM, van den Berg WB. Expression of transforming growth factor- $\beta$  (TGF $\beta$ ) and the TGF $\beta$  signalling molecule SMAD-2P in spontaneous and instability-induced osteoarthritis: role in cartilage degradation, chondrogenesis and osteophyte formation. *Ann Rheum Dis*. 2006;65:1414-1421.
10. Kaneko H, Ishijima M, Futami I, Tomikawa N, Kosaki K, Sadatsuki R, Yamada Y, Kurosawa H, Kaneko K, Arikawa-Hirasawa E. Synovial perlecan is required for osteophyte formation in knee osteoarthritis. *Matrix Biol*. 2013;32(3-4):178-187. doi: 10.1016/j.matbio.2013.01.004.
11. Hashimoto S, Creighton-Achermann L, Takahashi K, Amiel D, Cooutts

- RD, Lotz M. Development and regulation of osteophyte formation during experimental osteoarthritis. *Osteoarthritis Cartilage*. 2002;10(3):180-187.
12. Kilkenny C, Browne WJ, Cuthill IC, Emerson M, Altman DG. Improving bioscience research reporting: the ARRIVE guidelines for reporting animal research. *Osteoarthritis Cartilage*. 2012;20(4):256-260. doi: 10.1016/j.joca.2012.02.010.
  13. Murata K, Kanemura N, Kokubun T, Morishita Y, Fujino T, Takayanagi K. Acute chondrocyte response to controlling joint instability in an osteoarthritis rat model. *Sport Sci Health*. 2016. doi:10.1007/s11332-016-0320-y. [Epub ahead of print]
  14. Oprenyeszki F, Chausson M, Maquet V, Dubuc JE, Henrotin Y. Protective effect of a new biomaterial against the development of experimental osteoarthritis lesions in rabbit: a pilot study evaluating the intra-articular injection of alginate-chitosan beads dispersed in an hydrogel. *Osteoarthritis Cartilage*. 2013;21(8):1099-1107. doi: 10.1016/j.joca.2013.04.017.
  15. Gerwin N, Bendele AM, Glasson S, Carlson CS. The OARSI histopathology initiative - recommendations for histological assessments of osteoarthritis in the rat. *Osteoarthritis Cartilage*. 2010;18 Suppl 3:S24-34. doi: 10.1016/j.joca.2010.05.030.
  16. Pritzker KPH, Gay S, Jimenez SA, Ostergaard K, Pelletier JP, Revell PA, Salter D, van den Berg WB. Osteoarthritis cartilage histopathology: grading and staging. *Osteoarthritis Cartilage*. 2006;14(1):13-29.
  17. Little CB, Barai A, Burkhardt D, Smith SM, Fosang AJ, Werb Z, Shah M, Thompson EW. Matrix metalloproteinase 13-deficient mice are resistant to osteoarthritic cartilage erosion but not chondrocyte hypertrophy or osteophyte development. *Arthritis Rheum*. 2009;60(12):3723-3733. doi: 10.1002/art.25002.
  18. Udo M, Muneta T, Tsuji K, Ozeki N, Nakagawa Y, Ohara T, Saito R, Yanagisawa K, Koga H, Sekiya I. Monoiodoacetic acid induces arthritis and synovitis in rats in a dose- and time-dependent manner: proposed model-specific scoring systems. *Osteoarthritis Cartilage*. 2016;24(7):1284-1291. doi: 10.1016/j.joca.2016.02.005.
  19. Arunakul M, Tochigi Y, Goetz JE, Diestelmeier BW, Heiner AD, Rudert J, Fredericks DC, Brown TD, McKinley TO. Replication of chronic abnormal cartilage loading by medial meniscus destabilization for modeling osteoarthritis in the rabbit knee in vivo. *J Orthop Res* 2013;31(10):1555-1560. doi: 10.1002/jor.22393.
  20. Onur TS, Wu R, Chu S, Chang W, Kim HT, Dang AB. Joint instability and cartilage compression in a mouse model of posttraumatic osteoarthritis. *J Orthop Res*. 2014;32(2):318-323. doi: 10.1002/jor.22509.

21. Egloff C, Hart DA, Hewitt C, Vavken P, Valderrabano V, Herzog W. Joint instability leads to long-term alterations to knee synovium and osteoarthritis in a rabbit model. *Osteoarthritis Cartilage*. 2016;24(6):1054-1060.
22. Mansour JM, Wentorf FA, DeGoede KM. In vivo kinematics of the rabbit knee in unstable models of osteoarthrosis. *Ann Biomed Eng*. 1998;26(3):353-360.

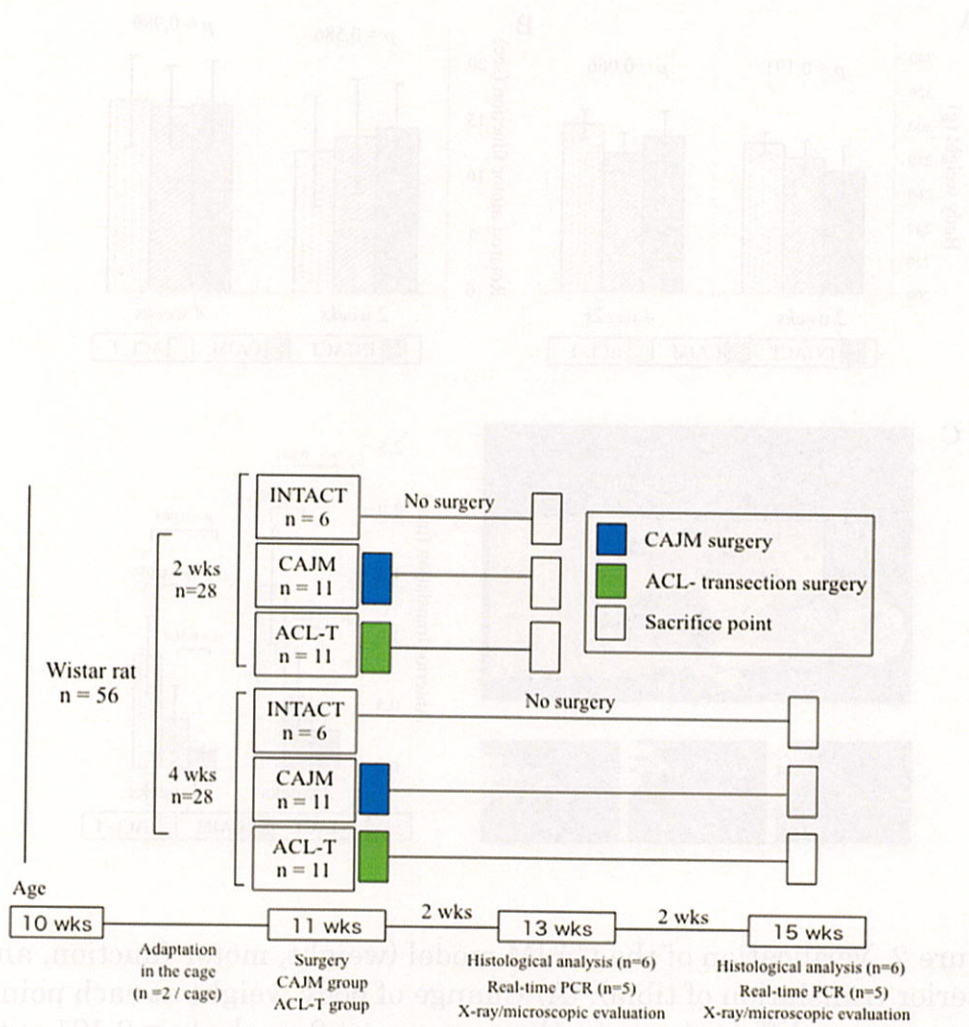


**Figure 1.** Flow chart illustrating experimental protocol.

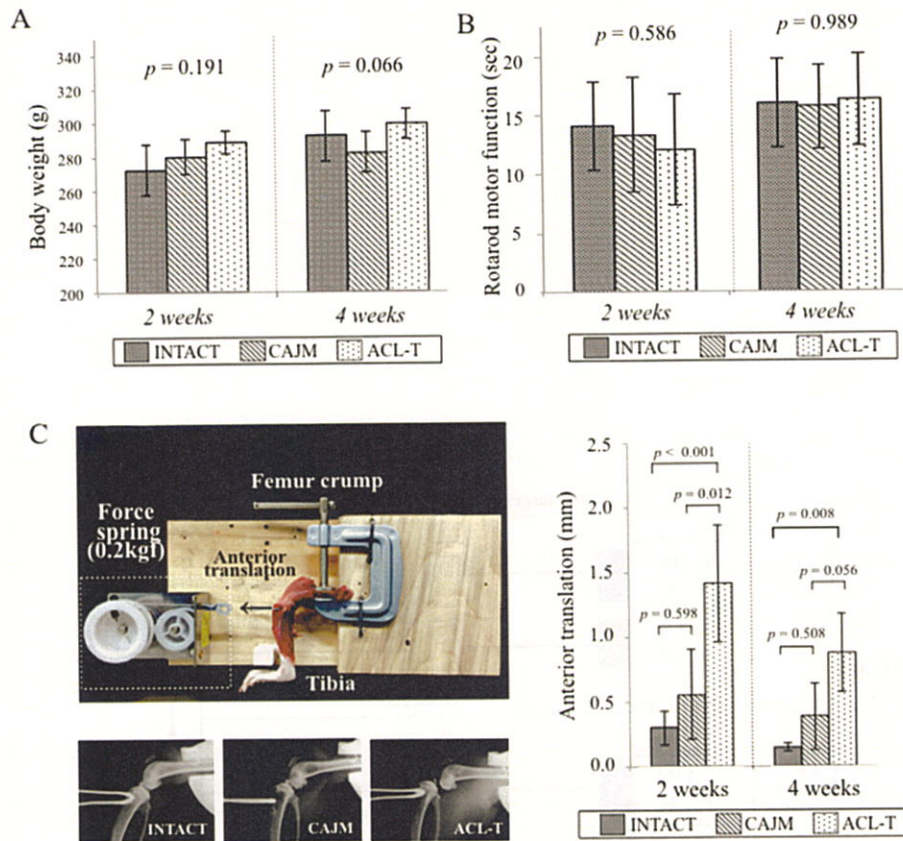


Figure 2. Verification of the CAJM model (weight, motor function, and anterior translation of tibia). (A) Change of body weight at each point. There was no different among three groups at 2 weeks ( $p = 0.191$  with ANOVA) and 4 weeks ( $p = 0.066$  with ANOVA). (B) Motor function evaluation using rotarod analysis at each point. There was no different among three groups at 2 weeks ( $p = 0.586$  with ANOVA) and 4 weeks ( $p = 0.989$  with ANOVA). (C) Anterior translation evaluation method and results. A custom knee instability evaluation system was used to quantify the anterior laxity. The femur was held with a manual clamp, and the tibia was retracted forward by a 0.2 kgf constant force spring. A soft x-ray radiography was used to evaluate the anterior translation, and the displacement was calculated. At 2 weeks, the degree of anterior translation was significantly increased in the ACL-T group as compared with that in the CAJM group ( $p < 0.001$  with post-hoc Tukey method). At 4 weeks, the ACL-T group showed significantly increased anterior translation as compared with that in the INTACT group ( $p = 0.008$  with post-hoc Tukey method). All data are expressed as means with 95% confidence interval limits. The exact P-values between the compared groups (based on a one-way analysis of variance with Tukey's post-hoc test) are displayed on the graph.

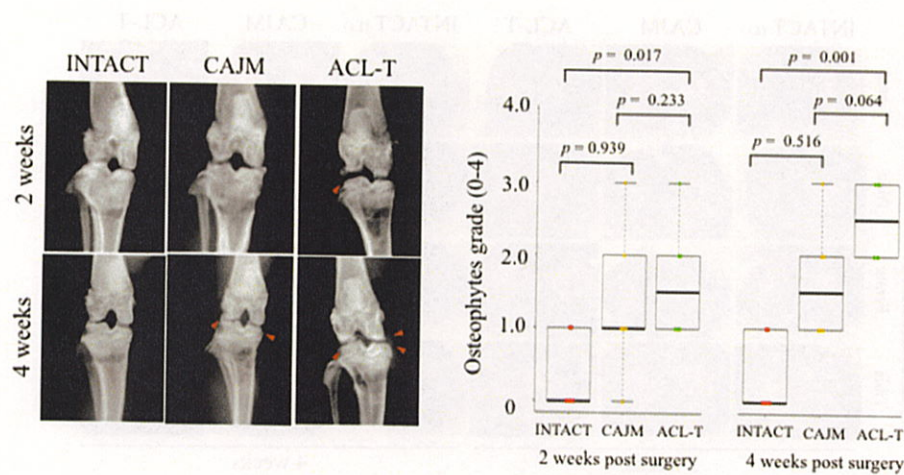


Figure 3. Knee osteophyte formation evaluation with radiography. Time course of soft X-ray radiography of knee joints in INTACT, CAJM, and ACL-T groups at 2 and 4 weeks. Both the ACL-T and CAJM groups showed osteophyte formation (red triangle). The radiographic images were graded, and the ACL-T group scored higher than the INTACT group at 2 weeks ( $p = 0.017$  with post-hoc Mann-Whitney U-test with Bonferroni correction) and 4 weeks ( $p = 0.001$  with post-hoc Mann-Whitney U-test with Bonferroni correction), respectively. The data are expressed as the median at 25% and 75%. The exact P-values between the compared groups (based on the Kruskal-Wallis test followed by the Mann-Whitney U-test for pair-wise difference) are shown on the graph.

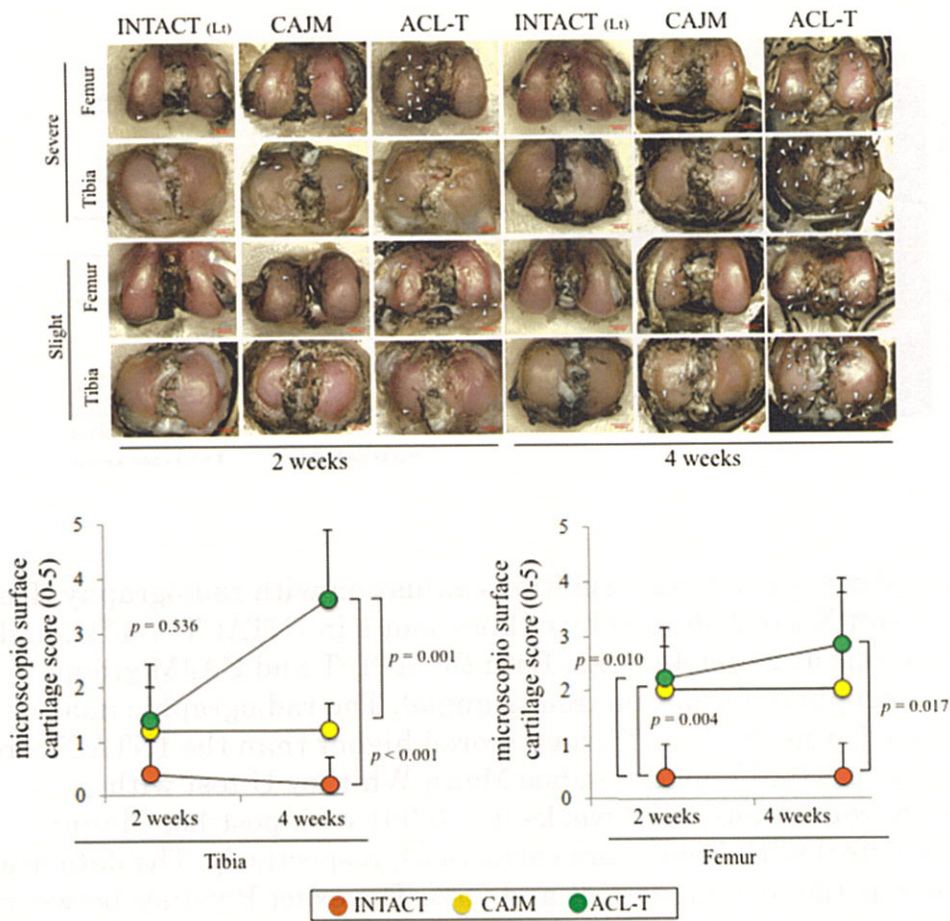


Figure 4. Macroscopic analysis of tibial and femoral cartilage. Representative imaging of Indian ink staining. The most severe change and slightest change in each group were selected. The white arrow heads indicate the cartilage degeneration point and area. Semi-quantification of microscopic features with analysis based on previous scoring systems. The data are expressed as means with lower and upper 95% confidence interval limits. The exact P-values between the compared groups (based on a one-way analysis of variance and Tukey's post-hoc test) are shown on the graph.

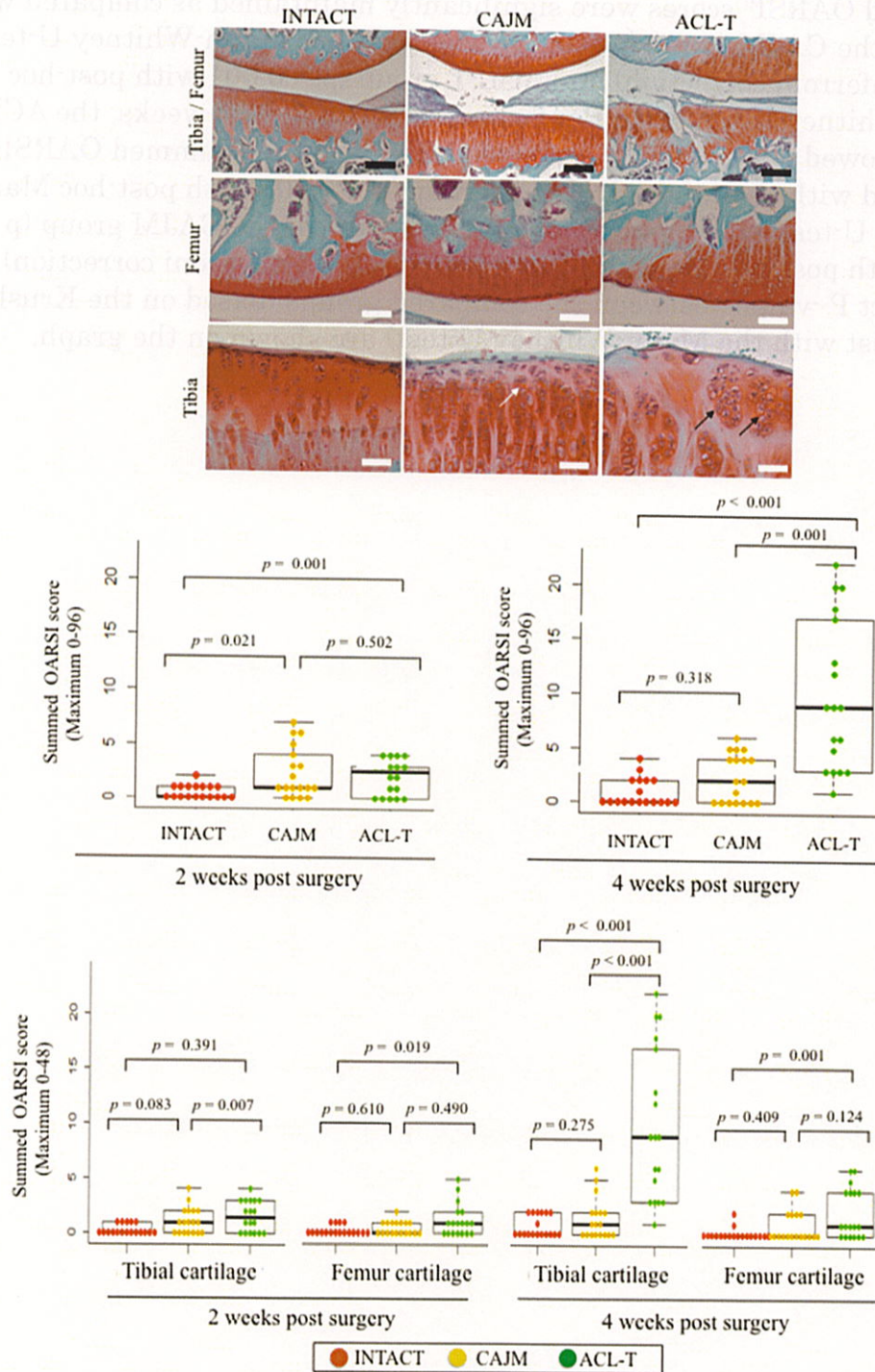


Figure 5. Specific histological findings of articular cartilage at 4 weeks, and OARSIS scoring at 2 and 4 weeks. Cartilage sections with Safranin O and fast green staining in the INTACT, CAJM, and ACL-T groups. The CAJM group exhibited enlargement of the cartilage lacuna and increased chondrocytes (white arrow), whereas the ACL-T group exhibited a

confirmed cluster of chondrocytes (block arrow) and surface fibrillation. OARSI scores at 2 and 4 weeks. At 2 weeks, the INTACT group's "Summed OARSI" scores were significantly maintained as compared with those of the CAJM group ( $p = 0.021$  with post-hoc Mann-Whitney U-test with Bonferroni correction) and ACL-T group ( $p = 0.001$  with post-hoc Mann-Whitney U-test with Bonferroni correction). At 4 weeks, the ACL-T group showed a significantly increased OARSI score (Summed OARSI) as compared with that of the INTACT group ( $p < 0.001$  with post-hoc Mann-Whitney U-test with Bonferroni correction) and of the CAJM group ( $p < 0.001$  with post-hoc Mann-Whitney U-test with Bonferroni correction). The exact P-values between the compared groups (based on the Kruskal-Wallis test with the Mann-Whitney U-test) are shown on the graph.



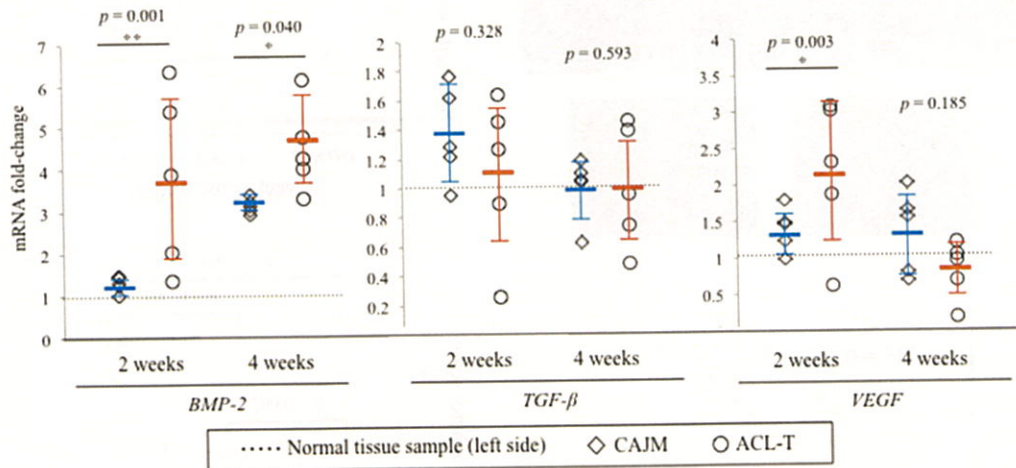


Figure 7. mRNA expression levels in the synovial membrane. Synovial membrane tissue samples harvested at the 2- and 4-week time points were evaluated to investigate the mRNA expression of factors associated with osteophyte formation as a proportion of the normal tissue samples (ratio: 1.0). At 2 weeks, the mRNA expression levels of the BMP-2 had significantly increased in the ACL-T group as compared to those in the CAJM group ( $p = 0.001$  based on post-hoc Mann-Whitney U-test). The VEGF mRNA expression was also significantly increased in the ACL-T group ( $p = 0.003$  based on post-hoc Mann-Whitney U-test). At 4 weeks, the BMP-2 mRNA expression was significantly increased in the CAJM group. The data are expressed as the fold change with 95% confidence interval limits.

## Supplementary methods

### Controlling abnormal joint movement inhibits response of osteophyte formation

Kenji Murata MSc , Takanori Kokubun, PhD , Yuri Morishita, MSc,  
Katsuya Onitsuka , Shuhei Fujiwara , Aya Nakajima , Tsutomu Fujino, MSc ,  
Kiyomi Takayanagi PhD , Naohiko Kanemura, PhD

#### Surgical information

As described previously, the ACL-T and CAJM models were established after anesthetization of the rats with pentobarbital, the right knee joint was exposed to the medial capsule without disrupting the patellar tendon (Fig.1a), and the ACL was transected completely (Fig.1b). In both group, bone tunnel were established by creating along the anterior aspect of the proximal tibia (Fig.1c). To achieve a damping force in the knee joint after the ACL transection, a bone tunnel to the anterior proximal tibia was created, and a nylon thread was passed through the tunnel (Fig.1d). The thread was tied and secured to the posterior distal femur, thereby damping the anterior drawing force of the femur on the tibia (Fig.1e-g). A schematic representation of the surgical procedure is provided in the bottom panel.

The CAJM rat model is designed to restore biomechanical function following ACL transection by using a nylon suture placed along an orientation similar to the original cruciate ligament on the outer side of the joint. Unlike in ACL reconstruction, abnormal joint movements can be dampened, although intra-articular suturing of the ligament is not possible. The moreover, CAJM model was not limited range of motion for flexion and extension (Fig.2)

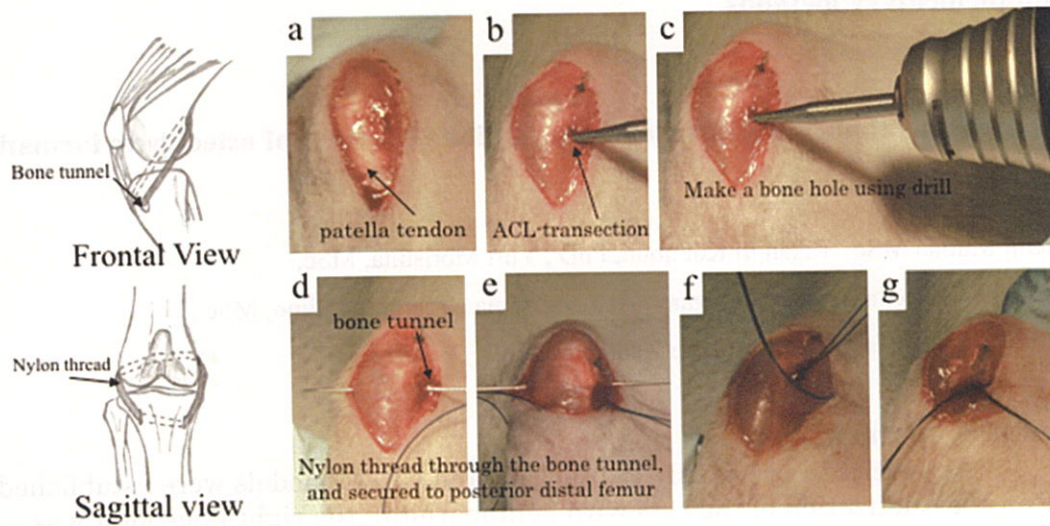


Fig.1. Schematic frontal and sagittal views of a controlled abnormal joint movement (CAJM) model showing tibia achieved by creating bone tunnel using rotary drill and nylon thread passed beside the femur condyle.

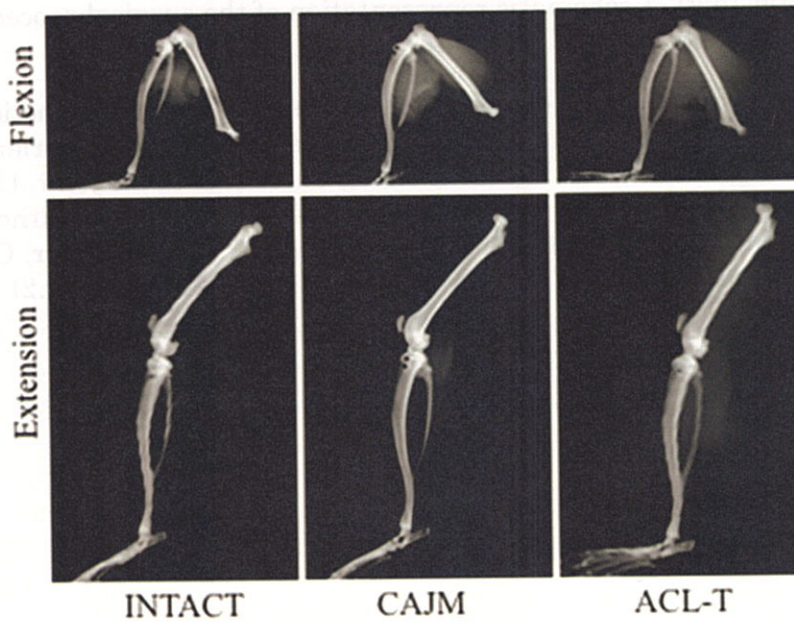


Fig.2. Influence of controlling joint instability among INTACT, ACL-T and CAJM models. Soft x-ray radiographs were taken using a soft radiogram M-60. There was no different for flexion and extension angle.

## Supplemental table

### Controlling abnormal joint movement inhibits response of osteophyte formation

Kenji Murata MSc, Takanori Kokubun, PhD, Yuri Morishita, MSc,

Katsuya Onitsuka, Shuhei Fujiwara, Aya Nakajima, Tsutomu Fujino, MSc,

Kiyomi Takayanagi PhD, Naohiko Kanemura, PhD

Table 1. X-ray scoring system<sup>18</sup>

Grade	X-ray feature
0	No osteophytes
1	Doubtful osteophytes
2	Minimal osteophytes, possibly with narrowing, cysts, and sclerosis
3	Moderate or definite osteophytes with moderate joint space narrowing
4	Severe, with large osteophytes and definite joint space narrowing

Table 2. Histological osteophyte formation scoring system<sup>21</sup>

Score	Histological feature
Size	0 None
	1 Small (approximately the same thickness as the adjacent cartilage)
	2 Medium (1–3 times the thickness of the adjacent cartilage)
	3 Large (3 times the thickness of the adjacent cartilage)
Maturity	0 None
	1 Predominantly cartilaginous
	2 Mixed cartilage and bone with active vascular invasion and endochondral ossification
	3 Predominantly bone

Table 3. Microscopic cartilage surface and bone scoring for rats<sup>22</sup>

Score	Features
0	Intact articular surface
1	$\leq 10$ punctate depressions per condyle
2	$> 10$ punctate depressions per condyle
3	Erosion ( $\leq 50\%$ of joint surface)
4	Erosion ( $> 50\%$ of joint surface)
5	Bone destruction